

F. CHEN
Corrected copy

PLASMA PHYSICS

SUMMER INSTITUTE
PRINCETON UNIVERSITY
1962

LECTURE NOTES

• PROBE TECHNIQUES

Francis F. Chen

Copyright © 1962 by Francis F. Chen, Princeton,
New Jersey. No part of this book may be reproduced
in any form or by any means without permission except
that the Government of the United States of America or
its designees shall have a royalty-free, non-exclusive,
irrevocable license to reproduce, translate, and use
all or any portion of this book.

PREFACE

This volume is one of a series prepared for use of participants in the Summer Institute in Plasma Physics held at Princeton University June 25 - August 3, 1962. An attempt has been made to make this volume serve also as a complete, up-to-date survey of probe and sheath theory, since no such review article existed up to the present time, and the need for such an article has been expressed to the author on a number of occasions. Hence the material contained herein considerably exceeds that which will actually be used in the Summer Institute.

The author would appreciate comments on or corrections to the text.

June 7, 1962

TABLE OF CONTENTS

	<u>Page</u>
1. Introduction	1
1.1 Introduction	1
1.2 The Current-Voltage Characteristic	4
2. Sheath Formation	7
2.1 The Debye Shielding Length	7
2.2 The Child-Langmuir Law	8
2.21 Case of Finite Temperature	10
2.3 The Sheath Criterion	13
2.31 The Case $T_1 = 0$	15
2.32 Physical Meaning of the Sheath Criterion	17
2.33 The Case $T_1 \neq 0, u_o = 0$	21
2.34 The Case $T_1 \neq 0, u_o \neq 0$	26
2.4 The Collisionless Plane Discharge	27
2.5 Sheath Stability	31
2.6 Effect of Magnetic Field	32
2.7 Sheaths in More Than One Dimension	32
3. Probe Theory in the Absence of Collisions and Magnetic Fields	33
3.1 Probe Current in a Prescribed Electric Field	34
3.11 Thin Sheath: Space Charge Limited Current	35
3.12 Thick Sheath: Orbital Motions	39
3.13 Range of Validity of Orbital Theory	44
3.14 Summary of Langmuir's Theory	47
3.2 The Transition Region	49
3.21 Maxwellian Distribution	50
3.22 Isotropic Distributions	51
3.3 Saturation Ion Currents: Unknown Electric Field	54
3.31 Zero Temperature Limit	54
3.32 Finite Temperature: Orbital Motions	59
3.33 Case of Mono-energetic, Isotropic Ion Distribution	62
3.34 Summary of Theories of Ion Collection	67
3.4 Plane Probes	69

	<u>Page</u>
4. Probe Theory in the Presence of Collisions	70
4.1 Probe at Space Potential	71
4.2 Saturation Current in the Limit $\lambda \ll h$	76
4.21 Cylindrical Probe	76
4.22 Spherical Probe	80
4.23 Plane Probe	82
4.3 Summary of Probe Theories with Collisions	83
5. Probe Theory in the Presence of a Magnetic Field	85
5.1 Overall View of the Problem	86
5.2 Electron Current near the Space Potential	89
5.3 "Collisionless" Theory of a Probe in Strong Magnetic Fields	95
5.4 Summary of Probe Theories with a Magnetic Field	106
6. Floating Probes	109
6.1 Floating Potential	109
6.2 Time Response	111
6.3 Effects of Oscillations	112
6.4 Double Probes	113
7. Double Sheaths	120
7.1 Electron Emission: General Formulation	122
7.2 Space Charge Limited Emission	133
7.3 Emitting Probes	137
7.4 Secondary Emission	140
8. Practical Applications	142

ELECTROSTATIC PROBES AND SHEATHS: A SURVEY

by

Francis F. Chen

1. Introduction

1.1 One of the fundamental techniques, in fact, the first one, for measurement of the properties of plasmas is the use of electrostatic probes. This technique was first developed by Langmuir as early as 1924, and consequently is sometimes called the method of Langmuir probes. Basically, an electrostatic probe is merely a small metallic electrode, usually a wire, inserted into a plasma. The probe is attached to a power supply capable of biasing it at various voltages positive and negative relative to the plasma, and the current collected by the probe then provides information about the conditions in the plasma.

It is a fortunate property of plasmas that under a wide range of conditions the disturbance caused by the presence of the probe is localized, and the probe can act truly as a probe in the sense that its very presence has no effect on the quantities it is measuring. We shall find, however, that under certain circumstances, particularly in the presence of a strong magnetic field, the disturbance is not localized, and the probe current then depends not only on the plasma parameters (density and electron and ion temperatures), but also on the way in which the plasma is created and maintained. In such a case the method becomes obviously less useful.

In spite of the difficulties which arise when probes are used in present-

day plasmas, the method is an important one because it has one advantage over all other diagnostic techniques: it can make local measurements. Almost all other techniques, such as spectroscopy or microwave propagation, give information averaged over a large volume of plasma.

Experimentally, electrostatic probes are extremely simple devices, consisting merely of an insulated wire, used with a dc power supply, and an ammeter or an oscilloscope. Nature, however, makes us pay a penalty for this simplicity: the theory of probes is extremely complicated. The basic equations of probe theory are the Boltzmann equation for each type of particle

$$\frac{\partial f_j}{\partial t} + \underline{v}_j \cdot \underline{\nabla} f_j + \frac{q_j}{m_i} \left[-\underline{\nabla} V + \frac{1}{c} \underline{v}_j \times \underline{B} \right] \cdot \underline{\nabla} f_j = \left(\frac{\partial f_j}{\partial t} \right)_{\text{coll.}} \quad (1.1-1)$$

and Poisson's equation

$$\nabla^2 V + 4\pi(q_i n_i + q_e n_e) = 0 \quad (1.1-2)$$

where

$$n_j = \int f_j(\underline{r}_j, \underline{v}_j) \underline{d}^3 \underline{v}_j \quad (1.1-3)$$

These are the same equations that are used in practically all aspects of plasma physics; the difference here is that $\nabla^2 V$ cannot be assumed to vanish and that we are concerned with the conditions at a boundary of the plasma and therefore Eq. (1.1-2) must be solved with certain boundary conditions. This is considerably more difficult than, say, finding a dispersion relation for plasma waves, in which

all one has to do is set a determinant equal to zero. In fact, just the formulation of the boundary conditions is not easy. In many problems in other fields of plasma physics the distribution functions f for ions and electrons can be assumed to be approximately Maxwell-Boltzmann. In probe theory, however, only one distribution -- that of the particles repelled by the probe -- is approximately Maxwellian; the other species of particle, which is collected by the probe, has a distribution which must be calculated from (1.1-1). This means that we are generally faced with a self-consistency problem in which the potential V must be found which satisfies both (1.1-1) and (1.1-2). Even when the collision term can be neglected, this generally leads to a non-linear integral equation which can be simplified only in specific cases to a point where the solution is analytic or, at least, simple enough that the dependences on the plasma parameters can be seen.

It will be our purpose to summarize, with a minimum of algebra and, hopefully, a maximum of physical insight, the result of those specific cases in which the theory of probes has given useful results and to indicate the experimentally interesting cases in which the mathematical difficulties of the theory have so far been insuperable. We shall pay particular attention to two aspects which are of particular importance in present-day physics: the case of a plasma in a strong magnetic field, and the case of electron or ion emission at a plasma boundary. The importance of strong magnetic fields is obvious; the subject of the sheath on an emitting surface is of importance not only because probes tend to be heated to incandescence in hot plasmas but also because of the current interest in thermionic converters and in the production of laboratory discharges.

We shall not be able to cover the experimental aspects of probes, nor shall we be concerned with other (non-electrostatic) types of probes which may be inserted into a plasma, such as magnetic probes, microwave probes, or scintillator probes.

1.2 The Current-Voltage Characteristic

In order to get an over-all view of the situation, let us look at a typical plot of probe current versus probe voltage, as shown in Fig. 1.1.

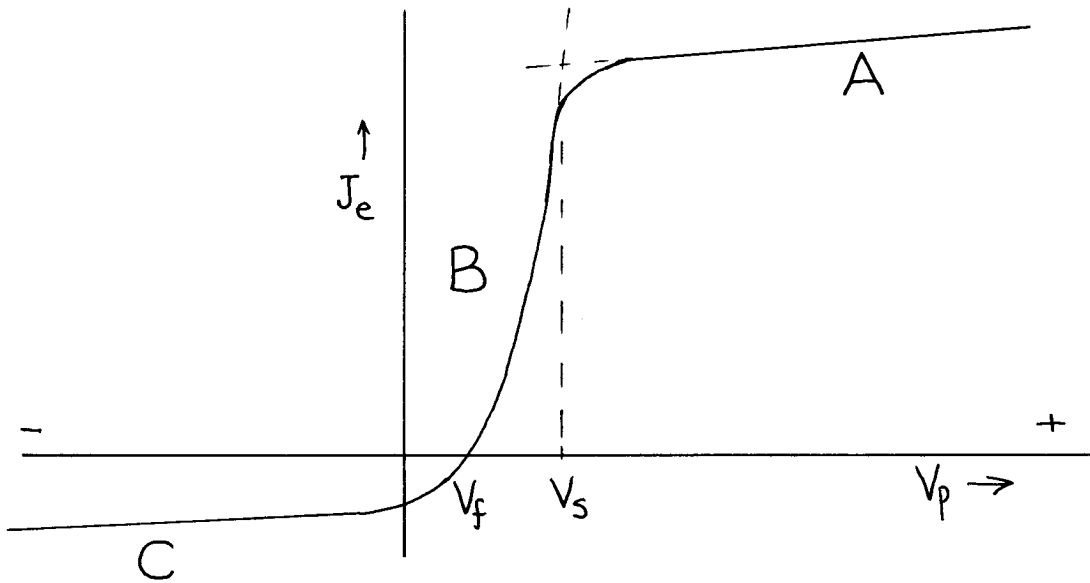


Fig. 1.1

Here negative, or electron, current to the probe is plotted against V_p , the probe voltage with respect to an arbitrary reference point. This plot may be obtained continuously in a steady-state discharge, or point by point in a pulsed discharge, the probe bias being changed from pulse to pulse; or the entire curve may be obtained in a few microseconds in a pulsed discharge by the use of a fast sweeping voltage source.

The qualitative behavior of this curve can be explained as follows. At the point V_s , the probe is at the same potential as the plasma (this is commonly called the space potential). There are no electric fields at this point, and the charged particles migrate to the probe because of their thermal velocities. Since electrons move much faster than ions because of their small mass, what is collected by the probe is predominantly electron current. If the probe voltage is made positive relative to the plasma, electrons are accelerated toward the probe. Moreover, the ions are repelled, and what little ion current was present at V_s vanishes. Near the probe surface there is therefore an excess of negative charge, which builds up until the total charge is equal to the positive charge on the probe. This layer of charge is called a sheath, and outside of it there is very little electric field, so that the plasma is undisturbed. It is characteristic of a plasma that the sheath is usually very thin; to the extent that this is true, the probe is truly probing in the sense that it does not disturb its environment. The electron current is that which enters the sheath through random thermal motions; and since the area of the sheath is relatively constant as the probe voltage is increased, we have the fairly flat portion A of the probe characteristic. This is called the region of saturation electron current.

If now the probe potential is made negative relative to V_s , we begin to repel electrons and accelerate ions. The electron current falls as V_p decreases in region B, which we shall call the transition region of the characteristic. If the electron distribution were Maxwellian, the shape of the curve here, after the contribution of the ions is subtracted, would be exponential. Finally, at the

point V_f , called the floating potential, the probe is sufficiently negative to repel all electrons except a flux equal to the flux of ions and therefore draws no net current. An insulated electrode inserted into a plasma would assume this potential.

At large negative values of V_p almost all the electrons are repelled, and we have an ion sheath and saturation ion current (region C). This is similar to region A; but there are two points of asymmetry between saturation ion and saturation electron collection aside from the obvious one of the mass difference, which causes the disparity in the absolute magnitude of the currents. The first point is that the ion and electron temperatures are usually unequal, and it turns out that sheath formation is considerably different when the colder species is collected than when the hotter species is collected. The second point is that when there is a magnetic field, the motion of the electrons is much more affected by the field than the motion of the ions. These two points, which were neglected in the original theory of Langmuir, are responsible for making impossible the simple and straightforward application of probes as originally proposed by Langmuir.

It is evident that the formation of sheaths plays an important role in probe theory. For this reason, the next section will be devoted to an explanation of the basic characteristics of sheaths.

2. Sheath Formation

2.1 The Debye Shielding Length

Let us consider what happens when a potential V is introduced at some point in an infinite plasma in equilibrium. We can imagine, for instance, that a perfectly transparent grid is inserted into the plasma. If the ions and electrons are in thermal equilibrium, their densities are given by the Maxwell-Boltzmann distribution:

$$n_i = n_o e^{-eV/kT_i} \quad (2.1-1)$$

$$n_e = n_o e^{eV/kT_e} \quad , \quad (2.1-2)$$

where we have assumed singly charged ions for simplicity. The potential in the plasma is given by Poisson's equation, which, for simplicity, we shall write in one dimension:

$$\frac{d^2V}{dx^2} = -4\pi e(n_i - n_e) \quad . \quad (2.1-3)$$

To get a rough idea of the scale length of the potential distribution, let us expand the exponentials in (2.1-1) and (2.1-2) and substitute into (2.1-3):

$$\frac{d^2V}{dx^2} = 4\pi n_o e \left(\frac{eV}{kT_e} + \frac{eV}{kT_i} \right) = 4\pi n_o e^2 \left(\frac{1}{kT_e} + \frac{1}{kT_i} \right) V \quad .$$

Hence

$$V \sim e^{-x/h} \quad , \quad \text{where}$$

$$h^2 = \frac{kT_i T_e}{T_i + T_e} \frac{1}{4\pi n_o e^2} \quad . \quad (2.1-4)$$

This shows that as we approach our grid, the potential rises exponentially from its value in the plasma with a characteristic length \underline{h} , which is called the Debye length. We note that when T_i and T_e are much different from each other, the Debye length is dependent primarily on the smaller temperature.

Numerically the value of \underline{h} is usually extremely small, smaller than any other characteristic length such as the radius of the plasma, the probe radius, or a mean free path. This means that a potential introduced on a probe is localized and shielded from the rest of the plasma so that the disturbance caused by the probe has a chance of being negligible.

2.2 The Child-Langmuir Law

The previous example was an extreme simplification inasmuch as the grid producing the potential disturbance was perfectly transparent. In practice, one species of particle will be repelled and one collected, and the distribution of the collected species cannot be Maxwellian. Let us now examine another idealized situation, that of two infinite parallel plane plates, one of which emits particles and is at zero potential, and the other of which is perfectly absorbing and is at a potential V . This is shown in Fig. 2.2.

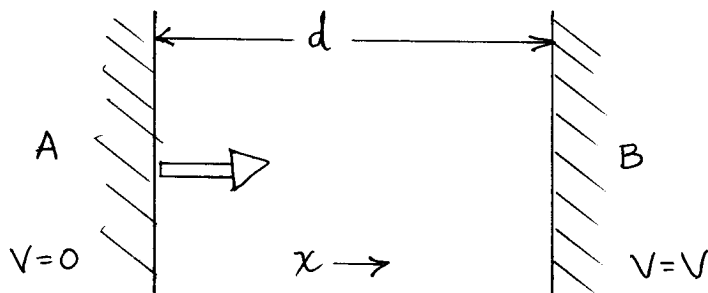


Fig. 2.2

Consider first the case of emission at plane A of only one species of particle, with charge $-e$ and mass m , emitted at zero velocity. The particle velocity at a position where the potential is V is then

$$v = (2eV/m)^{1/2} \quad . \quad (2.2-1)$$

If the emitted current density is j , the particle density at x will be

$$n(x) = \frac{j}{-e} \left[\frac{2eV(x)}{m} \right]^{-1/2} \quad . \quad (2.2-2)$$

Poisson's equation becomes

$$\frac{d^2V}{dx^2} = 4\pi j \left(\frac{2eV}{m} \right)^{-1/2} \quad .$$

Multiplying by dV/dx and integrating from $x = 0$, we have

$$\begin{aligned} \frac{1}{2} \left(\frac{dV}{dx} \right)^2 &= 4\pi j \int_0^V \left(\frac{2eV}{m} \right)^{-1/2} dV \\ &= 4\pi j \left(\frac{2m}{e} \right)^{1/2} V^{1/2} + \left(\frac{dV}{dx} \right)_0 \quad . \end{aligned} \quad (2.2-3)$$

By space-charge-limited flow, we mean that $(dV/dx)_0$ vanishes. We then have

$$V^{-1/4} dV = (8\pi j)^{1/2} \left(\frac{2m}{e} \right)^{1/4} dx \quad . \quad (2.2-4)$$

Integrating from $x = 0$ to $x = d$, we have

$$\frac{4}{3} V^{3/4} = (8\pi j)^{1/2} \left(\frac{2m}{e} \right)^{1/4} d$$

or

$$j = \left(\frac{2e}{m} \right)^{1/2} \frac{V^{3/2}}{9\pi d^2} \quad , \quad (2.2-5)$$

which is the Child-Langmuir 3/2-power law for space-charge-limited current flow between two planes separated by a distance \underline{d} with a potential V between them.

2.21 Case of Finite Temperature

The next easiest case to consider is that in which the particles are emitted at a temperature T , the geometry remaining the same as before. Let us assume that the velocity distribution at plane A is half of a Maxwellian distribution, as is the case for electron emission from a hot plate. The distribution function at $x = 0$ is then

$$\begin{aligned} f(0, v) &= 2n_o \left(\frac{m}{2\pi kT}\right)^{1/2} e^{-mv^2/2kT} & v > 0 & \quad (2.21-1) \\ &= 0 & v < 0 & \quad . \end{aligned}$$

The Boltzmann equation (1.1-1) reduces in this case to

$$v \frac{\partial f}{\partial x} = \frac{q}{m} \frac{dV}{dx} \frac{\partial f}{\partial v} \quad , \quad (2.21-2)$$

where \underline{q} is the charge of the particle. This says that \underline{f} is a function of $\frac{1}{2}mv^2 + qV$, the total energy. The distribution function at x is then given by (2.21-1) with v^2 replaced by $v^2 + (2qV/m)$:

$$f(x, v) = 2n_o \left(\frac{m}{2\pi kT}\right)^{1/2} e^{-m(v^2 + \frac{2qV}{m})/2kT}, \quad v > \left(\frac{-2qV}{m}\right)^{1/2}. \quad (2.21-3)$$

We can save a lot of writing from now on if we introduce dimensionless variables, at the risk of losing the immediate recognition of the physical meaning of each

equation. Since we are interested in a potential V which accelerates the particles, we have that $qV < 0$. Thus we shall choose

$$\eta = -\frac{qV}{kT} \quad . \quad (2.21-4)$$

Also we shall introduce a thermal velocity

$$v_t = \left(\frac{2kT}{m}\right)^{1/2} \quad (2.21-5)$$

and let

$$u = v/v_t \quad . \quad (2.21-6)$$

Finally, the unit of distance will be the Debye length, so that

$$\xi = x(kT/4\pi n_0 q^2)^{-1/2} \quad . \quad (2.21-7)$$

In these units velocity and potential are directly related ($u^2 \sim \eta$), and the total energy is simply $(u^2 - \eta) \frac{kT}{2}$. The velocity distribution (2.21-3) becomes

$$f(\eta, u) = \frac{2n_0}{v_t \sqrt{\pi}} e^{-(u^2 - \eta)}, \quad u^2 > \eta \quad . \quad (2.21-3)'$$

The density is then

$$n(\eta) = v_t \int_{\sqrt{\eta}}^{\infty} f(\eta, u) du = n_0 e^{\eta} (1 - \text{erf} \sqrt{\eta}), \quad (2.21-8)$$

where the error function is defined by

$$\text{erf } x = \frac{2}{\sqrt{\pi}} \int_0^x e^{-t^2} dt \quad . \quad (2.21-9)$$

Poisson's equation is now

$$\frac{d^2 V}{dx^2} = -4\pi q n, \text{ or}$$

$$\eta'' = \frac{d^2 \eta}{d\xi^2} = e^\eta (1 - \operatorname{erf} \sqrt{\eta}). \quad (2.21-10)$$

Again using the integrating factor η' , we have upon integration

$$\frac{1}{2} \eta'^2 = e^\eta (1 - \operatorname{erf} \sqrt{\eta}) + \frac{2}{\sqrt{\pi}} \eta^{1/2} + \frac{1}{2} \eta_0'^2. \quad (2.21-11)$$

The integral of the error function has been carried out by using (2.21-9) and reversing the order of integration.

The potential distribution is then found by integrating (2.21-7). The resulting curve has the behavior shown in Fig. 2.3.

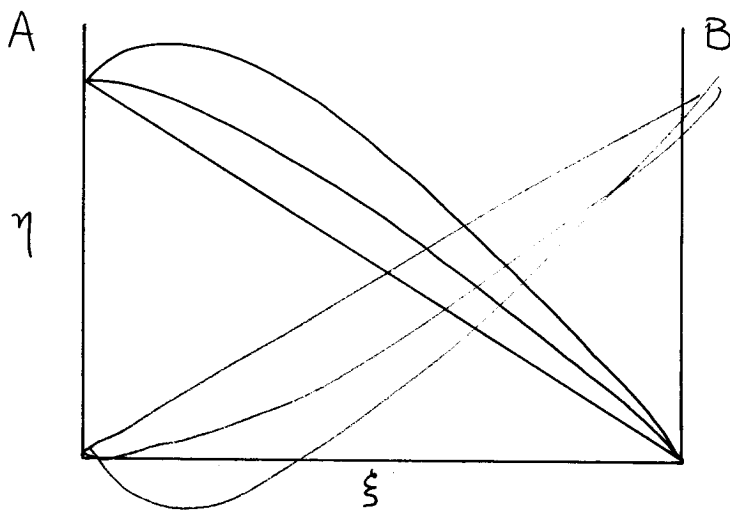


Fig. 2.3

For very small n_0 , there is no space charge, and $\eta(\xi)$ is a straight line. As n_0 is increased, the curve becomes more and more concave upwards until the slope $\eta'(0)$ becomes zero. Then space charge limitation occurs, since there is no longer any electric field acting on the particles as they leave surface A. If n_0 is further increased, a retarding field must be set up in order to reflect the excess of particles emitted over the number that the space charge will allow through. Thus a potential maximum η_m at $\xi = \xi_m$ must occur, and it is obvious that Eq. (2.21-7) must be integrated starting from this point, with $\eta'_m = 0$. The entire solution, including that for the region to the left of ξ_m , has been given by Langmuir [1961, IV, p. 373 ff.]; however, for our purposes η_m and ξ_m are usually so small that they can be set equal to zero. The integral of (2.21-7) has no ^{simple} analytic form, but to first order the space-charge-limited current is given by

$$j = \left(\frac{2e}{m}\right)^{1/2} \frac{1}{9\pi} \frac{(V - V_m)^{3/2}}{(d - x_m)^2} \left(1 + \frac{2.66}{\sqrt{\eta}}\right) \quad (2.21-8)$$

Comparison with (2.2-5) shows that the effect of a finite temperature is slight.

2.3 The Sheath Criterion

Let us now introduce a second species of charged particle, so that we have a species 1 which is accelerated from A to B and a species 2 of equal and opposite charge which is repelled from B. We want eventually to identify surface A with the surface of the plasma and B with the surface of a wall or probe. Since a plasma is very nearly neutral (by definition), we require that $n_1 \approx n_2$ at A.

One is likely to feel dissatisfied with an arbitrary division of a gas dis-

charge into a "plasma" region, in which quasi-neutrality obtains, and a "sheath" region in which large potential drops can occur; therefore, let us digress briefly to discuss this dichotomy. This sharp division between plasma and sheath was originally suggested by the experimental observation that potential drops were always confined to small regions near electrodes; however, it is not merely for convenience that such a separation is made. The equations governing the plasma, where collisions and ionization take place but where quasi-neutrality can be assumed, are entirely different from those governing the sheath, where charges can build up but where there are no collisions. (If the collision free path were comparable to the Debye length, the plasma would be so weakly ionized that one might say it is not a plasma at all.) This is then a boundary-layer problem, in which the solutions for the interior and exterior regions must be matched at the interface and must tend to the proper asymptotic limits in their respective regions. Even with this division the operations can rarely be solved analytically. A continuous solution of the plasma-sheath transition, if the equations could be set up, would involve a large numerical calculation. Such a calculation would not be expected to yield results much different from those based on distinct plasma and sheath regions, since this is generally a good approximation, and indeed must be, as indicated earlier, in order for probes to work as probes.

In solving the problem of the sheath, certain boundary conditions must be met to ensure a smooth transition to the plasma. It is our purpose in this section to see what these requirements are.

2.31 The Case $T_1 = 0$

We now return to the problem of the collisionless motion of two types of charged particle between two infinite planes with a potential difference between them. For simplicity, we shall treat first the somewhat degenerate case in which $T_1 = 0$, i . e . , the accelerated particles have no random motion. In this case we must give them a non-vanishing drift velocity v_o at A, since otherwise their velocity at A would be 0 and their density infinite if their current is to be finite. This difficulty can be avoided by going to the spherically-symmetric case, where density falls as $1/r^2$, but then we would lose the simplicity of the particle orbits which we have in the one-dimensional case.

Since there can be no particles of type 1 traveling from B to A, the distribution function of 1 is

$$f_1(0, v) = n_o \delta(v - v_o) \quad v_o > 0$$

$$f_1(x, v) = n_o \delta\left[\left(v^2 + \frac{2q_1 V}{m_1}\right)^{1/2} - v_o\right] \quad . \quad (2.31-1)$$

We now assume that the potential B is so large that almost all particles 2 are repelled; their distribution will then be Maxwellian:

$$f_2(x, v) = n_o \left(\frac{m_2}{2\pi k T_2}\right)^{1/2} e^{-m_2\left(v^2 + \frac{2q_2 V}{m_2}\right)/2kT_2} \quad . \quad (2.31-2)$$

With the dimensionless variables

$$\eta = -\frac{q_1 V}{kT_2}, \quad u = v \left(\frac{m_1}{2kT_2} \right)^{1/2}, \quad \xi = x \left(\frac{4\pi n_0 q_1^2}{kT_2} \right)^{1/2}, \quad (2.31-3)$$

this becomes

$$f_2(\eta, u) = n_0 \left(\frac{m_2}{\pi m_1} \right)^{1/2} \frac{1}{v_s} e^{-\frac{m_2}{m_1} u^2 - \eta}, \quad (2.31-4)$$

where we have set $q_1 = -q_2$, and where $v_s = (2kT_2/m_1)^{1/2}$. Note that since particles 1 are accelerated, $q_1 V$ is always negative, and therefore η always positive. Similarly, (2.31-1) becomes

$$f_1(\eta, u) = n_0 v_s^{-1} \delta[(u^2 - \eta)^{1/2} - u_0]. \quad (2.31-5)$$

The densities are found by integrating with respect to $v_s du$:

$$n_2 = n_0 e^{-\eta}$$

$$n_1 = n_0 \int \delta(y - u_0) \frac{y dy}{(y^2 + \eta)^{1/2}} = n_0 (1 + \eta u_0^{-2})^{-1/2}. \quad (2.31-6)$$

Poisson's equation is then

$$\eta'' = n_0 [(1 + \eta u_0^{-2})^{-1/2} - e^{-\eta}]. \quad (2.31-7)$$

With the usual integrating factor η' , the integral from 0 to x is

$$\frac{1}{2} \eta'^2 = n_0 \left\{ 2u_0^2 [(1 + \eta u_0^{-2})^{1/2} - 1] + e^{-\eta} - 1 \right\} + \frac{1}{2} \eta_0'^2. \quad (2.31-8)$$

For the moment, let us neglect η' . The left-hand side in (2.31-8) must be positive; hence

$$2u_o^2 [(1 + \eta u_o^{-2})^{1/2} - 1] > 1 - e^{-\eta} \quad (2.31-9)$$

Near the origin $\eta = 0$, this inequality becomes, upon expanding,

$$2u_o^2 \left[\frac{1}{2} \eta u_o^{-2} - \frac{1}{8} \eta^2 u_o^{-4} \right] > \eta - \frac{1}{2} \eta^2$$

Must go to second order - this corresp. to 2nd deriv. of $\int nd\eta$ - hence to n

$$u_o = \left(\frac{m_1 v_o^2}{2kT_2} \right)^{1/2} > \frac{1}{2^{1/2}} \quad (2.31-10)$$

This is the original sheath criterion derived by Langmuir [1961, V] and Bohm [1949]. It states that in order for the sheath equation to have a solution for small η there is a restriction on the streaming velocity assumed for particles 1 at plane A: namely, that it be larger than $(kT_2/m_1)^{1/2}$.

2.32 Physical Meaning of the Sheath Criterion

The most common application of this criterion is in the case of ion collection, in which ions are particles 1 and electrons particles 2. In many discharges the ion temperature is much lower than the electron temperature, so that the assumption $T_1 = 0$ is applicable. Equation (2.31-10) then says that the ions must stream into the sheath boundary with an energy greater than $\frac{1}{2}kT_e$, which is much larger than their thermal energy. We shall see later how they may gain such an energy in the plasma.

The reason for this restriction on the cold particles can be seen by plotting the density, as given by (2.31-6), logarithmically against potential η , as shown in Fig. 2.4.

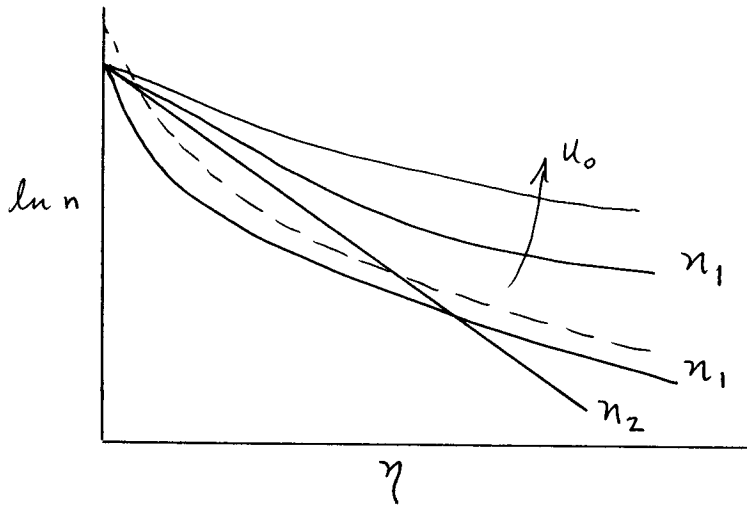


Fig. 2.4

The trapped particles 2 have a density which appears as a straight line on the semi-log plot. If η'' is rigorously zero, the curve for n_1 starts at the same point n_0 as does n_2 , and its initial slope depends on u_0 . If u_0 is small, n_1 is less than n_2 for small η . Referring to Poisson's equation,

$$n_0 \eta'' = n_1 - n_2 \quad ,$$

we see that if $\eta' = 0$ and η is to be positive, η'' must be positive near $\eta = 0$.

If u_0 is too small, η'' is negative, and this will not permit a monotonic solution for $\eta(\xi)$. The solution will oscillate between two values of η , corresponding to an imaginary value of η'^2 . If u_0 were large, we see from Fig. 2.4 that n_1 is always larger than n_2 , and the problem does not arise. The critical condition is that

$$\left(\frac{dn_1}{d\eta}\right)_0 = \left(\frac{dn_2}{d\eta}\right)_0 \quad . \quad (2.32-1)$$

From (2.31-6), this is just

$$-\frac{n_0}{2} u_0^{-2} = -n_0 \quad , \quad \text{or} \quad u_0^2 = \frac{1}{2} \quad ,$$

the same condition as (2.31-10).

In this treatment we have assumed $\eta = \eta' = \eta'' = 0$ at the origin. If this were strictly true, the only solution would be the trivial one $\eta = 0$. In actuality the sheath solution must be matched to the plasma solution at a point where both η' and η'' are slightly positive. The situation is illustrated in Fig. 2.5.

Take η'' , η'''' , etc. from 2.31-7 all are 0.

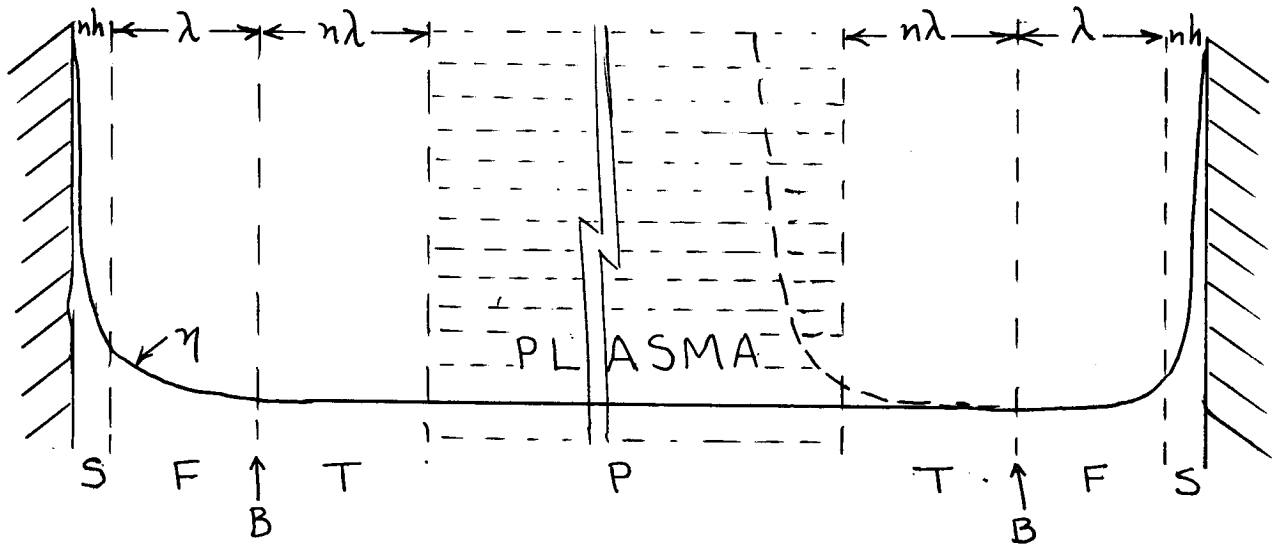


Fig. 2.5

Here a one-dimensional discharge bounded by two walls has been schematically divided into several regions. In region P there is a plasma in which the collision and ionization processes dominate. Region S is the sheath region, several Debye lengths in thickness, where the wall potential (which confines the electrons) is developed abruptly. The potential barrier, as seen by the electrons, is shown. In region F, of the order of an ion mean free path in thickness, the collisionless equations we have been using must hold. At the same time, quasi-neutrality must also obtain in F, since otherwise the abrupt

rise of potential would occur in F rather than in S. Between P and F is a transition region T in which plural collisions occur, and neither the collision-dominated nor the free-fall equations apply. We are concerned with the value of η' and η'' at the boundary B between T and F.

If, in T and P, we did not use the proper equations but instead continued using Eq. (2.31-7), the resulting curve for η might look like that shown by the dotted line. The curve must be symmetric about some point ξ_0 , since (2.31-7) is invariant under a reflection in ξ . At ξ_0 we have $\eta' = 0$, $\eta'' \neq 0$. If we move our coordinate system to start at ξ_0 , we need consider only this boundary condition; the general conclusions will be the same. If $\eta'' > 0$, n_{10} will be larger than n_{20} , and the density curve will look like the dotted one in Fig. 2.4. It is clear that now u_0 may be decreased until n_1 crosses n_2 , but that the area above n_2 must always be larger than the area below n_2 in order for the expression for η'^2 to be positive. The critical value of u_0 is now that which makes these areas equal, and there will be one such value for each value of η'' .

An upper limit to η''_0 can be obtained by assuming that $\eta'' = \eta''_0$ everywhere. Since in actuality $\eta'' \geq \eta''_0$, we have

$$\eta'' \geq \eta''_0, \quad \eta' \geq \eta''_0 \xi, \quad \eta \geq \frac{1}{2} \eta''_0 \xi^2.$$

In order that the η curve not develop abruptly until the sheath region is reached, we require that η be less than, say, 1 when x is of the order of λ . Thus,

$$\eta''_0 \leq \frac{2h^2}{\lambda^2}. \quad (2.32-2)$$

* This way of estimating η''_{max} is n.g. since $\eta(x)$ does not have to be monotonic
 Must estimate η''_{max} from plasma region -20-

It can be shown that

$$u_o = \frac{1}{2^{1/2}} \left[1 - \left(\frac{\eta_o''}{1 + \eta_o''} \right)^{1/2} \right], \quad (2.32-3)$$

so that the reduction in u_o is less than something like h/λ . Since h/λ is generally very small, the sheath criterion (2.31-10) is not greatly affected by the assumptions about η_o'' and η_o' , and is valid as long as $T_1 = 0$. In the next section we shall say more about this in the general case.

2.33 The Case $T_1 \neq 0, u_o = 0$

We have found that in the collection of cold particles there is a severe condition on their initial velocity. The question now is whether such a condition also occurs for hot particles. We assume that the accelerated particles 1 have a half-Maxwellian distribution, as in (2.21-3)':

$$f_1(\eta, u) = \frac{2n_{1o}}{v_t \sqrt{\pi}} e^{-(u^2 - \eta)}, \quad u^2 > \eta \quad (2.33-1)$$

Here η and u are normalized to quantities pertaining to species 1. The distribution of species 2 is Maxwellian:

$$f_2(\eta, u) = \frac{n_{2o}}{\sqrt{\pi}} \left(\frac{m_2}{m_1} \right)^{1/2} \frac{1}{v_t} e^{-\alpha \left(\frac{m_2}{m_1} u^2 + \eta \right)}, \quad (2.33-2)$$

where

$$\alpha = \frac{T_1}{T_2} \quad (2.33-3)$$

is the parameter we wish to evaluate.

Integrating over $v_t du$, we have for the densities

$$\begin{aligned} n_1 &= n_{10} e^{\eta} (1 - \operatorname{erf} \sqrt{\eta}) \\ n_2 &= n_{20} e^{-\alpha \eta} \end{aligned} \quad (2.33-4)$$

Here we must not set $n_{10} = n_{20}$ for the following reason. The derivative of n_1 is

$$\begin{aligned} \frac{d}{d\eta} n_1 &= n_{10} \left[e^{\eta} (1 - \operatorname{erf} \sqrt{\eta}) - e^{\eta} \frac{2}{\sqrt{\pi}} \frac{d}{d\eta} \int_0^{\sqrt{\eta}} e^{-t^2} dt \right] \\ &= n_{10} \left[e^{\eta} (1 - \operatorname{erf} \sqrt{\eta}) - \frac{2}{\sqrt{\pi}} \cdot \frac{1}{2} \eta^{-1/2} \right] \end{aligned} \quad (2.33-5)$$

Thus as $\eta \rightarrow 0$, $dn_1/d\eta \rightarrow -\infty$. If $n_{10} = n_{20}$, it is clear from Fig. 2.4 that n_1 will be less than n_2 for small η regardless of the value of α . We must therefore allow η_0'' to be finite, as in the last section, so that $n_{10} \neq n_{20}$; then a solution will be possible for some values of α .

Let

$$\eta_0'' = \delta = (n_{10} - n_{20})/n_{10} \quad (2.33-6)$$

Then Poisson's equation is

$$\eta'' = e^{\eta} (1 - \operatorname{erf} \sqrt{\eta}) - (1 - \delta) e^{-\alpha \eta} \quad (2.33-7)$$

The first integral is, for $\eta_0' = 0$,

$$\frac{1}{2} \eta'^2 = e^{\eta} (1 - \operatorname{erf} \sqrt{\eta}) - 1 + \frac{2}{\sqrt{\pi}} \eta^{1/2} + \frac{1 - \delta}{\alpha} (e^{-\alpha \eta} - 1) \quad (2.33-8)$$

Therefore if

$$g(\eta) = e^{\eta} (1 - \operatorname{erf} \sqrt{\eta}) - 1 + \frac{2}{\sqrt{\pi}} \eta^{1/2}$$

(2.33-9)

and

$$h(\eta) = \frac{1 - \delta}{\alpha} (1 - e^{-\alpha\eta}) ,$$

we have the condition

$$g(\eta) > h(\eta) .$$

(2.33-10)

The functions g and h are shown schematically in Fig. 2.6.

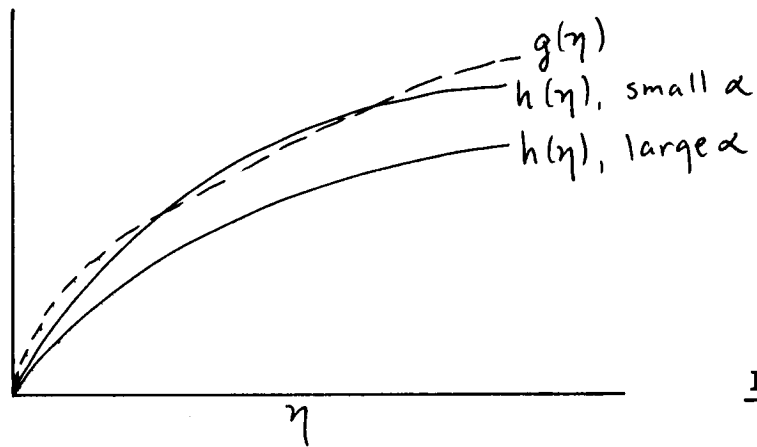


Fig. 2.6

For sufficiently large α , $h(\eta)$ will always lie under $g(\eta)$, and the inequality (2.33-10) will be satisfied. For small α the two curves will cross, giving a region of η in which η'^2 is negative. The critical value of α , α_c , occurs when the two curves are just tangent, or

$$g(\eta) = h(\eta)$$

$$g'(\eta) = h'(\eta) .$$

(2.33-11)

Elimination of η between these two equations will give a relation between α_c and δ . Note that $g' = h'$ is simply the equation $n_1 = n_2$. The density plot in this

case is shown in Fig. 2.7.

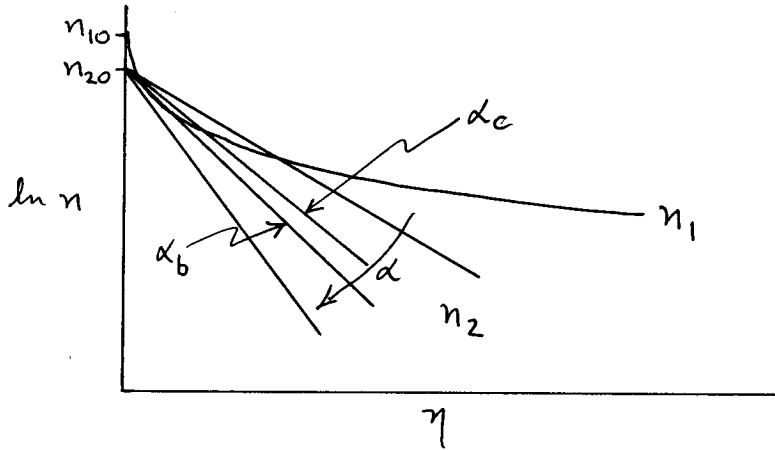


Fig. 2.7

As α is decreased in Fig. 2.7, the line representing n_2 begins to cross n_1 in two places. When the second intersection occurs just when the areas under the two curves are equal, then Eqs. (2.33-11) are satisfied, and we have the critical value of α .

To solve (2.33-11) and (2.33-9), we note that for very small δ the value of η which satisfies (2.33-11) must be small, as is apparent from Fig. 2.7. We may then expand (2.33-9), keeping only terms of order $\eta^{1/2}$. The expansion in half powers converges slowly, so we are depending on the fact that δ is ordinarily extremely small (less than 1%). We also make the approximation that the value of α_c will be close to the value α_b at which the curves $n_1(\eta)$ and $n_2(\eta)$ are tangent to each other. To find α_b we need only to solve the equations

$$n_1 = n_2, \quad n_1' = n_2', \quad \text{or}$$

$$\begin{aligned} e^{\eta} (1 - \text{erf} \sqrt{\eta}) &= (1 - \delta) e^{-\alpha \eta} \\ e^{\eta} (1 - \text{erf} \sqrt{\eta}) &= (1 - \delta) (-\alpha) e^{-\alpha \eta} + \frac{1}{\sqrt{\pi}} \eta^{-1/2}. \end{aligned} \quad (2.33-12)$$

Subtracting and expanding in $x = \eta^{1/2}$, we have

$$0 = (1 - \delta)(1 + \alpha)e^{-\alpha\eta} - \frac{1}{\sqrt{\pi}} x^{-1}$$

$$1 \cong \pi^{1/2}(1 - \delta)(1 + \alpha)x(1 - \alpha x^2)$$

$$x \cong [\pi^{1/2}(1 - \delta)(1 + \alpha)]^{-1} \quad . \quad (2.33-13)$$

From (2.33-12a), we have to this order, since $\text{erf } x \cong \frac{2}{\sqrt{\pi}} x$,

$$1 - \frac{2}{\sqrt{\pi}} x \cong 1 - \delta, \quad \text{or} \quad x \cong \frac{\sqrt{\pi}}{2} \delta \quad . \quad (2.33-14)$$

Combining the last two equations, we have finally

$$\frac{\pi}{2} \delta (1 - \delta)(1 + \alpha) = 1$$

$$1 \cong \frac{\pi}{2} \delta (1 + \alpha)$$

$$\alpha_b \cong \frac{2}{\pi\delta} - 1 \cong \frac{2}{\pi\delta} \cong \alpha_c \quad (2.33-15)$$

$$\alpha > \alpha_c$$

The maximum value of δ is given by (2.32-2), in which the Debye length \underline{h} must be evaluated with T_2 , the temperature of the particle in equilibrium. Thus for acceleration of a species with temperature T_1 and no drift velocity, we must have

$$\alpha = \frac{T_1}{T_2} > \frac{\lambda^2}{\pi h_2^2} \quad . \quad (2.33-16)$$

This is a severe condition which is rarely satisfied. This does, however, bear out the previously mentioned fact that the nature of the sheath problem is different when $T_1 \gg T_2$ than when $T_2 \gg T_1$.

2.34 The Case $T_1 \neq 0, u_o \neq 0$

When the collected particle is allowed to have a drift velocity $v_t u_o$ at plane A toward plane B, the condition on α given by (2.33-16) is greatly mollified. In this case the distribution function is

$$f_1(\eta, u) = \frac{2n_{1o}}{1 + \operatorname{erf} u_o} \frac{1}{\sqrt{\pi} v_t} e^{-[(u^2 - \eta)^{1/2} - u_o]^2} \quad (2.34-1)$$

Unfortunately the density cannot be expressed in closed form, so that the general solution must be obtained numerically. We shall not do this, but it is clear that the answer will give a relation which α and u_o must satisfy for each value of δ . Since the maximum value of δ is fixed by the ratio λ/h_2 , one has a criterion in which either the temperature T_1 or the drift velocity u_o must be sufficiently large in order for a monotonic solution of Poisson's equation to exist.

When the hotter species is collected, the drift velocity necessary to satisfy the sheath criterion is usually small compared with the thermal velocity; this does not seem hard to attain. However, when the colder species is collected, as in the collection of cold ions, the drift velocity is many times the thermal velocity of the ions, and some mechanism must exist in the plasma region to produce this directed motion.

We have so far assumed that the wall potential η_w at plane B was so high

that none of species 2 is collected. For lower values of η_w a correction can be made to the Maxwellian distribution so that the density reads

$$n_2 = \frac{n_{20}}{2} e^{\alpha\eta} [1 + \operatorname{erf} \alpha^{1/2} (\eta_w - \eta)^{1/2}] \quad . \quad (2.34-2)$$

This is obtained from (2.33-2) by omitting the particles traveling to the left with velocities greater than $\eta_w^{1/2}$. If η_w becomes as small as 3, say, the distribution is no longer approximately Maxwellian and is governed by how the particles are produced in the plasma region. In such a case there is no clear separation of the sheath problem from the description of the entire discharge.

We have also found that in the case $T_1 = 0$ the sheath criterion is the same as the condition $n_1'(\eta) = n_2'(\eta)$. We shall make use of this later in connection with double sheaths.

2.4 The Collisionless Plane Discharge

We have seen that in order for a sheath to form when the collected particles are cold they must have a large drift velocity by the time they enter the collision-free region. This drift velocity is most easily acquired by falling through a potential drop in the plasma or transition region. However, we have seen in Sec. 2.1 that potential drops large compared with the temperature of the colder species cannot occur in a plasma in equilibrium except near a boundary. The reason that such potential drops can and do exist in plasmas is due to the fact that the ions are usually not in equilibrium. They are continuously being created by the ionization mechanism and are relatively slow moving, so that their density distribution is dictated by the ionization and not by the

Maxwell-Boltzmann law. In such a case we can have a steady-state situation which is not in equilibrium. To demonstrate how ionization can produce large potential drops in the plasma, we shall next consider the simple case of a plane parallel discharge in which the ions do not make any collisions. Langmuir and Tonks [1961, V] have considered the general case where there are collisions; however, the collisionless case is particularly simple because an analytic solution has been given by Harrison and Thompson [1959].

Imagine that a plasma is created between two infinitely large parallel plates separated by $2L$. The ionization function is $q(x)$ ion pairs per cm^3 per sec, where x is the distance from the mid-plane. The ionization is produced by some such mechanism as ultraviolet radiation which has no other effects. The ions fall freely to the wall from rest under the influence of an electric field. The ion density at x is then given by

$$n_i(x) = \int_0^x \frac{q(x') dx'}{v(x, x')} \quad , \quad (2.4-1)$$

where

$$v(x, x') = \left[\frac{2e}{M} (V(x') - V(x)) \right]^{1/2} \quad , \quad (2.4-2)$$

V being 0 at the mid-plane and negative elsewhere.

In addition to the usual dimensionless quantities

$$\begin{aligned} \eta &= -eV/kT_e \\ u &= v/v_s & v_s &= (2kT_e/M)^{1/2} \\ \xi &= x/h & h^2 &= kT_e/4\pi n_0 e^2 \quad , \end{aligned} \quad (2.4-3)$$

we also have

$$g = qh/n_0 v_s \quad .$$

Here M is the ion mass, kT_e the electron temperature, $+e$ the ion charge, and n_0 the plasma density at the mid-plane.

In terms of these variables, Poisson's equation becomes, as a consequence of (2.4-1) and (2.4-2),

$$\frac{d^2 \eta}{d\xi^2} = \int_0^\eta \frac{g(\eta') \frac{d\xi}{d\eta'} d\eta'}{(\eta - \eta')^{1/2}} - e^{-\eta} \quad (2.4-4)$$

if the electron distribution is Maxwellian. If we assume $d^2 \eta / d\xi^2 = 0$, the resulting integral equation for η can fortunately be inverted by a standard formula; the result is

$$\pi g(\eta) \frac{d\xi}{d\eta} = \eta^{-1/2} - 2F(\eta^{1/2}) \quad , \quad (2.4-5)$$

where

$$F(x) = e^{-x^2} \int_0^x e^{t^2} dt \quad . \quad (2.4-6)$$

The function F is small at both large and small x and has a single maximum, at which it has the value $(2x)^{-1}$. Thus at a critical value of η equal to 0.854, the right-hand side of (2.4-5) vanishes, so that $d\eta/d\xi \rightarrow \infty$. The $\eta - \xi$ curve looks as follows (Fig. 2.8):

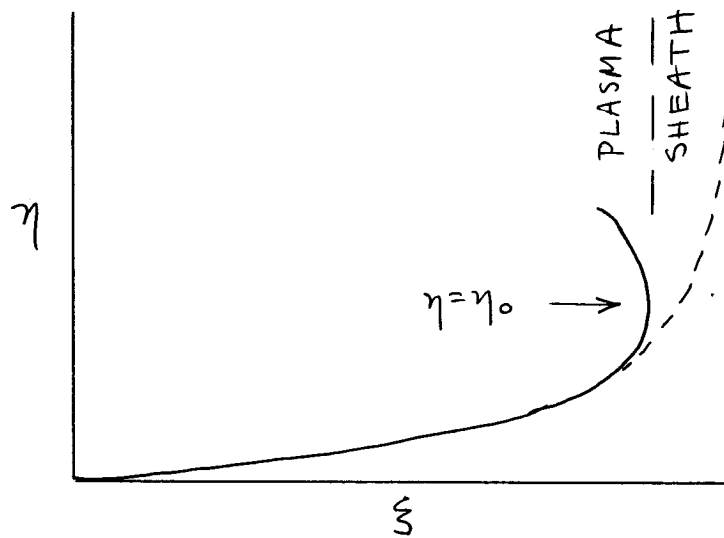


Fig. 2.8

The quasi-neutral approximation ($d^2\eta/d\xi^2 = 0$) that we have made therefore breaks down in the neighborhood of $\eta = 0.854$, and this point is quite independent of the function $g(\eta)$ although the shape of the $\eta - \xi$ curve of course is not. This point ($\eta_0 = 0.854$) can conveniently be defined as the sheath edge, since it is the point where the plasma equation breaks down. The sheath solution (dotted line) will presumably join smoothly on to the plasma solution.

The point to note is that at this junction the ions already have energies up to $0.854 kT_e$ as a consequence of the potential drop in the plasma. The square of the average ion velocity at $\eta = 0.854$ turns out to be $(\bar{u}_0)^2 = 0.654$, as compared to 0.5 previously computed (2.31-10) for mono-energetic ions. Of course at the point the sheath solution takes over, $\eta < 0.854$ and \bar{u}_0 is somewhat less; this is counterbalanced by the fact that the values of η' and η'' (greatly exaggerated in Fig. 2.8) are not 0 at this point, so the sheath criterion is somewhat less stringent. When all these effects are put together, the result is that the ions have just enough energy to allow a sheath solution to exist. This energy is

acquired from electric fields in the plasma, and these fields can exist in the plasma because of the non-thermal effects of the ionization process, which puts ions in places where they would not be in equilibrium.

2.5 Sheath Stability

In the case of cold ion collection by a wall or probe, we have seen that the sheath criterion requires that the ions have a comparatively large directed velocity toward the boundary. On the other hand, we know that double-peaked velocity distributions such as this (the ion and electron peaks being non-coincident) may be unstable against excitation of waves. In fact, the velocity (2.31-10) is just the critical velocity for excitation of ion waves when $kT_i = 0$. The question is, then, is it possible for sheaths to form without oscillations, and for us to consider only the time-independent sheath equations, as we have done? This question is difficult to answer in general because it is difficult to calculate the ion velocity distribution which would actually exist. However, in the simple collisionless case considered in Sec. 2.4, this distribution turns out to be independent of the ionization function $q(x)$ and is therefore easy to find. The result is that unless $q(x)$ completely vanishes in the sheath, the situation is stable; and our failure to consider time-dependent solutions is justified, at least in the case considered.

When a magnetic field is present, other instabilities can occur. In particular, D'Angelo and Motley of this Laboratory have recently discovered that ion waves near the cyclotron frequency propagating almost perpendicular to B can be excited by quite a small relative drift between electrons and ions.

Therefore the sheath on a wall intersecting lines of force may be unstable. This question has not been thoroughly investigated.

2.6 Effect of Magnetic Field

The mechanism of sheath formation in the presence of a strong magnetic field has not been analyzed in detail in the literature. Recently, however, there have been a few papers concerned with the effect on a sheath of a weak magnetic field, which affects the motions of the electrons only. [Allen and Magistrelli, *Nuovo Cim.* 18, 1138 (1960); P. L. Auer, *Nuovo Cim.* 22, 550 (1961)]. The result is that the critical ion energy u_o^2 for sheath formation should be divided by a factor $1 + \alpha$, where α is the ratio of the electron drift velocity parallel to the wall to the $E \times B$ drift velocity. The effect of the self-magnetic field of a discharge (that caused by the discharge current) is in a direction to make the sheath criterion less stringent.

2.7 Sheaths in More Than One Dimension

The case of emission by spherically and axially symmetric surfaces in the absence of a plasma has been calculated by Langmuir [1961, III and IV]. The plasma solution for a discharge in such geometries has been given by Tonks and Langmuir [1961, V]. There is no qualitative difference from the results of the one-dimensional analysis.

The situation is different in the case of the sheath criterion. If, on the one hand, the sheath were thin compared with the radius of curvature of the surface, one would expect that the one-dimensional sheath criterion need only be slightly modified. On the other hand, if the sheath edge were many radii of

curvature away from the electrode in question, the concept of a sheath criterion is of doubtful value. This is because the density at each point consists both of particles going toward the electrode (in the case, say, of ion collection by a small sphere) and of particles coming away from the probe. The existence of the latter current is possible because particles with finite angular momentum can make an orbit around the probe and miss it. The calculation of the ion density therefore is no simple problem.

Even the case of $T_1 = 0$, $u_0 = 0$ is soluble in the spherically symmetric case. In the plane case the density goes as $\eta^{-1/2}$ and becomes infinite at $\eta = 0$. In the spherical case, however, there is a factor $(4\pi r^2)^{-1}$ in the density which can cancel this divergence and give $n_1 = n_2$ at infinity. Moreover, if ions, say, start at rest at infinity and the total inward current is I , then the ion density will be proportional to $r^{-2} \eta^{-1/2}$. If η falls off as r^{-4} for large r , then n_i is a constant at large r . Since $n_e \sim e^{-\eta}$, the requirement that $n_i \geq n_e$ is satisfied even though the ion temperature is zero. This is greatly different from the plane case. We shall treat this problem in detail in the section on saturation ion currents.

3. Probe Theory in the Absence of Collisions and Magnetic Fields

The information obtainable from a probe is contained in the probe characteristic (Fig. 1.1). The plasma parameters which one hopes to determine are the electron and ion temperatures kT_e and kT_i , the plasma density n , and the plasma potential V_s . The probe characteristic consists of four main

parts: the saturation electron current (A), the transition region (B), the floating potential V_f , and the saturation ion current (C). In simplest terms, part A gives information about $n\sqrt{T_e}$; part B gives T_e ; part C gives $n\sqrt{T_e}$ again; V_s is obtainable from either V_f or the point at which B changes to A; and the ion temperature is not given by probes. The exact way in which these plasma parameters are related to the probe characteristic will depend on the shape of the probe and the relative magnitudes of the collision length, the probe dimensions, the Debye length, the Larmor radius, and so forth.

We shall discuss first the simplest case -- that in which both collisions and magnetic fields are negligible. This case is essentially that covered by the original theory of Langmuir. There is, however, one exception; that is, in dealing with saturation ion current the effect of acceleration of ions in the plasma region (which we discussed in connection with the sheath criterion) was at first unknown to Langmuir. For the proper treatment of ion saturation current we shall have to turn to comparatively recent work. We shall confine ourselves to plasmas consisting of singly charged positive ions and electrons. Extensions of the theory to include negative ions or multiply charged ions is straightforward. The main difference from the analysis of Sec. 2 is that now we shall have to consider particle orbits in more than one dimension.

3.1 Probe Current in a Prescribed Electric Field

We now turn to the problem of sheath formation on actual probes, which are normally not planar but cylindrical or spherical, since such shapes do not disturb the plasma as much as a large flat surface. Particles can now move in

orbits in a central force field, and the density is no longer a simple function of potential as it was in the one-dimensional case. Again we have Poisson's equation

$$\nabla^2 V = -4\pi(q_1 n_1 + q_2 n_2) \quad ,$$

but now not only is the Laplacian more complicated but also n_1 is a complicated integral involving V . The solution for V must even in the simplest case be found numerically. However, in some physical situations the probe current can be found without knowing the exact behavior of $V(\underline{r})$. In these situations the original theory of Langmuir is applicable. In describing this theory we shall assume that the function $V(\underline{r})$ is already known.

3.11 Thin Sheath: Space Charge Limited Current

Suppose that the prescribed electric field is such that the potential drop around a charged spherical or cylindrical probe attracting particles of type 1 is concentrated in a thin layer of radius \underline{s} surrounding the probe of radius \underline{a} . Suppose further that the velocity distribution is essentially Maxwellian at the edge of the sheath. This situation applies, for instance, to part A of the probe characteristic (saturation electron current), since in most plasmas $T_e \gg T_i$, and we have seen in Sec. 2.3 that the collection of the hotter species does not require a large drift velocity at the sheath edge. If $s - a \ll a$ so that all particles entering the sheath hit the probe, and if the probe is perfectly absorbing, then the probe current is simply

$$I = j_r A_s \quad (3.11-1)$$

where A_s is the area of the sheath, and j_r is the random current density

crossing a unit area in one direction. For a Maxwellian distribution, this is given by

$$j_r = \frac{1}{4} n \bar{v} = \frac{1}{2} n \left(\frac{2kT}{\pi m} \right)^{1/2} \quad (3.11-2)$$

We have omitted the charge e_1 and are therefore considering particle currents. The factor $1/4$ in j_r is composed of two factors of $1/2$. The first accounts for the fact that at the sheath edge the density is half the plasma density -- the half consisting of particles heading toward the probe. The second factor of $1/2$ is merely the average of the direction cosine over a hemisphere. To the extent that $s - a \ll a$, A_s is equal to A_p , the probe area; and the current is independent of voltage in this limit.

The physical situation is clarified by Fig. 3.1.

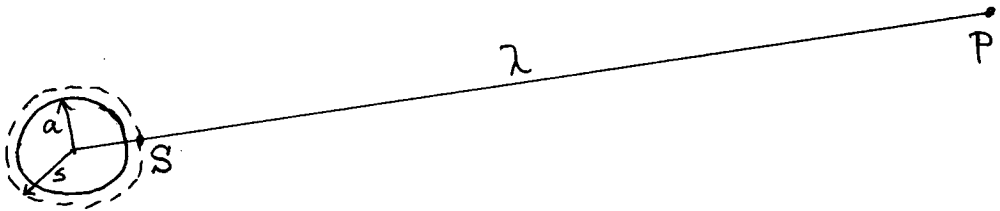


Fig. 3.1

The collision mean free path λ is assumed to be much larger than s or a . The population at point P consists of particles which made their last collision approximately a distance λ from P . Since the probe subtends only a very small solid angle at P , the shadowing effect of the probe has negligible effect, and the

distribution at P is closely Maxwellian. At point S, however, there can be no particles coming from the probe, and therefore the density must gradually change from n at P to $\frac{1}{2}n$ at S, if there is no ionization anywhere on the diagram. Since the particles of type 2, which are repelled by the probe, are in thermal equilibrium, their density is given by

$$n_2 = n e^{-eV/kT_2} \quad . \quad (3.11-3)$$

By assumption, all electric fields are concentrated within the sheath. However, in order to satisfy (3.11-3) and quasi-neutrality at S, we must have

$$\frac{e_2 V_s}{kT_2} = \ln 2 \quad , \quad (3.11-4)$$

the potential at ∞ being 0. Our initial prescription for $V(\underline{r})$ can be approximately true in practice only if kT_2 is very small. This is the reason this theory can be used for the collection of hot electrons in a gas of cold ions but would not be nearly correct in the case of cold ion collection.

Although we have considered the potential distribution and hence the sheath thickness $s - a$ to be prescribed, this is sometimes not necessary. In mercury discharges of the type used by Langmuir, the sheath was visible, and its thickness could be measured, so that a measured value of A_s could be used in (3.11-1). Even if A_s cannot be measured, it can be calculated from the space charge equations. If we neglect the density of particles 2 in the sheath, the problem is the same as one we have already considered in Sec. 2.21: that of space charge limited emission from a plane A (the sheath edge) to a plane B (the

probe surface). Thus the current density is given by Eq. (2.21-8):

$$j = \left(\frac{2}{em}\right)^{1/2} \frac{1}{9\pi} \frac{|V_p - V_s|^{3/2}}{(s-a)^2} \left(1 + \frac{2.66}{\sqrt{\eta}}\right), \quad (3.11-5)$$

where $\eta = |e(V_p - V_s)/kT_1|$. If $V_s = 0$, j can be equated to j_r to give a value of the sheath thickness $s - a$; this can then be used to compute A_s .

If $s - a$ were not infinitely small, the equation for planar geometry could not be used. Instead, the corresponding space charge equations for cylinders and spheres must be used. These are given by Langmuir [1961, III]:

$$\text{Cylinder:} \quad j = \frac{1}{9\pi} \left(\frac{2}{em}\right)^{1/2} \frac{|V_p - V_s|^{3/2}}{a^2 \beta^2} \left(1 + \frac{2.66}{\sqrt{\eta}}\right) \quad (3.11-6)$$

$$\text{Sphere:} \quad j = \frac{1}{9\pi} \left(\frac{2}{em}\right)^{1/2} \frac{|V_p - V_s|^{3/2}}{a^2 \alpha^2} \left(1 + \frac{2.66}{\sqrt{\eta}}\right), \quad (3.11-7)$$

where

$$\beta = \gamma - 0.4\gamma^2 + \dots$$

$$\alpha^2 = \gamma^2 - 0.6\gamma^3 + \dots$$

and

$$\gamma = \ln \frac{a}{s}.$$

When $s - a \ll a$, one can expand the logarithm and recover (3.11-5).

3.12 Thick Sheath: Orbital Motions

In the opposite limit of a thick sheath ($s \gg a$), not all particles entering the sheath will hit the probe because of the possibility of orbital motions. If the potential varies slowly enough (a condition we shall derive later), the probe current is still independent of the exact shape of $V(\underline{r})$. This is because the laws of conservation of energy and angular momentum concern only the initial and final values of the energy and angular momentum.

Consider the orbit of a particle in an attractive central force field. Let its initial velocity be v_o and impact parameter, p . At its point of closest approach to the center (in either a spherically or a cylindrically symmetric system), let its velocity be v_a and its radius \underline{a} . Then the conservation laws state (for $eV < 0$):

$$\frac{1}{2} m v_o^2 = \frac{1}{2} m v_a^2 + eV \quad (3.12-1)$$

$$p v_o = a v_a \quad (3.12-2)$$

Solving for p , we have

$$p = a \left(1 + \frac{V}{V_o} \right)^{1/2}, \quad (3.12-3)$$

where $-eV_o = \frac{1}{2} m v_o^2$. If we identify \underline{a} with the probe radius, we see that any particle with \underline{p} smaller than that given by (3.12-3) will hit the probe and be collected. Hence the effective collecting radius of the probe is the larger value \underline{p} , and this is independent of the shape of the potential distribution. It is clear, therefore, that for a mono-energetic beam of particles, or for an isotropic dis-

tribution of mono-energetic particles at infinity, the probe current is given by:

$$\text{Cylinder:} \quad I = 2\pi r^a \ell j_r \left(1 + \frac{V}{V_0}\right)^{1/2} \quad (3.12-4)$$

$$\text{Sphere:} \quad I = 4\pi r^2 j_r \left(1 + \frac{V}{V_0}\right) \quad (3.12-5)$$

Thus for a cylindrical probe the saturation electron current increases with the square root of the probe voltage. The current is limited by the impact parameter p and not by the sheath size, which can be infinitely large.

So far we have considered mono-energetic particles coming in from infinity. To do the more general problem we must take into account the finite size of the sheath and also the distribution of energies at the sheath edge. Again we shall presuppose that the potential distribution is known and that the entire potential drop occurs within a sphere or cylinder of radius s . Let eV be negative (attractive probe), and let u and v denote the radial and tangential components of velocity. Conservation of energy and angular momentum imposes the following relations between quantities at the sheath edge ($r = s$) and at the probe ($r = a$):

$$u_s^2 + v_s^2 = u_a^2 + v_a^2 + \frac{2eV_a}{m} \quad (3.12-6)$$

$$s v_s = a v_a \quad .$$

Solving for u_a , we have

$$u_a^2 = u_s^2 + v_s^2 \left(1 - \frac{s^2}{a^2}\right) - \frac{2eV_a}{m} \quad (3.12-7)$$

A necessary condition for a particle to hit the probe is that $u_a^2 \geq 0$. This is not a sufficient condition, since u^2 must not vanish anywhere between s and a; sufficiency will be discussed in the next section. This condition then imposes limits on the value of v_s :

$$v_s^2 \leq \left(u_s^2 - \frac{2eV_a}{m} \right) \left(\frac{s^2}{a^2} - 1 \right)^{-1} \equiv v_s^{*2} \quad (3.12-8)$$

This argument clearly holds for both cylinders and spheres. If $f(u, v)$ is the distribution function at s, the current to a cylindrical probe is obviously the sheath area times the integral of $uf(u, v)$ taken over all u from 0 to ∞ and over all v from $-v_s^*$ to $+v_s^*$:

$$j = n \int_0^{\infty} du u \int_{-v_s^*}^{+v_s^*} f(u, v) dv \quad (3.12-9)$$

$$I = A_s j \quad (3.12-10)$$

where we have suppressed the subscript s.

Of particular interest is Maxwell's distribution in two dimensions:

$$f(u, v) = \left(\frac{m}{2\pi kT} \right) e^{-m(u^2 + v^2)/2kT} \quad (3.12-11)$$

The integration of (3.12-9) using this distribution and Eq. (3.12-8) is straightforward and analytic. The answer is given by Langmuir [1961, IV]; the answer for the equation analogous to (3.12-9) for spheres is also given:

$$I = A_a j_r F \quad (3.12-12)$$

$$\text{Cylinder:} \quad F = \frac{s}{a} \operatorname{erf} \Phi^{1/2} + e^\eta [1 - \operatorname{erf}(\eta + \Phi)^{1/2}] \quad (3.12-13)$$

$$\text{Sphere:} \quad F = \frac{s^2}{a^2} [1 - e^{-\Phi}] + e^{-\Phi} \quad , \quad (3.12-14)$$

where

$$\eta = - \frac{eV}{kT} \quad (3.12-15)$$

$$\Phi = \frac{a^2}{s^2 - a^2} \eta^2 \quad (3.12-16)$$

$$\eta + \Phi = \frac{s^2}{s^2 - a^2} \eta^2 \quad (3.12-17)$$

and j_r and $\operatorname{erf} x$ are given by (3.11-2) and (2.21-5), respectively.

We note two limiting cases: $s - a \ll a$ and $s \gg a$. In the thin sheath limit, the arguments of the error functions are large, and we can use the approximation

$$1 - \operatorname{erf} x \approx \frac{1}{\sqrt{\pi}} \frac{e^{-x^2}}{x} \quad (3.12-18)$$

3.12-13

When this is inserted into ~~(3.11-20)~~, the result is $F = s/a$, and we recover

Eq. (3.11-1), as expected. Similarly, for large Φ we can neglect the exponentials in (3.12-14) and recover Eq. (3.11-1) for spheres.

Schulz & Brown
determine s from
sp. ch. eqn. as on p. 37

In the thick sheath limit, Φ is small, and we can neglect it relative to η .

The error function for small x is given by

$$\operatorname{erf} x \approx \frac{2}{\sqrt{\pi}} x, \quad (3.12-19)$$

and the exponential $e^{-\Phi}$ by $1 - \Phi$. Thus (3.12-13) and (3.12-14) become:

$$\text{Cylinder:} \quad F \cong \frac{2}{\sqrt{\pi}} \eta^{1/2} + e^{-\eta} (1 - \operatorname{erf} \eta^{1/2}), \quad (3.12-20)$$

$$\text{Sphere:} \quad F \cong \eta + 1. \quad (3.12-21)$$

If, in addition, $\eta \gg 1$, (3.12-20) and (3.12-18) yield

$$\text{Cylinder:} \quad F \cong \frac{2}{\sqrt{\pi}} (\eta^{1/2} + \frac{1}{2} \eta^{-1/2}) \cong \frac{2}{\sqrt{\pi}} (\eta + 1)^{1/2}. \quad (3.12-22)$$

Thus for large sheath radii I varies as V for spheres, in agreement with (3.12-5), while I varies as $V^{1/2}$ for cylinders, in agreement with (3.12-4). The latter is true only if $\eta \gg 1$ as well.

Equation (3.12-22) suggests that the slope of the electron saturation current as well as its absolute magnitude may be a useful datum. From (3.12-12) we have

$$I = A_a j_r \frac{2}{\sqrt{\pi}} (\eta + 1)^{1/2}$$

$$I^2 = \frac{4}{\pi} A_a^2 j_r^2 (\eta + 1). \quad (3.12-23)$$

Thus if I^2 is plotted against V_a , there should be a linear region where the slope is

$$\frac{2}{\pi} A_a^2 \frac{e}{m} n^2, \quad (3.12-24)$$

giving a value for n . The intercept of this line at $I = 0$ gives the value of e/kT . When such a linear plot of I^2 vs. V can be obtained, therefore, the density and electron temperature can be obtained separately, rather than in combination, as in Eq. (3.12-12).

In the weakly ionized plasmas investigated by Langmuir, it was actually possible to get a good linear plot of I^2 vs. V with cylindrical probes. This deviated from linearity at small V , where the approximation (3.12-22) becomes invalid, and at large V , where space charge limitation requires the use of (3.11-1). The use of Eq. (3.12-21) with spherical probes, however, turned out to be nearly impossible, since with actual probe sizes the condition $s \gg a$ could not be fulfilled; instead, spherical probes tended to draw space charge limited current.

Langmuir has also given approximate formulas for the very complicated case of a Maxwellian distribution with a superimposed drift [1961, IV].

3.13 Range of Validity of Orbital Theory

Aside from the requirements $\lambda \gg s$ and $\lambda \gg a$, the collisionless theory described above is subject to a requirement on the potential shape. This can be seen by imagining a potential which extends far from the probe ($s \gg a$) but which has most of the drop occurring in a thin layer around the probe. In

such a case one would use the formula for the case $s \gg a$, but obviously the true answer cannot differ much from that given by the formula for $s - a \ll a$. Such a potential has an "absorption radius" larger than \underline{a} which gives the effective collecting area inasmuch as all particles entering the surface at $r \gtrsim a$ are destined to hit the probe. The condition that no such absorption radius exists will now be derived.

From (3.12-7) we have the following expression for the radial velocity of a particle at the probe in terms of its initial velocity components:

$$u_a^2 = u_s^2 + v_s^2 \left(1 - \frac{s^2}{a^2}\right) + \phi_a \quad , \quad (3.13-1)$$

where we have let

$$\phi = -\frac{2eV}{m} \geq 0 \quad . \quad (3.13-2)$$

If $u_a^2 \geq 0$, the particle will hit the probe, provided that it is not repelled at some larger radius \underline{r} . The most stringent condition on ϕ is that even those particles barely able to reach the probe ($u_a = 0$) are not turned around at a larger radius \underline{r} . If they were turned around, all those which get past \underline{r} would strike the probe; and \underline{r} would be an absorption radius.

To get the most stringent condition on ϕ , we consider those particles with $u_a = 0$, for which

$$u_s^2 = v_s^2 \left(\frac{s^2}{a^2} - 1\right) - \phi_a \quad . \quad (3.13-3)$$

At any radius $r > a$, their radial velocity is given by

$$u_r^2 = u_s^2 + v_s^2 \left(1 - \frac{s^2}{r^2}\right) + \phi_r \quad (3.13-4)$$

in analogy to (3.13-1). Eliminating v_s^2 between the last two equations, we have

$$\begin{aligned} u_r^2 &= u_s^2 + \phi_r + \left(1 - \frac{s^2}{r^2}\right) \frac{u_s^2 + \phi_a}{(s^2/a^2) - 1} \\ &= \phi_r + u_s^2 \left[1 - \frac{a^2}{r^2} \frac{s^2 - r^2}{s^2 - a^2}\right] - \phi_a \left[\frac{a^2}{r^2} \frac{s^2 - r^2}{s^2 - a^2}\right] \quad (3.13-5) \end{aligned}$$

The condition that $u_r^2 > 0$ then gives this condition on ϕ_r :

$$\phi_r > g \phi_a - (1 - g)u_s^2 \quad , \quad (3.13-6)$$

where

$$g(r) = \frac{a^2}{r^2} \frac{s^2 - r^2}{s^2 - a^2} \quad . \quad (3.13-7)$$

If the initial distribution at \underline{s} includes particles with $u_s^2 = 0$, ϕ_r must satisfy the condition

$$\phi_r > g \phi_a \quad . \quad (3.13-8)$$

The meaning of this can be seen by letting \underline{s} approach infinity. Then the potential falls less rapidly than $1/r^2$:

$$s \rightarrow \infty: \quad \frac{\phi_r}{\phi_a} > \frac{a^2}{r^2} \quad . \quad (3.13-9)$$

This is a rather gradual variation with \underline{r} . This condition is not satisfied in a dense plasma, where the Debye length is small. Then the potential must drop abruptly from ϕ_a and hence fall below the $1/r^2$ curve.

Of course if an absorption radius exists this can be called the sheath edge, and the theory would then apply. However, in this case the velocity distribution at the sheath edge is unknown and must be calculated. This is essentially the problem we shall consider in Sec. 3.3. The potential may also be such that there are closed orbits within $r = s$. The population in these orbits would then depend on collisions, and the problem would no longer be tractable. This possibility is also considered in Sec. 3.3 on ion currents.

3.14 Summary of Langmuir's Theory

This theory applies when a) the hotter component of the plasma (usually electrons) is collected, so that the distribution at the sheath edge is approximately Maxwellian; b) the pressure in the discharge is low enough that the mean free path is much larger than the probe or sheath dimensions; and c) the plasma density or the probe potential is low enough that the potential distribution satisfies (3.13-8). The probe current is then independent of the exact shape of the potential.

When the sheath is thin compared to the probe radius, the current is limited by space charge and is given by (3.11-1). In this case the current varies with voltage only inasmuch as the sheath area changes; this change is given by (3.11-5, 6, 7). The saturation electron current magnitude then gives a value for $n(kT_e)^{1/2}$.

When the sheath is thick compared with the probe radius, the current is limited by orbital motions and is given approximately by (3.12-4, 5), or, more exactly, by (3.12-20, 21, 22). With intermediate sheath thicknesses, the current is always less than the smaller of (3.11-1) and (3.12-4, 5), and is given exactly by (3.12-12 to 17). In the thick sheath limit, part A of the probe characteristic appears as follows for different probe shapes (Fig. 3.2):

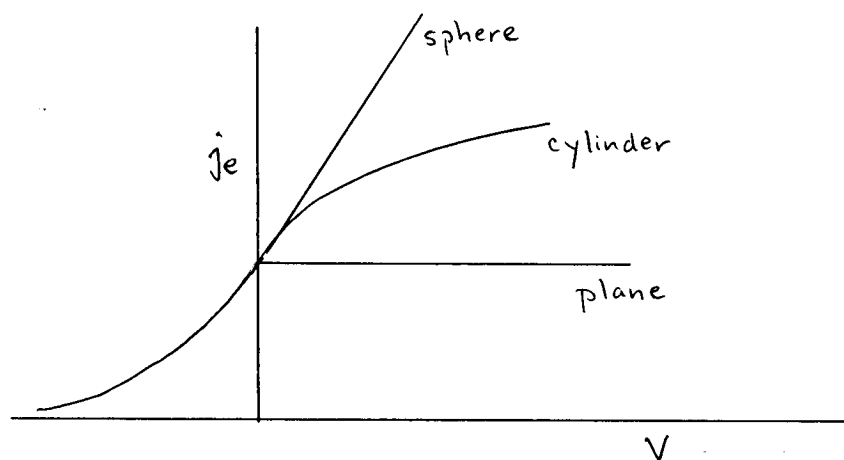


Fig. 3.2

The saturation electron current varies with V for spheres and as $V^{1/2}$ for cylinders; it does not change for planes since no orbits are possible and the sheath area is constant.

When the probe potential is increased in practice from $V = V_s$, there is at first a region in which the current is smaller than the space charge limited value and the orbital equations apply. For cylinders, Eq. (3.12-20) gives the current at small η ; for larger η , (3.12-22) applies, and the current varies as $\eta^{1/2}$. As η is further increased, space charge limitation sets in and either

(3.12-12 ff.) or (3.11-1) applies, depending on the probe size. The point of transition, which depends on s/a , moves to lower η as \underline{a} is increased or \underline{n} is increased. Thus the behavior shown in Fig. 3.2 does not appear except for very small probes and very small densities. For spheres (3.11-1) almost always applies since the transition occurs for very small η .

When a linear region on an $i^2 - V$ plot appears, one is fortunate to be able to calculate the density and the temperature separately from the slope and the intercept of the line -- Eqs. (3.12-23, 24).

As the voltage η is increased further, the sheath can ~~again~~ grow until again the equations for $s \gg a$ apply. However, now the condition (3.13-8) will probably be violated.

In most plasmas of today the Debye length is so small and the probe radius so large (so that the probe will not melt) that the Langmuir theory is useless, and the single formula (3.11-1) suffices to describe saturation electron current. Moreover, electron collection can seldom be used at all because the large currents involved seriously affect the plasma being measured.

3.2 The Transition Region

In region B of the probe characteristic the probe collects both ions and electrons. Fortunately, the ion current is much smaller than the electron current, because of the disparity in mass, and it can be subtracted out even if not accurately known. The probe, then, collects electrons moving against a repelling field. The current can be computed with the same formulas used in the section on orbital motions, but with $eV > 0$; however, for a Maxwellian

distribution the answer is the same regardless of the sheath and probe sizes and even the shape of the probe.

3.21 Maxwellian Distribution

Suppose the probe is charged negative to repel electrons and that it is perfectly reflecting. If the electron distribution is in thermal equilibrium, we know that the density follows the Boltzmann law

$$n = n_o e^{-\eta} \quad , \quad (3.21-1)$$

and that the distribution is still Maxwellian everywhere; only the density is changed by the potential. The random current hitting the probe is then merely

$$I = A_a j_r = A_a n \left(\frac{kT}{2\pi m} \right)^{1/2} \quad , \quad (3.21-2)$$

where n is evaluated at the probe surface. Using (3.21-1),

$$I = A_a n_o \left(\frac{kT}{2\pi m} \right)^{1/2} e^{-\eta} \quad , \quad (3.21-3)$$

where $\eta = |eV/kT|$. Now if the probe is perfectly absorbing, the Maxwellian distribution near the probe is deprived of electrons coming back from the probe. However, the distribution of those going toward the probe, which contribute to the current, is essentially unchanged, since it is determined by collisions far away from the probe, where the population is undisturbed by the presence of the probe. Therefore (3.21-3) is still approximately true for an absorbing probe, especially if η is large, so that the probe draws little current.

If $\ln I$ is plotted against η (or V), Eq. (3.21-3) predicts a straight line if the distribution is Maxwellian. The slope of the line is $|e/kT|$ and gives a

good measure of the electron temperature. In Langmuir's plasmas the $\ln I - V$ plot was linear over a ratio of 1000-1 in current. This was actually better adherence to the exponential law than one had a right to expect.

In the case of two groups of electrons at different temperatures, the $\ln I - V$ plot would be a broken line, as shown in Fig. 3.3.

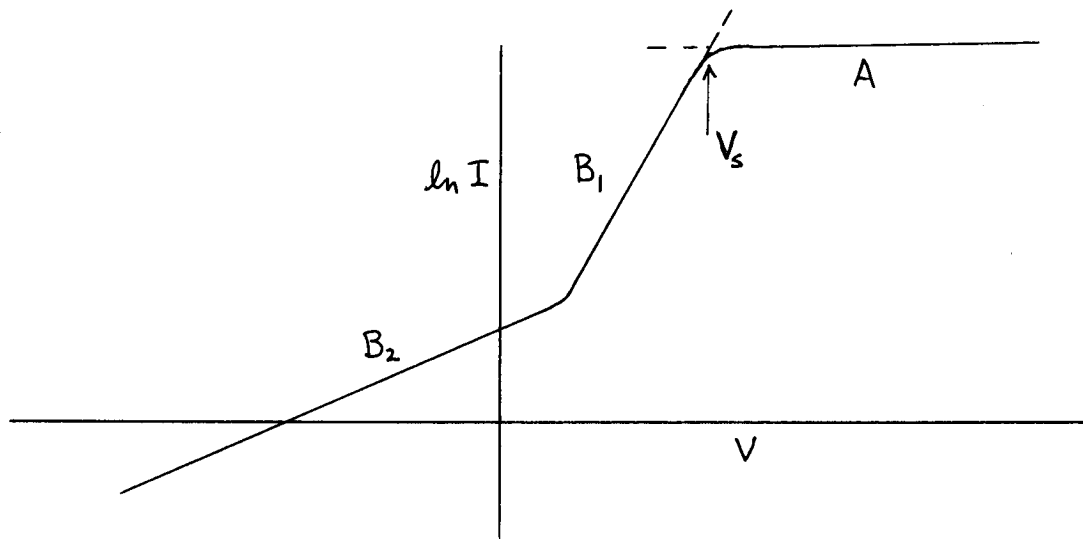


Fig. 3.3

The slopes of the two straight segments would give the temperatures of the two groups.

The space potential is often obtained by extrapolating parts A and B of the probe characteristic and finding the point of intersection; this is also shown in Fig. 3.3.

3.22 Isotropic Distributions

If the velocity distribution of electrons is not Maxwellian but is still isotropic, the shape of the transition region of the probe curve can give informa-

tion about the distribution function. This will be demonstrated for the case of a plane probe.

Let the isotropic distribution be $f(v)$, so that

$$n = \int_0^{\infty} f(v) d^3 v = 4\pi \int_0^{\infty} v^2 f(v) dv \equiv \int_0^{\infty} g(v) dv \quad (3.22-1)$$

Let a plane probe be at potential $-V$, so that electrons are repelled, and let

$$\phi = \left(\frac{-2eV}{m} \right)^{1/2} > 0 \quad (3.22-2)$$

The particle current density moving toward the probe at velocity \underline{v} and at an angle θ relative to the normal is

$$dj = v \cos\theta f(v) d^3 v \quad (3.22-3)$$

For each v , only those electrons with $\theta < \theta^*$ will be energetic enough to strike the probe, where

$$v \cos\theta^* = \phi^{1/2} \quad (3.22-4)$$

The minimum value of \underline{v} is obviously $\phi^{1/2}$. The total current density striking the probe is thus the integral of (3.22-3) over these limits:

$$\begin{aligned} j &= \int_{\phi^{1/2}}^{\infty} v^3 f(v) dv \int_0^{\theta^*} 2\pi \sin\theta \cos\theta d\theta \\ &= \int_{\phi^{1/2}}^{\infty} \frac{1}{2} v g(v) dv \int_0^{\cos\theta^*} -\cos\theta d(\cos\theta) = \int_{\phi^{1/2}}^{\infty} \frac{1}{4} v g(v) dv [\cos^2\theta]_{\cos\theta^*}^0 \end{aligned} \quad (3.22-5)$$

$$j = \frac{1}{4} \int_{\phi^{1/2}}^{\infty} v g(v) \left(1 - \frac{\phi}{v^2}\right) dv \quad . \quad (3.22-6)$$

If we differentiate with respect to ϕ , the integrated part drops out, leaving

$$\frac{dj}{d\phi} = \frac{1}{4} \int_{\phi^{1/2}}^{\infty} \frac{-g(v)}{v} dv \quad .$$

A second differentiation yields

$$\frac{d^2 j}{d\phi^2} = \frac{1}{4} \phi^{-1/2} g(\phi^{1/2}) \frac{1}{2} \phi^{-1/2} = \frac{1}{8} \frac{g(\phi^{1/2})}{\phi} \quad . \quad (3.22-7)$$

Thus the distribution function $g(v)$ is given by

$$g(\phi^{1/2}) = 8\phi j'' \quad . \quad (3.22-8)$$

Similar results have been obtained by Langmuir [1961, IV] for spherical and cylindrical probes.

Since a double differentiation of the probe curve is involved, the curve must be obtained extremely accurately before the distribution function can be found. This requires the plasma to be quiescent. A number of circuits have been given in the literature for performing the double differentiation electrically, by use of an oscillating probe voltage. In any case the accuracy required is such that this technique is not generally useful except in extremely quiescent plasmas.

3.3 Saturation Ion Currents: Unknown Electric Field

In the Langmuir theory it was assumed that the velocity distribution of the collected particles is known at the sheath edge. We have seen, however, in Sec. 2.3 that when the colder species is collected, as is usually the case in dealing with ion currents, the ions must have a drift velocity upon entering the sheath. Therefore, if the sheath edge is taken close to the probe, the ion velocity distribution is unknown. Alternatively, if one takes the sheath edge to be far away, to include the electric fields which impart this drift velocity to the ions, then an absorption radius exists, the condition (3.13-8) is not satisfied, and the Langmuir theory does not apply. This means that the ion current is not independent of the potential shape, and one must actually solve for the potential by using Poisson's equation. Since the ion density term in this equation is a complicated integral involving ion orbits, ^{the solution cannot be given explicitly} ~~this problem cannot be solved analytically~~ even in the simplest case.

In the case of a plane surface, we saw in Sec. 2.4 that the ion drift velocity is acquired in the plasma region, where ion production exists. For spheres and cylinders this is not necessary, and a well-posed problem exists even if one neglects collisions and ionization everywhere. Before tackling the complexities of orbits, we shall examine the simple case of ions starting at rest, so that all motions are radial.

3.31 Zero Temperature Limit

This special case is the theory of Allen, Boyd, and Reynolds [1956] for a spherical probe. Let I be the total ion current; in the absence of collisions

and ionization, I is conserved. If ions start from rest at ∞ , where $V = 0$, their velocity at \underline{r} , where the potential is V , is

$$v_i = \left(-\frac{2eV}{M}\right)^{1/2} = v_s \eta^{1/2}, \quad (3.31-1)$$

where

$$\eta = -eV/kT_e \quad \text{and} \quad v_s = (2kT_e/M)^{1/2}. \quad (3.31-2)$$

The ion density at \underline{r} is given by this velocity, the area, and the current I :

$$n_i = I / (4\pi r^2 v_s \eta^{1/2}). \quad (3.31-3)$$

With n_e given by Maxwell's distribution, Poisson's equation in spherical coordinates is:

$$\frac{1}{r^2} \frac{d}{dr} \left(r^2 \frac{dV}{dr} \right) = -4\pi e \left[\frac{I}{4\pi r^2 v_s \eta^{1/2}} - n_o e^{-\eta} \right]. \quad (3.31-4)$$

Introducing the usual dimensionless length

$$\xi = r/h = r(4\pi n_o e^2/kT_e)^{1/2}, \quad (3.31-5)$$

we can put this in the form
~~this becomes~~

$$\frac{1}{\xi^2} \frac{d}{d\xi} \left(\xi^2 \frac{d\eta}{d\xi} \right) = I(4\pi h^2 n_o v_s \eta^{1/2} \xi^2)^{-1} - e^{-\eta}. \quad (3.31-6)$$

We define a current I_λ such that

$$I_\lambda = 4\pi h^2 n_o v_s = (kT_e)^{3/2} (2/Me^4)^{1/2}. \quad (3.31-7)$$

From its form it is easy to see that I_λ is the random ion current crossing a Debye sphere, if the ions had the temperature of the electrons. Poisson's equation is, finally,

$$\left(\frac{d^2 \eta}{d\xi^2} + \frac{2}{\xi} \frac{d\eta}{d\xi} + e^{-\eta} \right) \eta^{1/2} \xi^2 = \frac{I}{I_\lambda} \quad (3.31-8)$$

An approximate solution of this can be obtained by defining a sheath edge.

The quasi-neutral equation, which obtains in the plasma region, is

$$\eta^{1/2} e^{-\eta} = \frac{I}{I_\lambda} \xi^{-2} \quad (3.31-9)$$

Differentiating this, we have

$$e^{-\eta} \left(\frac{1}{2} \eta^{-1/2} - \eta^{1/2} \right) \frac{d\eta}{d\xi} = \frac{-2I}{I_\lambda} \xi^{-3} \quad (3.31-10)$$

From this, we see that the coefficient of $d\eta/d\xi$ vanishes at $\eta = 1/2$, so that $d\eta/d\xi$ must be infinite there. This point marks the breakdown of the quasi-neutral solution and may be defined as the sheath edge. This is the same procedure used in Sec. 2.4 for the plane case. If $\eta = 1/2$ at the sheath edge, and $\xi \approx a/h$ there (a being the probe radius), then we have from (3.31-9)

$$I = I_\lambda a^2 h^{-2} 2^{-1/2} e^{-1/2} = A_a^2 2^{-1/2} e^{-1/2} n_o v_s = 0.61 A_a (kTe/M)^{1/2} n_o \quad (3.31-11)$$

We give this approximate solution because Bohm [1949] used the same

method to evaluate I for the case of mono-energetic ions with non-vanishing velocity. That calculation was very complicated because azimuthal motions had to be taken into account, but the method of approximation using a sheath edge was the same as given here. Bohm obtained coefficients of 0.57 and 0.54 instead of 0.61 in (3.31-11), for ion energies 0.01 and 0.5 times kT_e , respectively. Thus the saturation ion current is quite independent of kT_i and gives instead the product $n(kT_e)^{1/2}$. This is because ions are pulled into the sheath by a potential drop of order kT_e . The reverse would be true of saturation electron current if the electrons were colder than the ions.

The exact solution of (3.31-8) was obtained numerically by Allen et al. [1956]. Consider the asymptotic behavior of (3.31-8). The term corresponding to the ion density is $I/I_\lambda \eta^{1/2} \xi^2$. As $\xi \rightarrow \infty$ we see that if η varies asymptotically as ξ^{-4} , the ion density is finite at infinity. This is in contrast to the plane case, where as $v_i \rightarrow 0$, $n_i \rightarrow \infty$. If $\eta \rightarrow \xi^{-4}$, we see that η'' and $2\eta'/\xi$ approach zero, and (3.31-8) reduces asymptotically to the quasi-neutral equation, as expected. If we let $\zeta = \xi (I_\lambda/I)^{1/2}$, we have

$$\left(\frac{I_\lambda}{I}\right)^2 \left(\frac{d^2\eta}{d\zeta^2} + \frac{2}{\zeta} \frac{d\eta}{d\zeta} + e^{-\eta}\right) \eta^{1/2} \zeta^2 = 1 \quad (3.31-12)$$

The solutions of this for each value of I/I_λ agree at large ζ and are shown in Fig. 3.4a. The corresponding $\eta - \xi$ curves are shown in Fig. 3.4b.

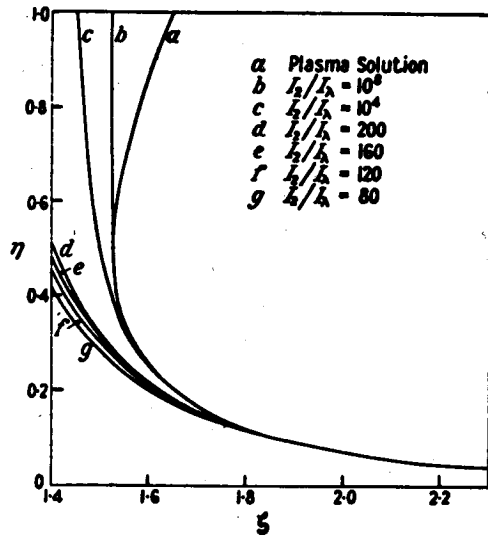


Fig. 3.4a

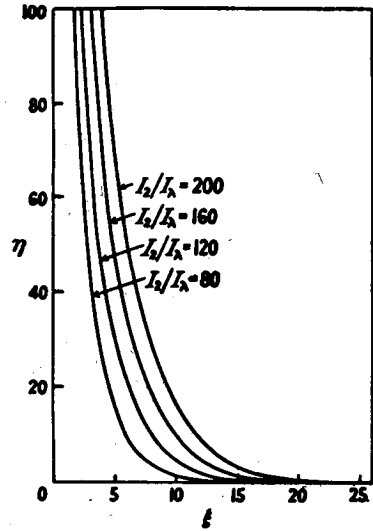


Fig. 3.4b

The probe potential for each value of I is found by the intersection of the appropriate potential curve with a vertical line at $\xi = a/h$. The shape of part C of the probe characteristic is found from these intersections; this is shown in Fig. 3.5 for various values of a/h . This variation of I with V was not computed by Bohm [1949].

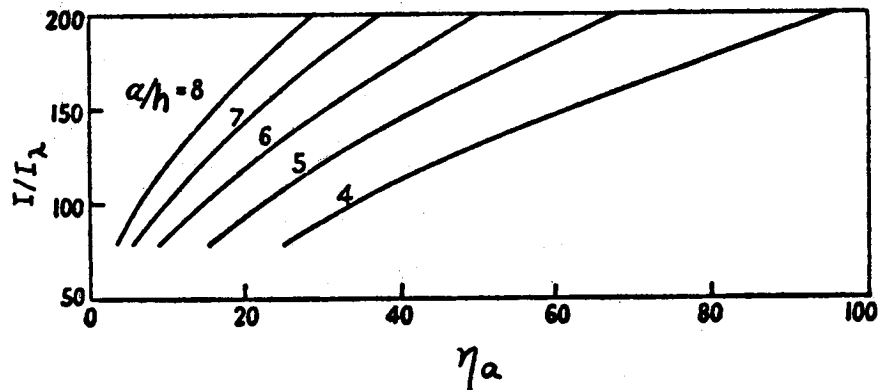


Fig. 3.5

3.32 Finite Temperature: Orbital Motions

When the ions have a finite angular momentum and can make orbits, the calculation of the ion density is so complicated that it will not be worthwhile to follow this in detail. Instead, we shall sketch the general procedure, following the method of Bernstein [1959].

Suppose that we have a spherical probe at negative potential, that the electrons are Maxwellian, and that the ion distribution is known at some large radius λ where the collisionless region ends. If there is spherical symmetry, Boltzmann's equation (1.1-1) has the general steady-state solution

$$f = f(E, J) \quad , \quad (3.32-1)$$

where E and J are the two constants of the motion, energy and angular momentum. If u and v are the radial and tangential components of velocity, V the potential, and e the ion charge, we have

$$E = \frac{1}{2} M(u^2 + v^2) + eV(r) \quad (3.32-2)$$

$$J = M r v \quad .$$

Solving for u , we have

$$\frac{1}{2} M u^2 = E - eV - J^2/2Mr^2 \quad . \quad (3.32-3)$$

Thus it is convenient to define an effective potential energy U , such that

$$U(r, J) = eV(r) + J^2/2Mr^2 \quad . \quad (3.32-4)$$

The distribution $f(E, J)$ can be divided into f^+ and f^- , corresponding respectively to ions moving away from and toward the probe. The function f^- is assumed to be known at some large radius and is therefore known everywhere. The complexity of the problem comes from finding f^+ . Obviously, f^+ will be zero for those orbits which intersect an absorbing probe and will be equal to f^- for those that do not. Thus in integrating over f to find the ion density to put into Poisson's equation, a procedure with which we are by now familiar, the domain of integration must be divided up, depending on whether $f^+ = 0$ or $f^+ = f^-$.

If $\lambda \gg a$ (λ and a being the mean free path and probe radius, respectively), one would expect that f^- would be almost Maxwellian at λ , since this distribution comes from ions which had a collision about λ cm away, and the probe subtends a very small angle at this distance. The distribution f^+ at λ will be depleted of those ions of low angular momentum which have hit the probe, but this small number does not greatly affect the total density there and does not affect the probe current, since these are particles traveling away from the probe. Thus the specification of f^- at λ should determine the problem if $\lambda \rightarrow \infty$, which is the regime of validity of the theory. Of course λ must not be equal to ∞ , since all angular momenta are infinite there, and the specification of f^- at ∞ would not tell anything about the distribution of angular momenta at finite radii.

The classification of orbits is best described by Bernstein's diagram of the effective potential energy U (Fig. 3.6):

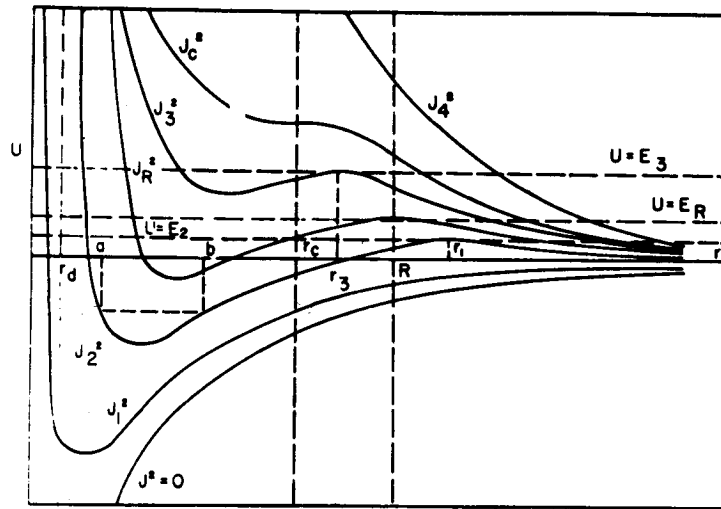


Fig. 3.6

For $J = 0$, the potential is everywhere negative, and the ion merely falls into the probe. For small J , we assume that the centrifugal force term in (3.32-4) dominates at sufficiently small radii, and there is a centrifugal barrier there. As J is increased, a maximum as well as a minimum will appear. At some critical J_c , the minimum will disappear, and there is only an inflection point. Finally, for very large J 's, the effective potential is always positive.

We note that for small J 's there is a potential well. Ions trapped in this well will make closed orbits around the probe and never reach $r = \lambda$. Therefore, the population in these orbits will not be determined by the specification of $f^-(E, J)$ at $r = \lambda$ but will depend sensitively on collisions near the probe. The existence of such trapped ions would alter the potential distribution in a manner which is difficult to predict and would invalidate the theory. Hence one of the results of this theory is that the probe radius must be larger than the radius of the inflection point in J_c^2 ; then no potential minimum can exist outside the probe and no particles can be trapped.

Consider now a probe of radius R and the curve J_R^2 which has its maximum at R . All ions with energy higher than E_R , the energy of this maximum, will be collected; and $f^+ = 0$ for such ions. Ions with $E < E_R$ will be either collected or reflected, depending on the relative magnitude of E and J^2 . At any radius $r_1 > R$, the ions with E smaller than the magnitude of the maximum in U at r_1 will not reach r_1 , and therefore $f^+ = f^-$. Ions with very large energy or very small angular momentum will be collected, and for these $f^+ = 0$, $f^- = f^-$. Thus when the density is computed, the distribution f must be integrated over the E, J phase space; and this space must be divided up into regions, depending on the probe radius R , in which f^+ and f^- are related in different ways to the known function f^- .

The ion density appears, then, as a complicated integral. This must be set equal, in Poisson's equation, to the Laplacian of V in spherical coordinates, minus the Maxwellian electron density term. This integro-differential equation has not been solved, even numerically, for the case of a continuous distribution of ion velocities at large radii.

3.33 Case of a Mono-energetic Isotropic Ion Distribution

The integral in n_i can be ~~carried out~~^{evaluated} if $f^-(E) \cong \delta(E - E_0)$. The solution of Poisson's equation still involves a difficult machine computation, but this has been done by Bernstein and Rabinowitz [1959]. It has also been done by Bohm, Burhop and Massey [1949] for the numerically much easier case in which the conditions at a "sheath edge" are assumed (cf. Sec. 3.31). We shall examine the final equation in order to gain some insight into the nature of the solution.

The following dimensionless parameters are used:

$$\begin{aligned}\xi &= r(4\pi n_0 e^2/kT_e)^{1/2} \\ l &= \frac{\psi}{\pi I_\lambda} (e^2/kT_e v_s), \quad v_s = (2kT_e/M)^{1/2} \\ \beta &= E_0/kT_e \\ \eta &= -eV/kT_e,\end{aligned}\tag{3.33-1}$$

where the notation is consistent with that used so far. In terms of these variables, Poisson's equation for the spherical case is

$$\begin{aligned}\frac{1}{\xi^2} \frac{d}{d\xi} \left(\xi^2 \frac{d\eta}{d\xi} \right) &= \frac{1}{2} \left(1 + \frac{\eta}{\beta} \right)^{1/2} + \frac{1}{2} \left(1 + \frac{\eta}{\beta} - \frac{l}{\beta^{1/2} \xi^2} \right)^{1/2} - e^{-\eta}, \quad \xi \geq \xi_0 \\ &= \frac{1}{2} \left(1 + \frac{\eta}{\beta} \right)^{1/2} - \frac{1}{2} \left(1 + \frac{\eta}{\beta} - \frac{l}{\beta^{1/2} \xi^2} \right)^{1/2} - e^{-\eta}, \quad \xi \leq \xi_0\end{aligned}\tag{3.33-2}$$

where ξ_0 is determined by the condition that the second bracket on the right-hand side and its derivative vanish at ξ_0 . It is the radius at which the maximum in the curve of $U(r)$ has a height equal to the initial ion energy E_0 . For $\xi < \xi_0$ the ion density is smaller than for $\xi > \xi_0$, because a number of ions are reflected by the potential hill to the right.

If we keep β finite and let ξ go to ∞ in (3.33-2), and expand in small η/β , the first of Eqs. (3.33-2) becomes

$$\frac{1}{\xi^2} \frac{d}{d\xi} \left(\xi^2 \frac{d\eta}{d\xi} \right) \cong 1 + \frac{1}{2} \frac{\eta}{\beta} - \frac{1}{4} \frac{l}{\beta^{1/2} \xi^2} - (1 - \eta) = \eta \left(1 + \frac{1}{2\beta} \right) - \frac{1}{4} \frac{l}{\beta^{1/2}} \frac{1}{\xi^2}.\tag{3.33-3}$$

Thus if η goes asymptotically as ξ^{-2} , the right-hand side can be made to vanish for large ξ ; this is the behavior expected in the plasma region.

On the other hand, if we let β (essentially the ion temperature) go to 0 first, ξ_0 must go to ∞ to make the second bracket on the right-hand side of (3.33-2) vanish. Thus we must expand the second of Eqs. (3.33-2) for large η/β . This gives

$$\begin{aligned} \frac{1}{\xi} \frac{d}{d\xi} \left(\xi^2 \frac{d\eta}{d\xi} \right) &= \frac{1}{2} \left(\frac{\eta}{\beta} \right)^{1/2} \left(1 + \frac{1}{2} \frac{\beta}{\eta} \right) - \frac{1}{2} \left(\frac{\eta}{\beta} \right)^{1/2} \left(1 + \frac{1}{2} \frac{\beta}{\eta} - \frac{\beta^{1/2}}{2\eta\xi} \right) e^{-\eta} \\ &= \frac{1}{4} \frac{\beta}{\eta^{1/2} \xi^2} e^{-\eta} \quad . \end{aligned} \quad (3.33-4)$$

This is the same as (3.31-8) derived before for $T_i = 0$. Here η must behave asymptotically as ξ^{-4} to achieve quasi-neutrality at large ξ .

The solution thus has the nature of a boundary layer problem in which η satisfies different equations for large and small ξ , and the solutions are matched at some radius, in this case ξ_0 . When the ions are strictly cold, the region of large ξ is never reached. This explains why the solution of Allen, Boyd, and Reynolds goes as ξ^{-4} instead of ξ^{-2} , as in the case of finite β . In practice ξ can never be allowed to go to infinity but only to some large distance λ . Whether η goes as ξ^{-2} or ξ^{-4} near λ will depend on whether λ is larger or smaller than ξ_0 , which, in turn, depends on the smallness of β . [The author is indebted to I. B. Bernstein for making this clear.]

For any given l , (3.33-2) gives a curve of η vs. ξ . These curves are shown in Fig. 3.7.

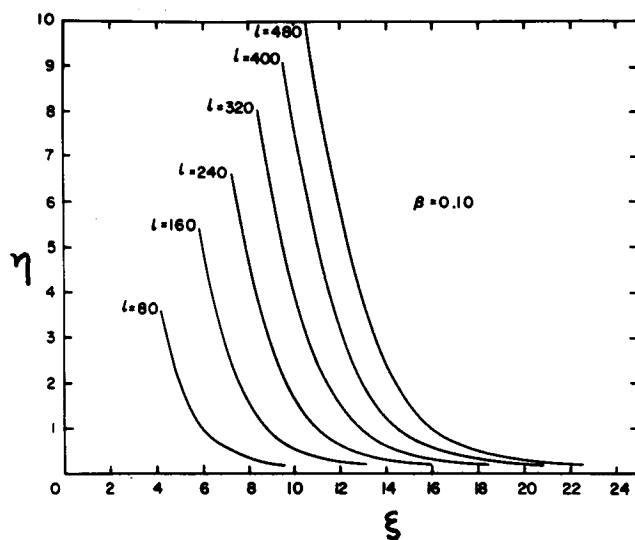


Fig. 3.7

A vertical line at $\xi = R$, the probe radius, then gives the probe potential at each current; this cross-plot gives the probe characteristic for saturation ion current (Fig. 3.8).

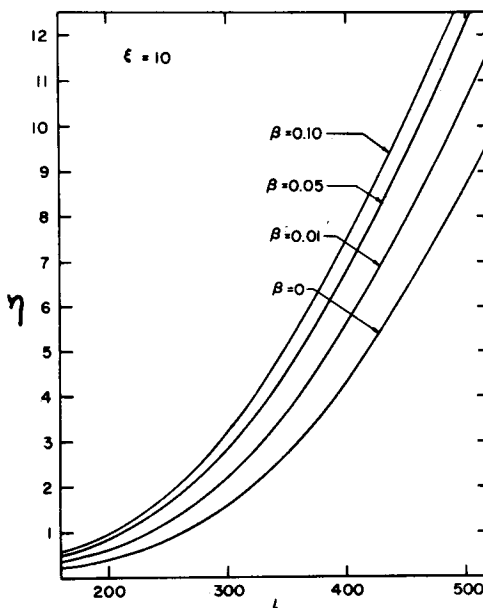


Fig. 3.8

Such a cross-plot must be made for each probe. One notes that the variation of probe current with ion temperature is slight ($\sim 20\%$), in agreement with Bohm [1949]. This result also justifies the use of a delta function distribution for the ions.

The case of a cylindrical probe has also been worked out analogously by Bernstein [1959]. In this case the appropriate dimensionless variables are the same as (3.33-1) with the exception

$$l = \frac{1}{4} \frac{\pi e^2}{kT_e} \frac{m}{2E_0} \frac{I^2}{n_0} \quad . \quad (3.33-5)$$

The fact that l now contains the density n_0 has the disadvantage that a large number of curves of l must be computed in order to give probe characteristics for the large range of plasma densities that may be of interest. Furthermore, the comparison with experiment is clumsier, since l involves not only n_0 , the quantity being sought, but also I^2 instead of I . To use this theory one must make many cross-plots from the dimensionless graphs of Bernstein. This is unfortunate, since cylindrical probes are the easiest to use experimentally.

To get information about kT_e or kT_i from the ion current and its variation with potential would be quite difficult. As the probe voltage is made more negative, the current would eventually become constant when the collisionless approximation that the mean free path is much larger than the sheath breaks down, and the current is limited by diffusion into the collisionless region. This transition point is not given in this theory.

3.34 Summary of Theories of Ion Collection

All of the theories presented so far are valid only for strictly collisionless, quiescent plasmas without magnetic fields. The geometry of the probe is assumed to be an ideal sphere with no supporting wires or an infinite cylinder with no end effects. In all cases the electron distribution is assumed to be Maxwellian; the collection of electrons at low voltages, which changes the electron concentration and hence the potential near the probe, is neglected.

The original Langmuir theory (Sec. 3.12) is valid for very low densities and small probes, where an absorption radius larger than the probe radius does not exist. This condition is generally not satisfied in ion collection if the ions are colder than the electrons. However, this theory may be applicable in the tenuous plasmas of outer space.

The theory of Bohm, Burhop, and Massey [1949] concerns the case of a spherical probe and mono-energetic ions of energy 0.01 and 0.5 times kT_e . The dependence on ion energy was found to be slight, and the approximate result for saturation ion flux was found to be

$$I = \frac{1}{2} n_0 A \left(\frac{kT_e}{M} \right)^{1/2} , \quad (3.34-1)$$

where A is the probe area, n_0 the plasma density, and M the ion mass. In deriving this result the approximation of a "sheath edge" was made; consequently, no dependence on probe voltage is given. The formula (3.34-1) is thus quite inexact but nonetheless quite useful. It shows immediately the dependence on the

plasma parameters, and it gives an absolute number which can be compared quickly with experiment. To this order of accuracy (3.34-1) can be used even for non-spherical probes and probes in a magnetic field, provided the appropriate area is substituted for A. This gives an immediate, order-of-magnitude check on the plasma density. ~~The density profile is given more accurately than the absolute density.~~ The density profile is given more accurately than the absolute density provided the electron temperature can be assumed to be constant or if its profile is known.

The theory of Allen et al. (Sec. 3.31) is also for a spherical probe and is limited to completely cold ions. The solution is exact to large radii, and the variation of ion current with probe voltage (i. e., the shape of part C of the characteristic) is given graphically. Since the dependence on ion temperature is small, the assumption of zero temperature is not restrictive. Comparison with experiment must be done graphically, and a separate cross-plot of the given curves must be made for each value of the probe radius measured in Debye lengths. This theory has the advantage that the equation is fairly easy to solve numerically, so that curves for additional values of the parameters can readily be obtained.

The theory of Bernstein and Rabinowitz (Sec. 3.33) is the most accurate and the most difficult to use. Again the solution is carried to large radii, and the variation with voltage given. Moreover, finite ion energies are considered; and the important cylindrical case given as well as the spherical case. Comparison with experiment, however, involves a tedious process of cross-plotting and

reduction of dimensionless parameters to real variables, for each assumed value of the plasma parameters. The numerical solution is so complicated that curves other than the ones given are difficult and expensive to obtain.

The case of a continuous distribution of ion energies has not been solved except in the Langmuir theory, which neglects the solution for $V(r)$. However, this problem is not expected to give an answer much different from those already obtained. All these theories suffer from the fact that the electric field from the probe accelerates ions from large distances; hence collisions and external electric fields, such as those required to maintain the discharge, are apt to influence the probe current.

see Hall's recent work

3.4 Plane Probes

So far we have been concerned mainly with spherical and cylindrical probes. The reason for this is that a plane probe must be quite large in order to avoid edge effects; and a large plate will seriously disturb the plasma being probed. In the case of an infinitely large plate, there can be no ions flowing away from the plate no matter how far away one goes, as long as ionization and collisions are neglected. Hence the unperturbed distribution at infinity can never be achieved. There is therefore really no collisionless theory of a plane probe. A small plane probe will act like a spherical or cylindrical probe in that the electric field will fall off radially. Equation (3.34-1) can be used in that case.

In strong magnetic fields particles are constrained to move along the field; hence all probes are essentially plane probes. Collisions must then be

taken into account, and the influence of the probe may be far-reaching. The probe current may be connected with the process which maintains the plasma, and in this case the probe ceases to be a simple device which measures only the plasma itself.

4. Probe Theory in the Presence of Collisions

In weakly ionized plasmas at high pressures the results of the previous section will be modified by collisions between the collected particles and neutral atoms. The species repelled by the probe will not be greatly affected by collisions, since it is ordinarily assumed to be in thermal equilibrium anyway. We now consider the effects of collisions not because the case of high pressures is important in modern plasmas but because this is a necessary prelude to the case of strong magnetic fields, in which particles can move transversely only by collisions.

The effects of collisions on the foregoing theory are two-fold. First, if the mean free path λ is less than the characteristic length of the potential (roughly h), the equation of motion of particles in the sheath will differ from the free-fall equation, and one would expect that the potential profile and hence the probe current would be altered. Second, if λ is not considerably larger than the probe radius a , the distribution of velocities at the edge of the collisionless region will differ from the undisturbed distribution, since the probe is large enough to block a non-negligible portion of the particles arriving at this edge.

This depletion of the plasma at the boundary of the collisionless region can only be calculated by considering the collision-dominated region. Thus the effects of collisions must be considered if either the condition $\lambda \gg h$ or the condition $\lambda \gg a$ is not satisfied.

4.1 Probe at Space Potential

The second effect, that of depletion of the plasma when $\lambda \gg a$ is not satisfied, can be readily illustrated in the case of a probe at space potential, when there are no electric fields to be taken into account. We shall give an improved version of the treatment of Bohm, Burhop, and Massey [1949], which is valid for almost any shape of probe.

Consider a probe of area A_p and any convex shape immersed in a plasma. One mean free path λ from its surface we draw an imaginary surface of area A_λ . Outside of this surface we shall assume that particle motion is collision dominated, while inside the motion is collisionless. If n_λ is the density at the surface A_λ , and if the velocity distribution were isotropic there, as would be the case if $A_p \ll A_\lambda$, the random flux crossing A_λ inwards would be

$$j_r = \frac{1}{4} n_\lambda \bar{v} \quad , \quad (4.1-1)$$

where \bar{v} is the average magnitude of the thermal velocity. The current striking the probe would then be this times the probe area:

$$I = \frac{1}{4} n_\lambda \bar{v} A_p \quad . \quad (4.1-2)$$

On the other hand, if $A_p \lesssim A_\lambda$, that is, if the mean free path were so short that the surface A_λ is very close to the surface A_p , then the distribution at A_λ cannot be isotropic, since there cannot be any particles there coming from the probe. In this case the density n_λ is only half as large, and the probe current is instead

$$I = \frac{1}{2} n_\lambda \bar{v} A_p \quad . \quad (4.1-3)$$

In general, for arbitrary λ ,

$$I = \frac{n_\lambda \bar{v} A_p}{4K} \quad , \quad (4.1-4)$$

where K is a constant varying between 1 and 1/2, depending on the relative magnitude of A_λ and A_p . For a sphere of radius a , consideration of the solid angle over which the velocities are distributed at A_λ shows that

$$K = 1 - \frac{1}{2} \left(1 + \frac{\lambda}{a}\right)^{-2} \quad . \quad (4.1-5)$$

$$1 - \frac{1}{2} \left[1 - \left(1 - \left\{1 + \frac{\lambda}{a}\right\}^{-2}\right)^{\frac{1}{2}} \right]$$

The current I can be computed another way. In the region outside A_λ , the particle current density is controlled by diffusion and mobility and is given by

$$\vec{j} = -D \nabla n - \mu n \nabla V \quad , \quad (4.1-6)$$

D and μ being the coefficients of diffusion and mobility, respectively. Since the probe is at space potential, we shall assume that there are no electric fields, and ∇V vanishes. We shall examine this assumption later. In the exterior region j is conserved, so that $\nabla \cdot \vec{j} = 0$. From (4.1-6) we see that if D is constant,

$$\nabla \cdot \vec{j} = -D \nabla^2 n = 0 \quad . \quad (4.1-7)$$

The probe current is the integral of the normal component of \vec{j} over any surface enclosing the probe. Choosing this surface to be A_λ , we have

$$I = \int_{A_\lambda} -\vec{j} \cdot d\vec{s} = D \int_{A_\lambda} \nabla n \cdot d\vec{s} \quad , \quad (4.1-8)$$

\vec{j} and $d\vec{s}$ being oppositely directed. This integral depends only on the geometry of the surface A_λ , since n is a harmonic function outside A_λ . This can be seen by making an analogy with the problem of electrostatics.

Consider a conductor with a surface A_λ immersed in a vacuum. Outside A_λ , the potential V satisfies Laplace's equation $\nabla^2 V = 0$. Integrating Poisson's equation

$$\nabla^2 V = -4\pi\rho$$

over the volume inside A_λ , we have for the total charge on the conductor

$$-4\pi q = \int \nabla^2 V d^3 r = \int_{A_\lambda} \nabla V \cdot d\vec{s} \quad . \quad (4.1-9)$$

We know that q depends only on the geometry and is given by the capacitance of the surface A_λ :

$$q = C(V_\lambda - V_\infty) \quad . \quad (4.1-10)$$

Since n and V satisfy the same equations, we can make an analogy between I and q . From (4.1-8, -9, and -10), we have

$$I = -4\pi q D = -4\pi C D (V_\lambda - V_\infty) = 4\pi C D (n_o - n_\lambda) \quad , \quad (4.1-11)$$

n_o being the density at ∞ .

Now we can equate this to the value of I computed for the collisionless region (4.1-4):

$$I = 4\pi CD(n_o - n_\lambda) = n_\lambda \bar{v} A_p / 4K \quad . \quad (4.1-12)$$

Solving for n_λ and I, we have

$$n_\lambda = n_o \frac{4\pi CD}{4\pi CD + \bar{v} A_p / 4K} \quad , \quad (4.1-13)$$

and

$$I = \frac{\bar{v} A_p}{4K} n_o \frac{4\pi CD}{4\pi CD + \bar{v} A_p / 4K} = \frac{n_o \bar{v} A_p}{4} \left[K + \frac{\bar{v} A_p}{16\pi CD} \right]^{-1} \quad . \quad (4.1-14)$$

Specializing now to the case of a sphere, we have that $A_p = 4\pi a^2$ and $C = a + \lambda$, this being the capacity of a sphere of radius $a + \lambda$. Then the probe current becomes, with K from (4.1-5),

$$I = \frac{n_o \bar{v} A_p}{4} \left[\frac{\bar{v}}{4D} \frac{a^2}{a + \lambda} + \frac{K}{2} \left(1 + \frac{\lambda}{a} \right)^{-2} \right]^{-1} \quad . \quad (4.1-15)$$

Since the classical diffusion coefficient is

$$D = \frac{\lambda \bar{v}}{3} \quad , \quad (4.1-16)$$

this becomes

$$I = \frac{n_o \bar{v} A_p}{4} \left[\frac{3}{4} \frac{a}{\lambda} \frac{a}{a+\lambda} + 1 - \frac{1}{2} \left(1 + \frac{\lambda}{a} \right)^{-2} \right]^{-1} \quad (4.1-17)$$

or

$$I = \frac{n_o \bar{v} A_p}{4} \left[\frac{3}{4} \sigma^{-1} (1 + \sigma)^{-1} - \frac{1}{2} \left(1 + \sigma \right)^{-2} + 1 \right]^{-1} \quad (4.1-18)$$

$$+ 1 - \frac{1}{2} \left\{ 1 - \left[1 - \left(1 + \sigma \right)^{-2} \right]^{\frac{1}{2}} \right\} \right]^{-1}$$

with

$$\sigma = \lambda/a \quad (4.1-19)$$

In the limit of large σ , (4.1-18) reduces to the collisionless random current, $I = n_o \bar{v} A_p / 4$. In the limit $\sigma \rightarrow 0$, (4.1-18) becomes

$$I = \frac{n_o \bar{v} A_p}{4} \cdot \frac{4}{3} \frac{\lambda}{a} \quad (4.1-20)$$

Thus in the limit of small λ , collisions reduce the probe current by approximately a factor λ/a .

We now return to the assumption of zero electric field. The expression for n_λ (4.1-13) is of course valid for either species of particle, as are all the formulas in this section. Since $D \sim \lambda \bar{v}$, \bar{v} will cancel out of the equation. All the remaining parameters depend only on geometry, except λ . Thus if λ is different for ions and electrons, n_λ will differ, and an electric field must be set up to reestablish quasi-neutrality. Consequently, for small λ/a it is not really possible to bias a probe at space potential, since its very presence changes the space potential. Our derivation of (4.1-20) must therefore be regarded as approximate.

4.2 Saturation Current in the Limit $\lambda \ll h$

We now consider the opposite extreme when a large voltage is put on the probe and electric fields are important. This problem is simplified if we assume that the mean free path is much shorter than any other length in the problem, including the Debye length, so that particle motion is collision-dominated everywhere, even in the sheath. We shall then see how this "diffusion sheath" differs from the collisionless sheaths we have considered up to now. We shall pay particular attention to the case of a cylindrical probe for two reasons: the integrals are tractable, and the result may be directly applicable to the case of a strong magnetic field.

4.21 Cylindrical Probe

Let an infinite cylindrical probe of radius a be immersed in a plasma of density n_0 . Let particles 1 be collected so that $e_1 V$ is negative, and let the potential be so high that particles 2 are essentially Maxwellian. Further, let the motion of particles 1 be completely collision-dominated, so that the flux is describable in terms of a diffusion coefficient D and a mobility μ (pertinent to species 1):

$$j_1 = -D \nabla n_1 - \mu n_1 \nabla V \quad . \quad (4.21-1)$$

Poisson's equation is

$$\nabla^2 V = -4\pi e_1 (n_1 - n_0 e^{-e_2 V/kT_2}) \quad . \quad (4.21-2)$$

For any probe current I , j_1 is known since I is conserved, and these two equations may be solved simultaneously for n_1 and V . To make further progress,

↑

we must now make the first of two important simplifications: that the probe potential is so large compared to kT_1 that the D term in (4.21-1) can be neglected relative to the μ term. This can be seen as follows. If Λ_n and Λ_V are the characteristic lengths of the gradients of n and V , then in view of Einstein's relation for classical diffusion,

$$\mu = \frac{eD}{kT} \quad , \quad (4.21-3)$$

we have

$$\frac{D\nabla n_1}{\mu n_1 \nabla V} \approx \frac{kT_1}{eV} \frac{\Lambda_V}{\Lambda_n} \quad . \quad (4.21-4)$$

Providing that the Λ 's are of the same order of magnitude, the D term is smaller than the μ term by the ratio kT_1/eV .

With this simplification, (4.21-1) gives the ion density:

$$n_1 = \frac{-j_1}{\mu \nabla V} \quad . \quad (4.21-5)$$

In cylindrical symmetry, the total current I per unit length ^{toward} the probe is

$$I = -2\pi r j_1 \quad . \quad (4.21-6)$$

With $e_2 = -e_1$, Poisson's equation now becomes, in cylindrical coordinates,

$$\frac{1}{r} \frac{d}{dr} \left(r \frac{dV}{dr} \right) = -4\pi e_1 \left[\frac{I}{2\pi r \mu_1 \frac{dV}{dr}} - n_o e^{e_1 V/kT_2} \right] \quad . \quad (4.21-7)$$

In dimensionless form this becomes

$$\frac{1}{\rho} \frac{d}{d\rho} \left(\rho \frac{d\eta}{d\rho} \right) = \frac{-\iota}{\rho \frac{d\eta}{d\rho}} - e^{-\eta} \quad , \quad (4.21-8)$$

where

$$\begin{aligned} \eta &= -e_1 V / kT_2 \\ \rho &= r/h \quad \quad h^2 = kT_2 / 4\pi n_0 e_1^2 \\ \iota &= I / I_0 \\ I_0 &= 2\pi n_0 \mu_1 kT_2 / e_1 \quad . \end{aligned} \quad (4.21-9)$$

From (4.21-8) it is clear that a quasi-neutral solution at large radii can be obtained only if $d\eta/d\rho$ approaches $-\iota/\rho$ as ρ approaches ∞ and η approaches 0.

Then the right-hand side vanishes at ∞ , corresponding to equal charge densities.

Thus the asymptotic behavior of η is

$$\eta \xrightarrow{\rho \rightarrow \infty} \int_{\infty}^{\rho} \frac{d\eta}{d\rho'} d\rho' \rightarrow \int_{\infty}^{\rho} \frac{-\iota}{\rho'} d\rho' \quad . \quad (4.21-10)$$

This integral diverges, so that strictly speaking the cylindrical problem is not a well-formulated one. Consideration of the D term, which we neglected, does not help the asymptotic behavior; the potential simply falls so slowly that one would expect an infinite current per cm to a cylindrical probe. In actuality this, of course, does not happen because there is a) ionization and b) end effects, so that I is not strictly constant with radius. From (4.21-10) it is apparent that any decrease, however slight, of I and hence of ι ^{with r} will make the integral converge.

The cylindrical probe at high pressures is therefore not a true probe in that its influence necessarily extends into the region where ion production is important.

The solution of (4.21-8) can be found if we impose a "sheath edge" at $\rho = s$ and assume that $d\eta/d\rho = 0$ at $\rho = s$. To solve this analytically we must also make our second approximation: that the potential is so high that the density of particles 2 can be neglected. Then Poisson's equation becomes

$$\frac{1}{\rho} \frac{d}{d\rho} \left(\rho \frac{d\eta}{d\rho} \right) = \frac{-\iota}{\rho \frac{d\eta}{d\rho}} ,$$

or

$$\frac{1}{\rho} \frac{df}{d\rho} = \frac{-\iota}{f} , \quad f \frac{df}{d\rho} = -\iota \rho \quad (4.21-11)$$

where

$$f(\rho) = \rho \frac{d\eta}{d\rho} .$$

Integrating from s to ρ , we have

$$\frac{1}{2} f^2 = \frac{1}{2} \rho^2 \left(\frac{d\eta}{d\rho} \right)^2 = \frac{\iota}{2} (s^2 - \rho^2) \quad (4.21-12)$$

$$\frac{d\eta}{d\rho} = \iota^{1/2} \left(\frac{s^2}{\rho^2} - 1 \right)^{1/2} \quad (4.21-13)$$

$$\eta - \eta_s = \iota^{1/2} \int_s^\rho \left(\frac{s^2}{\rho^2} - 1 \right)^{1/2} d\rho . \quad (4.21-14)$$

From No. 361.01 of Dwight's Tables of Integrals, we find finally that

$$\eta - \eta_s = \iota^{1/2} \left\{ (s^2 - \rho^2)^{1/2} - s \log \left[\frac{s}{\rho} + \left(\frac{s^2}{\rho^2} - 1 \right)^{1/2} \right] \right\} . \quad (4.21-15)$$

Substituting $\frac{a}{h}$ for ρ gives the probe potential. This is, then, the high-pressure equivalent of the Child-Langmuir space charge equation (3.11-6). If we convert (4.21-15) back to real units by (4.21-9), we will find that the dependences on kT_2 and n_0 cancel out; and, aside from the geometrical factor, the current I is proportional to $(V - V_s)^2$, as contrasted with $(V - V_s)^{3/2}$ in the collisionless case (3.11-6).

The condition $\lambda \ll h$ is usually not fulfilled in highly ionized plasmas, and this theory is then inapplicable. However, if there is a strong magnetic field, the mean free path is effectively reduced to r_L , the Larmor radius, in directions perpendicular to the field; and this may, for electrons, become smaller than \underline{h} . Since in the case of the infinite cylinder all motions are transverse to the axis, this theory is directly applicable in strong magnetic fields if μ is replaced by μ_{\perp} , or $\mu/\omega^2 \tau^2$.

4.22 Spherical Probe

The case of a sphere is entirely similar, except that one must replace (4.21-6) by

$$I = - 4\pi r^2 j_1 \quad (4.22-1)$$

and (4.21-9) by

$$I_0 = 4\pi h n_0 \mu k T_2 / e_1 . \quad (4.22-2)$$

Poisson's equation in spherical coordinates is then

$$\frac{1}{\rho^2} \frac{d}{d\rho} \left(\rho^2 \frac{d\eta}{d\rho} \right) = \frac{-\iota}{\rho^2} \frac{d\eta}{d\rho} - e^{-\eta} \quad (4.22-3)$$

In order to achieve a quasi-neutral solution, we must have for large ρ ,

$$\frac{d\eta}{d\rho} \rightarrow \frac{-\iota}{\rho^2} \quad (4.22-4)$$

or

$$\eta \rightarrow \frac{\iota}{\rho} \quad (4.22-5)$$

In this case the potential does fall fast enough to allow a solution which does not depend on conditions far from the probe.

If we neglect the exponential term and make the transformation $x = 1/\rho$, (4.22-3) becomes

$$x^4 \frac{d^2 \eta}{dx^2} = \iota \frac{dx}{d\eta}$$

$$\frac{d^2 \eta}{dx^2} \frac{d\eta}{dx} = \frac{\iota}{x^4} \quad (4.22-6)$$

In neglecting $e^{-\eta}$ we have, however, destroyed the asymptotic behavior and must assume a sheath edge at x_s . The last equation can be integrated once from x_s to x to give

$$\frac{d\eta}{dx} = \left(\frac{2}{3} \iota \right)^{1/2} \left(\frac{1}{x_s^3} - \frac{1}{x^3} \right)^{1/2} \quad (4.22-7)$$

The final integration must be done numerically.

4.23 Plane Probe

In this case we have

$$-j_1 = I \quad (4.23-1)$$

$$I_0 = n_0 \mu k T_2 / e_1 h \quad (4.23-2)$$

and

$$\frac{d^2 \eta}{d\xi^2} = \frac{-\iota}{d\eta/d\xi} - e^{-\eta} \quad (4.23-3)$$

For a quasi-neutral solution at $\xi = \infty$, $d\eta/d\xi$ must approach a constant, equal to $-\iota$. It is clear why this is so. Since j_1 is constant by (4.23-1), there must be a finite electric field to drive this current no matter how far from the probe one goes, as long as ionization is neglected. Hence the plane case is even worse than the cylindrical case asymptotically, and the probe current depends strongly on the ionization mechanism.

We can, nonetheless, solve the space charge problem of two parallel plates at $\xi = 0$ and $\xi = \xi_s$, with $d\eta/d\xi = -\iota$ and $\eta = 0$ at ξ_s . Multiplying (4.23-3) by $d\eta/d\xi$ and integrating from $\xi = \xi$ to $\xi = \xi_s$, we have

$$\begin{aligned} \frac{\iota^2}{2} - \frac{1}{2} \left(\frac{d\eta}{d\xi} \right)^2 &= -\iota (\xi_s - \xi) - e^{-\eta} + 1 \\ -\frac{d\eta}{d\xi} &= \left[\iota^2 + 2\iota (\xi_s - \xi) + 2e^{-\eta} - 2 \right]^{1/2} \quad (4.23-4) \end{aligned}$$

The final integration can be carried out if we neglect $e^{-\eta}$ ~~1~~.

$$\eta = \int_s^0 \frac{d\eta}{d\xi} d\xi = \int_s^0 [l^{-2} + 2l(s - \xi)]^{1/2} d\xi = (2l)^{1/2} \int_0^s (\frac{l}{2} + s - \xi)^{1/2} d\xi$$

$$= \frac{2}{3} (2l)^{1/2} [(\frac{l}{2} + s)^{3/2} - (\frac{l}{2})^{3/2}]$$

$$\eta = \frac{1}{3l} [(l^2 + 2ls)^{3/2} - l^{3/2}] \quad (4.23-5)$$

This gives the potential profile for space charge limited flow, to be compared with the collisionless formula (2.21-8). *For large ξ_s one finds that l is proportional to ξ_s^{-2} and η is proportional to ξ_s^{-2} on the potential axis.*

4.3 Summary of Probe Theories with Collisions

In the limit of small λ , the case considered in Sec. 4.2, the problem has been analyzed in detail recently by Su and Lam [1962]. This treatment is limited to the convergent spherical case. Two limiting cases are given. First, in the limit of high probe potentials the particles 2 are assumed to be Maxwellian. The joint solution of (4.21-1) and (4.21-2) is discussed, but in the actual numerical computations the D term is omitted, as in Sec. 4.2. However, the exponential density term is retained. Second, in the limit of small probe potentials the density of particles 2 cannot be assumed Maxwellian, and the D term cannot be omitted. However, it is possible in this case to expand in powers of η . Numerical probe curves for saturation ion current are given. Moreover, the criterion for validity of the small λ assumption is given to be

$$\left(\frac{\lambda}{a}\right)^{1/3} \left(\frac{\lambda}{h_i}\right)^{2/3} \ll 1 \quad , \quad (4.3-1)$$

where h_i is the ion Debye length and \underline{a} the probe radius. This condition refers to the case of small η and may be relaxed for large η . The generalization of this theory to all values of η has been carried out by I. Cohen [1962].

These curves show good saturation at high probe potentials; that is, the probe current is more constant than the collisionless theory would predict. This often occurs in experiment; and when it does occur, one should suspect that the current is diffusion limited.

When the mean free path is neither large nor small, the theory becomes extremely complicated, since there is no simple equation of motion. The first analysis of a probe at high pressures was made by Davydov and Zmanovskaja [1936], who assumed that $\lambda \approx h$, so that quasi-neutrality obtained in the diffusion region, and free-fall occurred in the sheath. Ionization was taken into account, but the sheath criterion (2.31-10) seemed to be unknown to them. In 1951, R. L. F. Boyd considered the case of intermediate mean free path by dividing space into four regions and matching boundary conditions at each interface: a sheath region in which $n_i \neq n_e$, an abnormal mobility region in which $n_i \approx n_e$ and $v_i \sim (\nabla V)^{1/2}$, a normal mobility region where (4.21-1) is satisfied, and an undisturbed plasma region. A result of this very complicated analysis was that the probe current cannot be computed without prior knowledge of the sheath thickness.

The transition from collisionless to collision-dominated probe collection was studied by Schulz and Brown [1955]. For no collisions, the Langmuir theory was used. With one collision in the sheath, the probe current was found to be

increased, since the orbital motion was disrupted. With several (2-10) collisions in the sheath, the ions can be scattered out, and a plural scattering calculation by Cobine was used. For many collisions in the sheath, Eq. (4.21-15) was used. Semi-empirical formulas were given for each case, and the theory was checked against microwave measurements of density, with extremely good agreement.

In all this work the classical diffusion and mobility constants were assumed. In fully ionized plasmas the diffusion coefficient varies with density, and these theories would not hold. However, the mean free path for Coulomb collisions is usually so long that the collisionless theory usually would apply, except in dense, cold, fully ionized plasmas.

5. Probe Theory in the Presence of a Magnetic Field

As we have already seen, probe theory in the absence of magnetic fields is sufficiently complicated that in most cases of interest numerical solutions of the equations are necessary. When a magnetic field is added, the problem becomes so difficult that it has received only very spotty treatment up to the present time. This is unfortunate, since most plasmas of interest today employ a magnetic field to aid in confinement; this applies both to plasmas of thermonuclear interest and to the Van Allen belts.

The main difficulties introduced by a magnetic field are twofold. First, particles are constrained to gyrate about the lines of force, so that particles move at different rates along and across the field. This introduces an aniso-

tropy which makes the problem at least two-dimensional. Second, the effective mean free path across the field is of the order of the Larmor radius, since particles can travel only this far without making a collision; and since the Larmor radius is quite small for electrons even for moderate fields, there is essentially no collisionless theory in such a case. In fact, for very strong fields any probe will resemble a plane probe, since particles can come to it from only one direction; and we have seen that the current to plane probes depends on the mechanism of plasma production in the entire volume and is not a local property of the plasma itself. We shall first consider the problem in general and then discuss the few specific cases which have been treated.

5.1 Overall View of the Problem

When a magnetic field is applied, the most noticeable effect is that the saturation electron current is decreased below its value in the absence of a field. The ratio of I_e to I_i is normally of the order of the ratio of electron to ion thermal velocities, i. e., $(kT_e/m)^{1/2}/(kT_i/M)^{1/2}$, and this is of the order of 10^2 . In a magnetic field weak enough that the ion Larmor radius r_{Li} is large compared to the probe radius \underline{a} and the Debye length \underline{h} and hence that I_i is not affected, but strong enough that r_{Le} is comparable to or smaller than the relevant dimensions, this ratio falls to 10 or 20. This is presumably because the available electron current, which normally is that diffusing to a sphere of radius of order λ , is decreased by the magnetic field B to that diffusing at a reduced rate across B into a cylindrical tube defined by the lines of force intercepted by the probe.

The normal diffusion coefficient D, as given by kinetic theory, is $\lambda\bar{v}/3$.

The diffusion coefficient across a magnetic field, in the case of classical collisions with neutrals, is

$$D_{\perp} = D / (1 + \omega^2 \tau^2) \quad , \quad (5.1-1)$$

where ω is the cyclotron angular frequency, and τ the mean collision time.

Equation (5.1-1) also holds for fully ionized gases. Since $\omega\tau$ for electrons is typically above 10^2 (at 100 gauss and 10 microns neutral pressure), D_{\perp} is severely reduced even at small fields. For ions, ω is decreased by m/M while $\tau = (n_0 \bar{\sigma} v)^{-1}$ is increased by approximately $(M/m)^{1/2}$, so that $\omega^2 \tau^2$ is at least 2000 times smaller than for electrons. Thus $D_{\perp i}$ is decreased severely only for large B, and the conditions assumed in the previous paragraph can actually occur. (For the derivation of (5.1-1) the reader is referred to Kadomtsev and Nedospasov, J. Nucl. Energy, Part C, 1, 230 (1960).) At large magnetic fields anomalous diffusion almost always occurs, in which D_{\perp} is much larger than the value in (5.1-1). An important function of probes is to measure the unknown anomalous value of D_{\perp} .

Another effect of the magnetic field is to destroy electron saturation; that is, part A of the probe characteristic continues to increase with voltage. This may be because the effective length of the flux tube into which electrons can diffuse to reach the probe increases continuously with voltage; however, this part of the characteristic has not been analyzed in detail, and it is not possible to give an exact physical picture.

As for the transition region, part B of the characteristic, it seems reasonable that at high negative voltages, when the drain of electrons is small, the plot of $\ln I_e / V_p$ should still be linear when the distribution is Maxwellian,

and the slope should still give the electron temperature. The sheath around a spherical probe will now be asymmetrical, but the addition of a magnetic field cannot change the state of thermodynamic equilibrium, and this state is such that the velocity distribution in any direction is exponential. However, for strong fields it is possible that a complete equilibrium is not reached, but instead the plasma is describable by different temperatures T_{\perp} for motions perpendicular to B and T_{\parallel} for parallel motions. In such a case one would expect that the slope of part B would give T_{\parallel} , since most electrons reach the probe by traveling along B . The exact analysis of this part of the characteristic has not been done.

Near the space potential, the absolute magnitude of the electron current has been estimated by Bohm et al. (Sec. 5.2), and the variation with potential by Bertotti (Sec. 5.3). However, the behavior is sufficiently obscure that at the present time it is not known which point on the characteristic corresponds to the space potential. The point of intersection found by extrapolating parts B and A of the characteristic is not necessarily near the space potential when there is a magnetic field as it is when there is not.

Part C of the characteristic, the ion saturation current, has so far defied all attempts at analysis in the case of a strong field, when r_{Li} is comparable to or smaller than other relevant lengths in the problem. In weak fields, as mentioned before, the ion current should not be greatly affected. Since the electron motion is affected, one would expect that the ion sheath around a negatively charged symmetrical probe would not necessarily be symmetric. The effect of this on the ion current has not been treated.

5.2 Electron Current near the Space Potential

The electron current at small positive probe voltages can be estimated in a manner similar to that in Sec. 4.1. This approach was originally suggested by Bohm, Burhop, and Massey [1959]. Consider a probe of arbitrary shape immersed in a plasma in a magnetic field. Let the positive probe potential be so large that very few ions are collected, but small enough that the electric field has little effect on the motions of electrons. Obviously these conditions are compatible only if $T_i \ll T_e$. Let the mean free path along B be λ , the Larmor radius be r_L , and the diffusion and mobility coefficients along and across the field be D , D_\perp , μ , and μ_\perp , where D_\perp is defined by (5.1-1) and μ_\perp is defined similarly.

As in Sec. 4.1, we assume that the motion across the last mean free path is unhindered, so that in terms of the density n_λ one mean free path away from the probe the current is given by (4.1-4):

$$I = A_p \frac{n_\lambda \bar{v}}{4K}, \quad (5.2-1)$$

where K is a constant varying from $1/2$ (if the surface A_λ is far from the probe) to 1 (if A_λ is close to the probe). With the magnetic field, the surface A_λ will be skewed, somewhat as shown in Fig. 5.1, since the length of a free path along B is λ , while across B it is only r_L . The exact shape is not important.

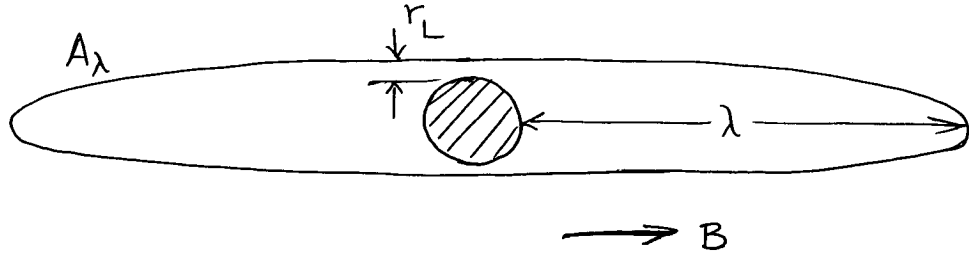


Fig. 5.1

In the region exterior to A_λ , we shall assume that the collision-dominated equations obtain and that current is conserved. The electron flux is given by

$$\vec{j} = -\mathbb{D} \cdot \nabla n + n \mu \cdot \nabla V \quad , \quad (5.2-2)$$

where \mathbb{D} and μ are diagonal matrices:

$$\mathbb{D} = \begin{pmatrix} D_\perp & 0 & 0 \\ 0 & D_\perp & 0 \\ 0 & 0 & D \end{pmatrix} \quad , \quad \mu = \begin{pmatrix} \mu_\perp & 0 & 0 \\ 0 & \mu_\perp & 0 \\ 0 & 0 & \mu \end{pmatrix} \quad . \quad (5.2-3)$$

The mobility term can be evaluated if we assume quasi-neutrality in the exterior region. Then n_e is equal to n_i , which in turn is given by the Boltzmann relation:

$$n_e = n_i = n_o e^{-eV/kT_i} \quad . \quad (5.2-4)$$

Thus,

$$\nabla n = n \left(\frac{-e}{kT_i} \right) \nabla V \quad . \quad (5.2-5)$$

Using this and the Einstein relation (4.21-3) (assuming the latter to hold even in

we find that
 a magnetic field), the current becomes

$$j = -D \cdot \nabla n \left(1 + \frac{T_i}{T_e}\right) \quad (5.2-6)$$

We shall ignore the correction factor $(1 + T_i/T_e)$ since this must be close to unity from our original model. Since current is conserved and D is assumed constant,

$$-\nabla \cdot j = D_{\perp} \nabla_{\perp}^2 n + D \frac{\partial^2 n}{\partial z^2} = 0 \quad (5.2-7)$$

If we let

$$\alpha = D_{\perp} / D \quad (5.2-8)$$

and

$$\zeta = \sqrt{\alpha} z \quad (5.2-9)$$

(5.2-7) becomes

$$0 = D_{\perp} \left(\nabla_{\perp}^2 n + \frac{\partial^2 n}{\partial \zeta^2} \right) = D_{\perp} \nabla_{\zeta}^2 n \quad (5.2-10)$$

where ∇_{ζ}^2 is the Laplacian in ζ -space, in which lengths in the direction of B have been contracted by a factor $\sqrt{\alpha}$. Thus \underline{n} is a solution of Laplace's equation in ζ -space.

The probe current is found in terms of n_{λ} by integrating j over A_{λ} :

$$I = \int_{A_{\lambda}} -j \cdot dS = \int_{A_{\lambda}} dS \cdot D \cdot \nabla n = D_{\perp} \int_{A_{\lambda}} dS_{\perp} \cdot \nabla_{\perp} n + D \int_{A_{\lambda}} dS_{\parallel} \cdot \frac{dn}{dz} \quad (5.2-11)$$

To transform the integrals to ζ -space, we note that $\partial/\partial z = \sqrt{\alpha} \partial/\partial \zeta$ and $dS_{\perp} = dS'_{\perp}/\sqrt{\alpha}$, while dS_{\parallel} and $\nabla_{\perp} n$ are unchanged by the transformation (the primes indicate quantities in ζ -space), so that

$$I = D \sqrt{\alpha} \int_{A'_{\lambda}} \nabla' n \cdot dS' \quad . \quad (5.2-12)$$

This integral can be evaluated for any simple surface A'_{λ} (the transformed surface A_{λ}), but there is no need to do this, since we saw in (4.1-11) that this is given in terms of the capacity of the surface A'_{λ} relative to infinity. Thus

$$I = 4\pi \sqrt{\alpha} CD(n_o - n_{\lambda}) \quad . \quad (5.2-13)$$

From this and (5.2-1), we have

$$I = A_p \frac{n_{\lambda} \bar{v}}{4K} = 4\pi \sqrt{\alpha} CD(n_o - n_{\lambda})$$

$$n_{\lambda} = \frac{n_o}{1 + \frac{A_p \bar{v}}{16\pi K \sqrt{\alpha} CD}} \quad , \quad (5.2-14)$$

and

$$I = \frac{n_o \bar{v} A_p}{4} \left[K + \frac{A_p \bar{v}}{16\pi \sqrt{\alpha} CD} \right]^{-1} \quad . \quad (5.2-15)$$

For strong fields we can neglect the first term in the brackets; then using

$D = \lambda \bar{v}/3$ and $A_p = 4\pi a^2$ for a sphere, we have

note change in denominator

$$I = \frac{n_o \bar{v} A_p}{4} \frac{4\sqrt{\alpha} C \lambda}{3a^2} = \frac{4\pi n_o \bar{v}}{3} \sqrt{\alpha} C \lambda \quad . \quad (5.2-16)$$

If, in calculating C, we assumed A_λ and hence A'_λ to be an infinite cylinder with its axis in the z-direction, or if we assumed the probe to be an infinitely long wire, we would find that $C \sim L/\ln(b/a)$, where \underline{a} is the radius of the surface A_λ , \underline{b} is the outer radius, and L the length of the region in question. Since we are interested in the limit $b \rightarrow \infty$, $L \rightarrow \infty$, the value of C depends on how these limits are approached. Thus we recover the result of Sec. 4.21 that an infinite cylindrical probe in the collision-dominated case is not a well-posed problem. The finite length of the surface A'_λ must be taken into account.

Returning to the case of a spherical probe, we note that the surface A_λ in this case can be approximated by a prolate spheroid of minor radius $a + r_L$ and semi-major axis $a + \lambda$. In ζ -space, the transformed surface A'_λ then has a radius \underline{b} perpendicular to B and a semi-axis \underline{d} along B, where

$$b = a + r_L \approx a \quad (5.2-17)$$

$$d = \sqrt{\alpha} (a + \lambda) \approx \sqrt{\alpha} \lambda \quad .$$

This spheroid is prolate or oblate depending on whether \underline{a} is less than or greater than $\sqrt{\alpha} \lambda$. The capacitance of such a spheroid can be found from standard texts to be

$$C = \frac{d(1 - p^2)^{1/2}}{\tanh^{-1}(1 - p^2)^{1/2}} \quad , \quad p = \frac{b}{d} \leq 1 \quad (5.2-18)$$

$$C = \frac{d(p^2 - 1)^{1/2}}{\tan^{-1}(p^2 - 1)^{1/2}}, \quad p = \frac{b}{d} \geq 1 \quad (5.2-19)$$

These formulas, together with (5.2-17) and (5.2-15) or (5.2-16), then give the saturation electron current at a small positive potential under the assumptions that $T_i \ll T_e$, that orbital motions can be neglected in the free-fall region, and that quasi-neutrality obtains elsewhere. The neglect of K in (5.2-15) is justified whenever the field is strong enough to make I much less than its zero-field value.

The expression for C diverges as $d \rightarrow \infty$ as one would expect; the potential in the infinite cylindrical case falls so slowly that if one could maintain a density n_0 at infinity, the current would be infinite. When $p \rightarrow 1$, the inverse tangent and hyperbolic tangent can be replaced by their arguments, and both expressions reduce to the spherical case, $C = b$. When $d = 0$, (5.2-19) reduces to the capacity of a disc:

$$C = \frac{2b}{\pi} \quad (5.2-20)$$

This differs only slightly from $C = b$. Thus in the range $p \gtrsim 1$ the probe current depends insensitively on the assumed length and shape of the surface A'_λ ; the opposite is true if $p \ll 1$. Fortunately, the interesting range of p centers around one. This may be seen as follows if one assumes classical diffusion:

$$p = \frac{b}{d} \approx \frac{a}{\sqrt{\alpha} \lambda} \approx \frac{a\omega}{\bar{v}} \quad (5.2-21)$$

For average laboratory conditions, $a = 10^{-2}$ cm, $\omega = 2 \times 10^{10}$ sec⁻¹ (1000 gauss), and $\bar{v} = 2 \times 10^8$ cm/sec ($kT_e \sim 10$ eV), p is just 1. At higher fields and larger

probe radii, in principle \underline{p} can be as large as 100; however, what normally happens at high fields is that transverse diffusion becomes much larger than the classical value, and this increase in α reduces \underline{p} back to the order of unity.

The dependence of I on D_{\perp} can be seen if we approximate C by $b (\approx a)$; then from (5.2-16),

$$I = \frac{n_o \bar{v} A_p}{4} \cdot \frac{4}{3} \frac{\lambda}{a} \sqrt{\alpha} \quad , \quad (5.2-22)$$

where \underline{a} is the probe radius, and $\alpha = D_{\perp}/D$. Thus \underline{I} varies only as the square root of D_{\perp} ; this is because part of the probe current comes from diffusion along B, and this is unaffected by a change in D_{\perp} .

Equations (5.2-22) and (3.34-1) are crude but useful approximations to the saturation electron and ion currents to an arbitrarily shaped probe in moderate magnetic fields ($r_{Li} \gg a$). If kT_e and λ are known, Eq. (5.2-22) gives the value of D_{\perp} whether it is classical or not. Unfortunately it is not clear at which point the characteristic λ should be measured.

5.3 "Collisionless" Theory of a Probe in Strong Magnetic Fields

In the previous section we considered the particle currents in the collision-dominated region but neglected the detailed behavior of the electric field and particle motions in the collisionless region near the probe. Now we shall describe the theory of B. Bertotti [1961], which treats this region but neglects the asymptotic behavior in the transverse direction. In order to obtain a tractable problem it has been necessary to reduce the problem to one dimension and to make a number of mathematical simplifications.

Consider a probe of cross-sectional area A_p in a strong magnetic field B. Let the probe voltage be so high that particles are essentially all repelled and

therefore are Maxwellian. This is of course true in the long run in spite of the magnetic field, since the latter cannot affect the thermodynamic equilibrium of particles 2. Because of the weak communication across lines of force, however, it takes longer to achieve this equilibrium in a field than without one, and we must assume that the time concerned is short relative to the confinement time of particles 2. The size of the Larmor radius of particles 2 then makes no difference; the density is given by the Boltzmann law whether the gyroradius is large or small. The gyroradius of the collected particle 1 will be assumed small compared to the probe radius.

The probe is assumed to collect only particles traveling along B in a tube of radius $a + r_L$, where a is the probe radius and r_L the gyroradius of particles 1, and $a \gg r_L$. The population of particles in this tube will be controlled by transverse diffusion into the tube from the undisturbed plasma. The diffusion coefficient D_{\perp} can be classical or anomalous (caused, say, by fluctuating electric fields), but the theory is most useful in the case of anomalous diffusion. Ordinary collisions suffered by a particle in the course of its travel along B in the tube defined by the probe are completely neglected. The theory is "collisionless" to the extent that a D_{\perp} which does not depend on collisions with particles can be used.

The basic assumption of this theory is that the radial fall-off of potential (and hence density) as one leaves the probe and the tube of force it intersects has a characteristic length of the order of the larger of r_L and \underline{h} , both of which are small compared with \underline{a} . Hence the undisturbed density n_o is reached

in a relatively short distance radially. All quantities will then be averaged over the cross-section of the tube, and this will become a one-dimensional theory in the dimension z , along B. As one goes away from the probe in the z -direction, the undisturbed density will be approached asymptotically, since there will be a larger and larger distance in which particles can diffuse into the tube and replenish the particles lost to the probe. The behavior of \underline{n} and \underline{V} in the z -direction will be given by the theory. This problem is very similar to the problem discussed in Sec. 2.4 of a collisionless discharge between infinite parallel plates. Instead of ionization we have here transverse diffusion which feeds particles into our one-dimensional space. There is here however a "recombination" mechanism due to the loss of particles from the tube due to the same diffusion mechanism which brought them in. This loss rate is specified by D_{\perp} and is taken into account in the theory, whereas recombination was neglected in Sec. 2.4.

The transverse diffusion is imagined to be given by a frequency \underline{s} , which is constant in space and time and gives the rate at which particles are exchanged between lines of force. Thus into a volume $\pi a^2 dz$ of the tube of force defined by a probe of circular cross-section, there are $\pi a^2 n_0 s dz$ particles per second transported from outside the tube (where the density is n_0), and there are $\pi a^2 n_1(z) s dz$ particles per second transported similarly out of this volume. The net flux is then found by dividing the difference by the area:

$$j = \frac{\pi a^2 s dz (n_0 - n_1)}{2\pi a dz} = \frac{1}{2} s a (n_0 - n_1) \quad . \quad (5.3-1)$$

The parameter \underline{s} can be related approximately to D_{\perp} by assuming that the radial gradient of \underline{n} has a scale length r_L , the gyroradius of particles 1; then the flux is also

$$j = D_{\perp} (n_o - n_1) / r_L , \quad (5.3-2)$$

and so

$$D_{\perp} \sim \frac{1}{2} s a r_L . \quad (5.3-3)$$

If n_1 and V are understood to be the average density and potential over a cross-section of our tube, they are related by the following one-dimensional Poisson equation for $e_1 = -e_2$:

$$\frac{d^2 V}{dz^2} = -4\pi e_1 (n_1 - n_o e^{-e_2 V / kT_2}) . \quad (5.3-4)$$

We shall employ the usual dimensionless variables:

$$\eta = -e_1 V / kT_2 > 0$$

$$\xi = z/h$$

$$h = (kT_2 / 4\pi n_o e_1^2)^{1/2} \quad (5.3-5)$$

$$u = v/v_s , \quad v_s = (2kT_2 / m_1)^{1/2}$$

$$\nu = n_1 / n_o .$$

Eq. (5.3-4) then becomes

$$\eta'' = \nu - e^{-\eta} , \quad (5.3-6)$$

and conservation of energy for particles 1 gives, for any positions ξ and ζ ,

$$u^2(\xi) - \eta(\xi) = u^2(\zeta) - \eta(\zeta) \quad . \quad (5.3-7)$$

We can also define a dimensionless diffusion coefficient Δ and a corresponding dimensionless \underline{s} :

$$\Delta = D_{\perp} / v_s h \quad (5.3-8)$$

$$\sigma = sh / v_s \quad ,$$

so that (5.3-3) becomes

$$\Delta \approx \frac{1}{2} \sigma a^* r_L^* \quad , \quad (5.3-3a)$$

where a^* and r_L^* are measured in units of \underline{h} .

The next task is to calculate \underline{v} in terms of $\underline{\sigma}$ and the initial velocities of particles 1. For simplicity Bertotti assumes that these have a uniform velocity $\pm u_0$ in the ξ -direction, half the particles going in each direction. The extension to a continuous velocity distribution complicates the equations but does not introduce any new effects. Let $\iota(\xi, \zeta)$ be the dimensionless particle current (normalized to $n_0 v_s$) which enters the tube in a unit length at ζ and reaches ξ . The current that enters at ζ , $\iota(\zeta, \zeta)$, is given by the diffusion parameter σ :

$$\iota(\zeta, \zeta) = \pm \frac{1}{2} \sigma \quad , \quad (5.3-9)$$

the $\pm 1/2$ indicating that half goes one way and half the other. As this component of current travels toward ξ , it is being diminished by diffusion out of the tube at a rate proportional to $\underline{\sigma}$ and to the density ι/u :

$$\frac{\partial \iota(\xi, \zeta)}{\partial \xi} = \frac{-\sigma \iota(\xi, \zeta)}{u(\xi, \zeta)}, \quad (5.3-10)$$

where \underline{u} is given by (5.3-7):

$$u^2(\xi, \zeta) = u_0^2 + \eta(\xi) - \eta(\zeta). \quad (5.3-11)$$

It is clear then that ι varies exponentially:

$$\iota(\xi, \zeta) = \pm \frac{1}{2} \sigma e^{-\sigma \tau(\xi, \zeta)}, \quad (5.3-12)$$

where $\tau(\xi, \zeta)$ is the time, normalized to h/v_s , taken to go from ζ to ξ :

$$\tau(\xi, \zeta) = \int_{\zeta}^{\xi} \frac{d\xi'}{u(\xi', \zeta)} > 0. \quad (5.3-13)$$

Of course, if u_0^2 were too small compared to η , some particles entering the tube heading away from the probe would be turned around by the potential. These would contribute twice to the density and would greatly complicate the equations. Hence we must assume for all η :

$$u_0^2 \geq \eta. \quad (5.3-14)$$

This means that the theory is limited to small probe potentials, and usually to electron collection, since if $T_i \ll T_e$, a probe potential ^{smaller than kt_i/e} ~~this small~~ would not be sufficient to repel most of the electrons and cause saturation. With this assumption, the density at ξ is given by the integral over all partial currents from $\xi = 0$ (at the probe) to $\xi = \infty$:

$$\nu(\xi) = \int_0^{\infty} \frac{\mathcal{L}(\xi, \zeta)}{u(\xi, \zeta)} d\zeta = \frac{1}{2} \sigma \int_0^{\infty} \frac{e^{-\sigma\tau(\xi, \zeta)}}{|u(\xi, \zeta)|} d\zeta \quad . \quad (5.3-15)$$

Because of the absolute value sign this is conveniently broken up into two integrals. Let $\rho = \zeta - \xi$. Then using (5.3-15) for $\underline{\nu}$ and (5.3-11) for \underline{u} , we have for Poisson's equation (5.3-6)

$$\eta'' + e^{-\eta} = \frac{\sigma}{2} \int_0^{\infty} \frac{e^{-\sigma\tau} d\rho}{[u_0^2 + \eta(\xi) - \eta(\xi + \rho)]^{1/2}} + \frac{\sigma}{2} \int_0^{\xi} \frac{e^{-\sigma\tau} d\rho}{[u_0^2 + \eta(\xi) - \eta(\xi + \rho)]^{1/2}} \quad , \quad (5.3-16)$$

where $\tau = \tau(\xi, \xi + \rho)$ is given by (5.3-13) and (5.3-11) in terms of η . This is an integro-differential equation for $\eta(\xi)$, with $\eta(0) = \eta_p$, $\eta(\infty) = 0$.

The probe current density \underline{j} is the integral over the partial currents $\mathcal{L} d\xi$:

$$j = n_0 v_s \int_0^{\infty} d\xi \mathcal{L}(0, \xi) = \frac{n_0 v_s \sigma}{2} \int_0^{\infty} e^{-\sigma\tau(0, \xi)} d\xi \quad (5.3-17)$$

by (5.3-12). Here τ is given by (5.3-13) and (5.3-11) once η is known.

The complexity of this equation is apparent. The nature of the solution can be seen, however, in a much simplified case, in which

$$\alpha = \frac{kT_2}{m_1 v_0^2} = \frac{1}{2} \left(\frac{v_s}{v_0}\right)^2 = \frac{1}{2u_0^2} \rightarrow 0 \quad . \quad (5.3-18)$$

In this case u_o is so large that in (5.3-11) \underline{u} can be replaced by $\underline{+} u_o$; in other words, the particle motion is unaffected by the potential. This corresponds to collection of one species which is much hotter than the other; usually this implies electron collection in the presence of cold ions. Also, the time τ in (5.3-13) is approximated by $\tau(\xi, \zeta) = u_o^{-1} |\xi - \zeta|$. Equation (5.3-16) then simplifies to

$$\eta'' + e^{-\eta} = \frac{\sigma}{2u_o} \int_0^{\infty} e^{-\sigma\rho/u_o} d\rho + \frac{\sigma}{2u_o} \int_0^{\xi} e^{-\sigma\rho/u_o} d\rho$$

$$\eta'' + e^{-\eta} = 1 - \frac{1}{2} e^{-\sigma\xi/u_o} \quad (5.3-19)$$

This equation has a rather peculiar behavior if we set $\sigma = 0$, corresponding to no transverse diffusion. Then

$$\eta''_o + e^{-\eta_o} - \frac{1}{2} = 0 \quad (5.3-20)$$

This means that quasi-neutrality can never be attained: the equation for η_o cannot be established for $\eta_o = 0$ and $\eta''_o = 0$. The physical meaning of this is clear. If there are no collisions and no transverse diffusion, the very presence of an absorbing probe removes all particles traveling toward the probe, and hence the density at ∞ can be only $(1/2)n_o$. On the other hand, if we first change the unit of distance so that

$$\xi^* = \sigma \xi / u_o \quad (5.3-21)$$

and (5.3-19) reads

$$\sigma^2 u_o^2 \frac{d^2 \eta_\infty}{d\xi^{*2}} + e^{-\eta_\infty} = 1 - \frac{1}{2} e^{-\xi^*} \quad (5.3-22)$$

and then let $\sigma \rightarrow 0$, we get

$$e^{-\eta_\infty} + \frac{1}{2} e^{-\xi^*} - 1 = 0 \quad (5.3-23)$$

or

$$\eta_\infty = -\ln\left[1 - \frac{1}{2} e^{-\sigma \xi/u_0}\right] \quad (5.3-24)$$

This solution and its derivatives do approach 0 for $\xi \rightarrow \infty$. In fact the quasi-neutral solution is guaranteed in this case because as $\sigma \rightarrow 0$ in (5.3-22) the differential operator is neglected.

This is therefore a boundary-layer type of problem in which two different equations obtain for different regions, and the solutions must be matched at the common boundary. The position of this boundary will depend on the size of $\underline{\sigma}$. We have met this situation before in Sec. 3.33 on ion collection, in which the non-uniform convergence occurred when the ion temperature approached zero.

The solution η_∞ of (5.3-24), then, applies to the quasi-neutral region far from the probe. There is a very gradual fall-off of potential corresponding to the gradual replenishment by diffusion of particles lost to the probe. At $\xi = 0$, $\eta_\infty = \ln 2$.

The solution η_0 of (5.3-20) is valid for the sheath region and must be matched to η_∞ by letting $\eta_0(\infty) = \ln 2$. With $\eta_0(0) = \eta_p$, η_0 can easily be found numerically. The first integration can be done analytically the usual way. Note that the scale length for η_0 is of order l (\underline{h} in real units), while for η_∞ it is u_0/σ (v_0/hs in real units), which is generally very much larger. Thus the last term in (5.3-19) can be set equal to $1/2$ in the sheath, and η_0 is the proper solution there.

The probe current follows from (5.3-17). In the limit of large u_o , τ is approximately ζ/u_o , so that the current density is approximately $j = \frac{1}{2} n_o v_s u_o = \frac{1}{2} n_o v_o$, which is just the thermal random current. With the first order correction found from the numerical solution of (5.3-20), the probe current density is

$$j = \frac{1}{2} n_o v_o (1 + 0.1642 \alpha) + \frac{1}{2} n_o v_o \alpha \int_0^{\infty} dz [\eta_o(z) - \ln 2] \quad , \quad (5.3-25)$$

where α is defined in (5.3-18). The integrand is always positive.

This result is clearly in contradiction to experiment, since it predicts an electron current in excess of the current (approximately $\frac{1}{2} n_o v_o$) which would be collected in the absence of a magnetic field. The reason is also clear and bears out our previous statement that there is really no collisionless probe theory for a magnetic field. We have seen that an infinite cylindrical probe collects infinite current in the collision-dominated case. Since any shape of probe acts like a long cylindrical probe in a magnetic field, since it collects particles along a long tube of force, one would expect that the surrounding plasma would be severely drained of electrons. Hence the original assumption that the plasma density has its undisturbed value n_o a small distance r_L radially away from the probe is invalid; the radial fall-off distance is actually very large. In this "collisionless" theory the density just outside the tube of force is assumed to be replenished to n_o by free motion along lines of force. However, because of the length of the scale distance for η_{∞} , these particles must travel a very long distance along z , and their motion is eventually limited by collisions. Thus the

decrease in j when $B \neq 0$ depends eventually on λ , the mean free path along B , as was found by Bohm (Sec. 5.2); and the largeness of (5.3-25) is due to the neglect of λ .

This theory can perhaps be salvaged, however, since for n_0 one merely has to substitute n_λ , as calculated by Bohm for the collision-dominated region (c.f. Eq. 5.2-14). This will give the correct magnitude of \underline{j} , while the last term in (5.3-25) will give its dependence on η_p , i.e., the shape of part A of the characteristic. This shape is somewhat unexpected, since the computation of the integral in (5.3-25) shows that the slope of \underline{j} increases with η_p . Thus according to this theory the floating potential occurs to the left of the inflection point in part B of the probe characteristic (Fig. 1.1), contrary to the case when $B = 0$. This has not been verified experimentally, since space potential is difficult to determine independently. The reason for \underline{j} to increase with η_p is merely that the sheath thickness δ increases with η_p ; hence there is a larger region where ∇n is large. The reason for the slope of \underline{j} to increase is more obscure. This is probably because electrons are accelerated more by higher η_p , so that they have less chance to be scattered out of the tube. This acceleration was neglected in calculating η_0 , as was diffusion; but it was included in the first order term in the expression for \underline{j} .

In a second paper by Bertotti the restriction to $\alpha \rightarrow 0$ was removed, but it was necessary to treat the case of slow diffusion, $\sigma \rightarrow 0$, in which the second integral in (5.3-16) could be neglected because the interval was finite. The restriction (5.3-14) on probe potential was also removed by considering particles

which are turned around by the electrostatic field. After a tedious calculation Bertotti arrives at an expression for \underline{j} valid for arbitrary $\underline{\alpha}$. In the limit of large η_p he finds that $j \sim \eta_p^{3/4}$. There is thus no saturation. However, this result is suspect for several reasons. First, the collisional effects mentioned above would certainly become important. Second, the asymptotic analysis in which η is divided into η_o and η_∞ is valid only if $\sigma\tau$ is small, i. e., the time of travel is small compared to σ^{-1} . For large sheaths this may not be true. Third, in the presence of gradients of η in both z and r directions, there is a second order drift which moves particles radially even when $\sigma = 0$. The neglect of this drift would not be valid if the value of σ is too small. The theory of Bertotti makes its primary contribution in demonstrating the mathematical nature of this boundary-layer problem.

5.4 Summary of Probe Theories with a Magnetic Field

As early as 1936 Spivak and Reichrudel made a study of electron collection in a weak magnetic field, primarily by cylindrical probes. Their point of view was that the Langmuir orbital theory (Sec. 3.12), which has the advantage that the probe current is independent of the potential distribution, had a limited range of applicability (the sheath had to be large), and that this range could be extended by applying a weak magnetic field. Electron collection is then controlled by orbital motions in the magnetic field over a larger range of possible potential distributions. The current is again independent of potential shape, and Poisson's equation and ion density are not considered. In order to solve the orbital problem, however, Spivak and Reichrudel had to assume a boundary at

which the magnetic field's effects abruptly stopped; and the velocity distribution at this boundary was assumed to be known. This rather unrealistic assumption limits the credibility of the theory, even though the resulting curves for parts A and B of the probe characteristic vary with B in a manner similar to that observed in experiments. Detailed comparison with experiment was attempted; but since the entire discharge changed with B, this was not definitive. In any case the theory is valid only for very weak fields (below 100 gauss) and very low densities.

In 1954-5, Bickerton considered electron collection by a plane placed parallel to a magnetic field. Three cases were considered: $h \ll r_L$, $h \gg r_L$, and $h \sim r_L$. The procedure was to assume that electron motion is prescribed by perpendicular diffusion and mobility (5.2-2) and that the electric field is given by Child's law (2.2-5) for space charge limited ion flow from the plasma to the collector. The latter assumption may be valid for the lower portion of the transition region of the probe characteristic, but Bickerton erroneously used this assumption even near space potential. With a known V and $j(n)$, the density in the sheath can be found in terms of that at the sheath edge. The latter was found from the quasi-neutral solution for the plasma region; convergence was achieved by including ionization.

For $h \ll r_L$, the electron motion inside the sheath is unaffected by the magnetic field, while that outside the sheath is unaffected by the electric field. If the velocity distribution is known at a distance $\sim r_L$ from the sheath edge, and all electrons entering the sheath are collected, consideration of orbits in the

outer region gives for the probe current density (for classical diffusion)

$$j = \frac{n_o \bar{v}}{4} \frac{\pi}{\omega \tau} e^{-\eta} \quad , \quad (5.4-1)$$

where ω is the electron gyrofrequency. If collisions during the last Larmor orbit are taken into account, the result quoted but not derived in Bickerton [1955] is

$$j = \frac{n_o \bar{v}}{4} \left[\frac{8 + \omega^2 \tau^2 (1 - e^{-2\pi/\omega\tau})}{2(4 + \omega^2 \tau^2)} \right] \quad . \quad (5.4-2)$$

This expression reduces to $n_o \bar{v}/4$ for $\omega = 0$ and to (5.4-1) for $\omega \rightarrow \infty$. The density n_o is that near the plane probe; its relation to the density at ∞ is not known, since no asymptotic analysis was given. Moreover, an abrupt sheath edge was assumed. Therefore some caution must be exercised in using (5.4-2). Although (5.4-1) resembles the result of Bohm (5.2-15) in that the current goes as $1/B$, the two theories do not agree in detail because of the difference in the original model.

The magnitude of the electron current near space potential is given by Bohm et al, (5.2-15), for a probe of arbitrary shape. This theory neglects electric fields and orbital motions and is valid only for $kT_e \gg kT_i$.

The variation of electron current with potential is given by Bertotti (5.3-25) for the case of a probe of arbitrary shape in a strong magnetic field, when the probe potential and the ion temperature are both small, and the transverse diffusion coefficient is constant. The result is not analytic. Collisions are neglected.

The variation of saturation probe current with potential is also given by

Bertotti [1962] for the case of slow diffusion and large potentials. The temperature ratio is arbitrary, so presumably this theory can be used for ion collection as well. However, the assumptions of the theory are so restrictive that extreme caution should be exercised in its use.

No satisfactory theory, particularly of the important regions B and C, of the probe characteristic in a magnetic field is available. *And about getting to from transition region - limited in range of beams - some improvement on double probe theory.*

6. Floating Probes

6.1 Floating Potential

Although space potential is usually the quantity of interest, what is easily measured is instead the floating potential, the voltage at which the probe draws no current. Therefore the exact relation between V_s and V_f is of interest. V_f is of course negative relative to V_s .

In the absence of a magnetic field an approximate relation can be obtained by using Eq. (3.34-1) for the ion current:

$$j_i = \frac{1}{2} n(kT_e/M)^{1/2} \quad (6.1-1)$$

Since most electrons are repelled, their distribution, if originally Maxwellian, remains so in the presence of the probe, and the electron current is merely the random current times the Boltzmann factor:

$$j_e = \frac{1}{4} n v_e e^{eV_f/kT_e} = \frac{1}{2} n \left(\frac{2kT_e}{\pi m} \right)^{1/2} e^{eV_f/kT_e} \quad (6.1-2)$$

V_f being negative. Setting j_i equal to j_e , we have

$$\frac{eV_f}{kT_e} = \frac{1}{2} \ln\left(\frac{\pi}{2} \frac{m}{M}\right) \quad (6.1-3)$$

Thus for hydrogen V_f is about 3.6 times kT_e negative relative to space, and the factor is somewhat larger for heavier elements. For a more exact answer, the numerical results for j_i (Sec. 3.34) must be used.

In the presence of a magnetic field the magnitude of V_f is uncertain because no theory exists for j_i at small negative probe potentials. If the field is so weak (less than a few hundred gauss, say) that r_{Li} is much larger than the Debye length and the probe radius, then it may be permissible to use (6.1-1) still. The electron current, however, will be constrained to flow along the field, even at quite low fields, so that the effective collecting area is reduced to something like the projection of the probe area on a plane perpendicular to B . Thus for a cylindrical floating probe perpendicular to B the electron current is, very approximately,

$$I_e = 4a \ell j_e \quad (6.1-4)$$

where \underline{a} and $\underline{\ell}$ are the radius and length, while the ion current is

$$I_i = 2\pi a \ell j_i \quad (6.1-5)$$

If we use (6.1-1) and (6.1-2) for j_e and j_i , the resulting value of eV_f/kT_e differs by only a constant equal to $\ln\frac{1}{2}\pi = 0.45$, and this is probably insignificant in view of the approximations made.

Since electron current is more seriously decreased by a magnetic field than ion current, it is probable that in general the floating potential is closer to the space potential with a magnetic field than without. However, the small

electron current lost to the floating probe may be supplied by the plasma so easily even with a magnetic field that the effect may be slight.

6.2 Time Response

In view of the uncertainties in interpreting probe currents, particularly in strong magnetic fields, one of the better uses for probes is for the measurement of local fluctuations in potential and electric field. For this the spatial resolution of probes is particularly suitable. If the difference $V_s - V_f$ stayed constant, as it would if kT_e were constant, one needs only to measure the voltage fluctuations on a floating probe to get the fluctuations of V_s . However, there is an upper limit to the frequency response, since it takes a finite time for the ion sheath on a floating probe to adjust to changes in the plasma conditions. This time can be roughly estimated by dividing the sheath thickness by the acoustic velocity, since this is the order of distance ions have to travel and the velocity to which ions can be pushed by electrons. Thus

$$\begin{aligned} \tau &\sim d/v_s \sim h/(kT_e/M)^{1/2} = \left(\frac{M}{4\pi n e^2}\right)^{1/2} \\ &= \frac{1}{\omega_{pi}} \end{aligned} \quad (6.2-1)$$

Floating probes can therefore measure potential fluctuations up to the order of the ion plasma frequency. The writer does not know of a theory of the time response of a floating probe.))

There is some experimental data on this in the paper of Kamke and Rose [1956]. In this experiment a probe collecting ion current was pulsed abruptly to

a potential 100 volts lower, and the time for the probe current to return to a steady value was measured. This turned out to be of the order of $1 \mu\text{sec}$, which is considerably slower than ω_{pi}^{-1} . However, this was done at high pressures, and ion motion was limited by collisions.

6.3 Effects of Oscillations

If the plasma being studied is electrostatically unstable, so that large fluctuations in local potential (compared to kT_e) occur, a probe biased at a steady voltage will be actually fluctuating relative to the plasma. Therefore, if the fluctuations in probe current are filtered out in taking the probe characteristic, the measured current is actually an average over a range of probe potentials. In the saturation current regions (A and C) this averaging does not affect the result greatly, since the current is fairly constant with voltage. In part B, the transition region, however, this averaging will not give the right probe curve, since the latter is a non-linear curve. The effect will be to smooth out the curve and give a spuriously high electron temperature.

Since the magnitude of this effect is difficult to determine theoretically, it was investigated experimentally in some unpublished work by the writer (Princeton Plasma Physics Laboratory Report MATT-62, 1961). The instantaneous plasma potential was obtained by a floating probe, and the instantaneous current was measured by a second probe biased at a constant potential. The instantaneous current and voltage thus found were displayed on the axes of an oscilloscope to give the probe curve. In a typical oscillatory discharge, a hot-cathode reflex arc, the effect of the oscillations on the measured value of kT_e

was found to be less than the 10% error in this value.

6.4 Double Probes

In most gas discharges there is an electrode in good contact with the plasma which can be used as a reference point for potential when applying a bias voltage to a probe. Such an electrode can be the anode or cathode of a discharge, or the metallic wall or limiter of an electrodeless discharge, such as that in a stellarator or a toroidal pinch. In some instances such a reference point is not available. Examples of this are a toroidal rf discharge in a glass tube or the plasma in the ionosphere. In such a case a double probe must be used. The double probe method was originally proposed by Johnson and Malter [1950], and we shall give a simplified version of their thorough analysis. This method was invented for use in decaying plasma, in which the plasma potential changed with time, so that it was difficult to maintain a constant probe-plasma potential difference. With two probes biased with respect to each other but insulated from ground, the entire system "floats" with the plasma and therefore follows the change of plasma potential.

Fig. 6.1 shows the geometry.

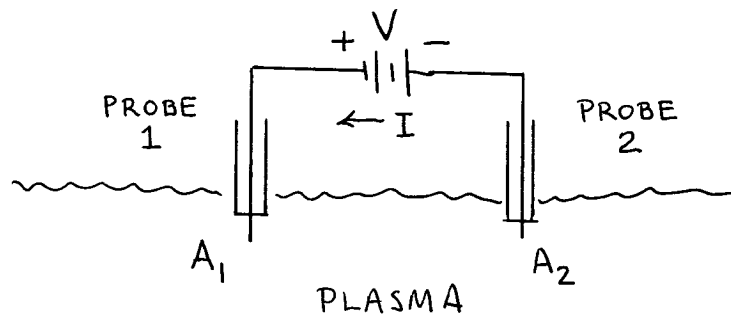


Fig. 6.1

Probes 1 and 2 have areas A_1 and A_2 , respectively, and are located in a plasma which has constant properties within the spacing of the probes. A voltage V is applied between 1 and 2, but the entire system is not connected to any electrode. For definiteness we shall assume V_1 is positive relative to V_2 , and therefore

$$V = V_1 - V_2 > 0 . \quad (6.4-1)$$

A current $I(V)$ flows between 2 and 1 and is positive if V is positive, by definition.

The potential distribution is shown schematically on Fig. 6.2.

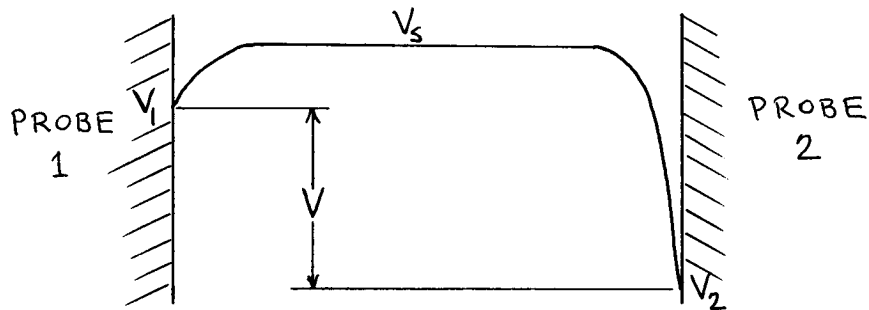


Fig. 6.2

Since the electron velocities are much higher than the ion velocities, the probes in general must both be negative with respect to space to prevent a net electron current from flowing to the whole system. This condition can be violated only if one probe is so much larger than the other that the ion current to the larger probe can cancel the saturation electron current to the smaller probe; we shall not consider such a case.

Fig. 6.3 shows what the probe characteristic will look like.

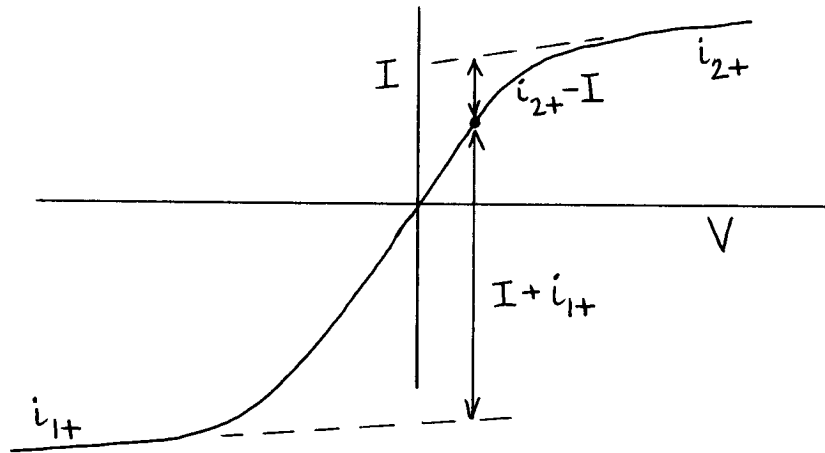


Fig. 6.3

This is drawn for the case $A_1 > A_2$; the curve will of course be symmetrical for $A_1 = A_2$. At $V = 0$, both probes are at floating potential and no net current goes to either one; hence $I = 0$. If V is now made slightly positive, V_1 will become less negative and V_2 more negative; thus more electrons will flow to 1 and fewer to 2. This results in a positive current flow from 2 to 1; that is, a positive I ; this is shown by the dot on Fig. 6.3. For large positive V 's, probe 2 will be very negative, drawing saturation ion current. Probe 1 will still be negative, but close enough to V_s to collect a sufficient electron current to cancel the ion current to probe 2. Thus the probe characteristic assumes the shape of the saturation ion characteristic of probe 2. With negative V the current is reversed, and the same general behavior occurs; the magnitude of the saturation current will be different if the probe areas are different.

This qualitative description reveals an important advantage of the double probe method: the total current to the system can never be greater than the

saturation ion current, since any electron current to the total system must always be balanced by an equal ion current. Thus the disturbance on the discharge is minimized. This has the disadvantage, however, that only the fast electrons in the tail of the distribution can ever be collected; the bulk of the electron distribution is not sampled.

To find the current $I(V)$ quantitatively, we define i_{1+} , i_{1-} , i_{2+} , and i_{2-} to be the ion and electron currents to probes 1 and 2 at any given V . The condition that the system be floating is

$$i_{1+} + i_{2+} - i_{1-} - i_{2-} = 0 \quad . \quad (6.4-2)$$

The current I in the loop is given by

$$i_{2+} - i_{2-} - (i_{1+} - i_{1-}) = 2I \quad . \quad (6.4-3)$$

If we add and subtract (6.4-2) and (6.4-3), we obtain

$$I = i_{1-} - i_{1+} = i_{2+} - i_{2-} \quad . \quad (6.4-4)$$

The currents i_{\pm} are given by Eq. (6.1-2) for the electron current density to a probe in the transition region:

$$i_{1-} = A_1 j_{\tau} e^{eV_1/kT_e} ; \text{ similarly for 2 } \quad . \quad (6.4-5)$$

Here j_{τ} is the random electron current density. Substituting this into the first of (6.4-4) and using (6.4-1), we have

$$\begin{aligned} I + i_{1+} &= A_1 j_{\tau} e^{eV_1/kT_e} = A_1 j_{\tau} e^{e(V+V_2)/kT_e} \\ &= \frac{A_1}{A_2} i_{2-} e^{eV/kT_e} \quad . \end{aligned} \quad (6.4-6)$$

From the second of (6.4-4),

$$\frac{I + i_{1+}}{i_{2+} - I} = \frac{A_1}{A_2} e^{eV/kT_e} \quad . \quad (6.4-7)$$

The basic assumption of this theory is that the probes are always negative enough to be collecting essentially saturation ion current; therefore, i_+ can be accurately estimated at any V by smoothly extrapolating the saturation portions of the double probe characteristic. The quantities in the numerator and denominator of (6.4-7) are then easily obtained; they are shown in Fig. 6.3. The slope of a logarithmic plot of this ratio against V then yields the electron temperature.

We note two special cases. If $A_1 = A_2$, then $i_{1+} \cong i_{2+} \cong i_+$, and (6.4-7) can be solved for I :

$$I = i_+ \tanh(eV/2kT_e) \quad . \quad (6.4-8)$$

This formula has been found to fit the experimental curve quite well. On the other hand, if $A_1 \gg A_2$, we can assume that probe 1 is essentially unaffected by probe 2 and is almost at floating potential, with $i_{1+} \cong i_{1-}$. Thus

$$I \ll i_{1+} = A_1 j_+ \quad . \quad (6.4-9)$$

Since $i_{2+} - I = i_{2-}$, Eq. (6.4-7) can be written

$$\frac{A_1 j_+}{1} \cong \frac{A_1}{A_2} i_{2-} e^{eV/kT_e} \quad ; \quad (6.4-10)$$

and

$$i_{2-} = A_2 j_+ e^{-eV/kT_e} = A_2 j_+ e^{-e(V_1 - V_2)/kT_e} \quad . \quad (6.4-11)$$

Since $i_{1+} \cong i_{1-}$, we have $j_+ \cong j_+ e^{eV_1/kT_e}$. With this, (6.4-11) becomes

$$i_{2-} = A_2 j_+ e^{eV_2/kT_e} . \quad (6.4-12)$$

This is just the transition current to a single probe, as one would expect, since probe 1 has become a large reference electrode. This case of $A_1 \gg A_2$ has application in space physics, where a nose cone casing often serves as a large reference probe.

The logarithmic plotting of (6.4-7) to determine kT_e is quite laborious. Since only a few electrons are sampled anyway, sufficient accuracy on kT_e can be obtained by merely measuring the slope of the characteristic at the origin. If we assume that i_+ is independent of V , we obtain from (6.4-4)

$$\frac{dI}{dV} = \frac{di_{1-}}{dV} = - \frac{di_{2-}}{dV} . \quad (6.4-13)$$

Using (6.4-5), we have

$$A_1 j_+ e^{eV_1/kT_e} \frac{e}{kT_e} \frac{dV_1}{dV} + A_2 j_+ e^{eV_2/kT_e} \frac{e}{kT_e} \frac{dV_2}{dV} = 0 . \quad (6.4-14)$$

From (6.4-1) we have

$$1 = \frac{dV_1}{dV} - \frac{dV_2}{dV} , \quad (6.4-15)$$

so that (6.4-14) becomes

$$A_1 e^{eV_1/kT_e} \frac{dV_1}{dV} + A_2 e^{eV_2/kT_e} \left(\frac{dV_1}{dV} - 1 \right) = 0 . \quad (6.4-16)$$

At $V = 0$, $V_1 = V_2$; and so

$$\left. \frac{dV_1}{dV} \right]_0 = \frac{A_2}{A_1 + A_2} \quad (6.4-17)$$

The first of (6.4-13) therefore becomes, at $V = 0$,

$$\left. \frac{dI}{dV} \right]_0 = \frac{A_1 A_2}{A_1 + A_2} j_{\tau} \frac{e}{kT_e} e^{eV_f/kT_e} \quad (6.4-18)$$

where V_f is the floating potential.

Since $A_1 V_1 = A_2 V_2$ we have

$$j_{+} = j_{\tau} e^{eV_f/kT_e} \quad (6.4-19)$$

Eq. (6.4-18) becomes
we have

$$\left. \frac{dI}{dV} \right]_0 = \frac{e}{kT_e} j_{+} \frac{A_1 A_2}{A_1 + A_2} \quad (6.4-20)$$

Finally, since $i_{1+} = A_1 j_{+}$ and $i_{2+} = A_2 j_{+}$, we have

$$\left. \frac{dI}{dV} \right]_0 = \frac{e}{kT_e} \frac{i_{1+} \cdot i_{2+}}{i_{1+} + i_{2+}} \quad (6.4-21)$$

From this, kT_e can be computed from the slope at the origin and the measured magnitudes of i_{1+} and i_{2+} .

Once kT_e is known, the plasma density can be calculated from either saturation current, with the help of one of the theories of ion collection summarized in Sec. 3.34.

add about "shadow" effect in mag field

7. Double Sheaths

An important complication to the theory of probes and sheaths is the emission of electrons from the probe or wall surface. This can be secondary emission due to ion bombardment or thermionic emission if the probe is heated by exposure to an intense discharge. The probe can also be heated to emission on purpose in order to gain more accurate information on the space potential.

When a surface emits electrons by either of these processes, these electrons may or may not actually leave the surface depending on whether or not they have enough energy to overcome any potential barriers which they may face. The energy of emitted electrons is quite low (c.f. Massey and Burhop, Electronic and Ionic Impact Phenomena, 1st ed., pp. 320, 554 (Oxford Univ. Press, 1952)). We must distinguish, however, between thermionic and secondary emission. In either case the energy distribution of the secondaries can be approximated by half of a Maxwellian distribution; but the equivalent temperature kT_p in the case of thermionic emission is about the same as the emitter temperature (about 0.2 eV), whereas for secondary emission, either by ions or by electrons, it is of the order of 1-3 eV. Thus for thermionic emission, the condition $kT_p \ll kT_e$ is almost always fulfilled (an exception being the case of thermally ionized Cs or K plasma). For secondary emission this condition would be satisfied in thermonuclear plasmas, where $kT_e > 10$ eV usually, but would not be satisfied in classical discharges, where $kT_e \sim 2$ eV. In what follows we shall focus our attention on the case $kT_p \ll kT_e$.

If kT_p is small, it is obvious that the case of a positive probe is unin-

velocities is exponential, the height of the barrier need be at most a small multiple of kT_p for any reasonable amount of emission from the surface. If $kT_c \ll kT_e$, the height of the barrier will in general be much smaller than the potential of the emitting probe or cathode.

The negative second derivative of η in the case of space charge limited emission indicates an excess of electrons in the immediate vicinity of the surface. Further out in the sheath, however, the curve has a positive second derivative in the region of the normal ion sheath. Thus there are two layers of charges in the sheath; this is what is known as a "double sheath".

Fig. 7.1 bears a striking resemblance to Fig. 2.3 for emission of electrons in a vacuum. The difference is that in a plasma there are plasma electrons and ions contributing to the space charge as well as emitted electrons. Moreover, the boundary condition on the left is no longer given by a simple conducting wall but by the sheath criterion for transition to the plasma region. With the preliminary work we have done in Sec. 2.3 this problem is straightforward but involves some algebra.

7.1 Electron Emission: General Formulation

The problem of the double sheath was first solved by Langmuir [Phys. Rev. 33, 954 (1929)]. Our treatment here is perhaps a little more accurate and systematic. It is given in detail since it is not to be found elsewhere. For simplicity we shall assume one-dimensional geometry and an absence of collisions in the sheath. We shall assume also that a steady-state solution is possible, and that the matching condition at the sheath boundary can be specified

by (2.32-1), namely,

$$\left(\frac{dn_i}{d\eta}\right)_o = \left(\frac{dn_e}{d\eta}\right)_o, \quad (7.1-1)$$

where the subscript o denotes quantities at the sheath edge ($\eta = 0, \xi \rightarrow \infty$). In order to get a closed expression for n_i we shall further assume that the ions are mono-energetic. In most instances ions will be much colder than electrons, and this approximation will be very good. The problem will be to calculate the space charge limited current for a given set of plasma parameters, and also the potential distribution, even when emission is not space charge limited. The result will then be applied to several problems, notably the calculation of the potential of a floating emitting probe.

Since this calculation can be applied to an emitting cathode as well as to a probe, we shall use the subscript c to denote quantities at the cathode (or probe) and the subscript p for quantities connected with the emitted, or "primary", electrons. Thus for thermionic emission, $kT_c = kT_p$. The algebra would be much simpler if we could assume $\eta_c \gg 1$; however, in some problems this is not satisfied, and we shall keep the calculation accurate down to almost $\eta_c = 1$. There can be few problems in which η_c is less than unity, since then plasma electrons stream freely to the collector, and it would be almost impossible to maintain the discharge. With a spherical or cylindrical probe, of course, one can sometimes draw saturation electron current without disturbing the discharge, but as stated above the case of positive probe potentials is uninteresting.

Poisson's equation now has a third term on the right, corresponding to

the density of emitted electrons:

$$\nabla^2 V = \frac{d^2 V}{dx^2} = -4\pi e(n_i - n_e - n_p) \quad . \quad (7.1-2)$$

This is supplemented by the boundary conditions

$$dV/dx = V = 0 \quad \text{at } x = \infty \quad . \quad (7.1-3)$$

Also, we have

$$\frac{d^2 V}{dx^2} = 0 = n_{oi} - n_{oe} - n_{op} \quad \text{at } V = 0 \quad (7.1-4)$$

and

$$V = V_c \quad \text{at } x = 0 \quad .$$

These relations and (7.1-1) are necessary to fix the behavior and relative magnitudes of the density terms.

We shall use the following dimensionless parameters:

$$\begin{aligned} \eta &= -eV/kT_e \\ \xi &= x/h \quad h = (kT_e/4\pi n_{oi} e^2)^{1/2} \\ u &= v/v_e \quad v_e = (2kT_e/m)^{1/2} \\ \nu &= n/n_{oi} \\ \beta &= T_e/T_p \\ \iota &= \frac{j_p}{n_{oi}} \left(\frac{m\pi}{2kT_e}\right)^{1/2} \quad . \end{aligned} \quad (7.1-5)$$

Eqs. (7.1-2) and (7.1-4) become

$$\eta'' = \nu_i - \nu_e - \nu_p \quad (7.1-2')$$

$$\nu_{oi} = \nu_{oe} + \nu_{op} \quad (7.1-4')$$

If the ions enter the sheath with a uniform velocity v_i , and if $\eta_i = mv_i^2/2kT_e$, then the ion density is given by (2.31-6):

$$\nu_i = \left(1 + \frac{\eta}{\eta_i}\right)^{-1/2} \quad (7.1-6)$$

Later η_i will be determined from (7.1-1).

If the plasma electrons are Maxwellian, their distribution is

$$f_e = C n_{oe} \left(\frac{m}{2\pi kT_e}\right)^{1/2} e^{-m(v^2 - \frac{2eV}{m})/2kT_e} \quad (7.1-7)$$

In dimensionless form, this is

$$f_e = C n_{oe} \frac{1}{\sqrt{\pi} v_e} e^{-(u^2 + \eta)} \quad (7.1-8)$$

The density n_e is found by integrating this over all possible velocities. Since we are concerned with η_c 's which may be small, we must not include electrons with positive u and energy greater than $\eta_c - \eta$, since these are lost to the collector.

Thus

$$n_e = v_e \int f_e du = \frac{C n_{oe}}{\sqrt{\pi}} e^{-\eta} \left[\int_{-\infty}^0 e^{-u^2} du + \int_0^{\sqrt{\eta_c - \eta}} e^{-u^2} du \right] .$$

We shall need the following definition and properties of the error function:

$$\operatorname{erf} x = \frac{2}{\sqrt{\pi}} \int_0^x e^{-t^2} dt, \quad \operatorname{erf} \infty = 1 \quad (7.1-9)$$

$$\frac{d}{dx} \operatorname{erf} x = \frac{2}{\sqrt{\pi}} e^{-x^2} \quad (7.1-10)$$

$$1 - \operatorname{erf} \sqrt{x} = (\pi x)^{-1/2} e^{-x} \left(1 - \frac{1}{2x} + \dots\right), \quad x > 1 \quad (7.1-11)$$

$$1 + \operatorname{erf} \sqrt{x} = 2 - (\pi x)^{-1/2} e^{-x} \left(1 - \frac{1}{2x} + \dots\right), \quad x > 1 \quad (7.1-12)$$

$$\int e^x \operatorname{erf} \sqrt{x} dx = e^x \operatorname{erf} \sqrt{x} - 2 \sqrt{\frac{x}{\pi}} \quad (7.1-13)$$

From (7.1-9), the electron density becomes

$$\nu_e = \frac{C}{2} \nu_{oe} e^{-\eta} (1 + \operatorname{erf} \sqrt{\eta_c - \eta}) \quad (7.1-14)$$

$$C = 2/(1 + \operatorname{erf} \sqrt{\eta_c})$$

If the cathode potential is so large that all electrons are reflected, the error function in (7.1-14) becomes unity, and the density reduces to the Boltzmann law.

As for the emitted electrons, their distribution is also given by (7.1-7)

except that V_c is their zero of potential and T_p their temperature. Thus (c f. 2.33-4)

$$f_p = 2n_{cp} \left(\frac{m}{2\pi k T_p}\right)^{1/2} e^{-m \left[v^2 - \frac{2e}{m}(V - V_c) \right] / 2k T_p} \quad (7.1-15)$$

or

$$f_p = 2n_{cp} \beta^{1/2} \frac{1}{\sqrt{\pi} v_e} e^{-\beta(u^2 + \eta - \eta_c)} \quad (7.1-16)$$

The density is found by integrating over $v_e du$. Since these electrons are accelerated as they move towards the plasma, there are no electrons with velocity less than $\sqrt{\eta_c - \eta}$. Thus

$$\begin{aligned}
 n_p &= 2n_{cp} \beta^{1/2} \pi^{-1/2} e^{\beta(\eta_c - \eta)} \int_{\sqrt{\eta_c - \eta}}^{\infty} e^{-\beta u^2} du \\
 &= n_{cp} e^{\beta(\eta_c - \eta)} (1 - \operatorname{erf} \sqrt{\beta(\eta_c - \eta)}) . \quad (7.1-17)
 \end{aligned}$$

To evaluate n_{cp} , we note that the emitted current j_p is

$$\begin{aligned}
 j_p &= \int_0^{\infty} v f_p dv = v_e^2 \int_0^{\infty} u f_p du \\
 &= 2n_{cp} \beta^{1/2} v_e \pi^{-1/2} \int_0^{\infty} u e^{-\beta u^2} du \\
 &= v_e n_{cp} (\pi\beta)^{-1/2} . \quad (7.1-18)
 \end{aligned}$$

Thus

$$n_{cp} = j_p \beta^{1/2} \pi^{1/2} / v_e = \iota \beta^{1/2} n_{oi} \quad (7.1-19)$$

by (7.1-5), and

$$\nu_p = \iota \beta^{1/2} e^{\beta(\eta_c - \eta)} (1 - \operatorname{erf} \sqrt{\beta(\eta_c - \eta)}) . \quad (7.1-20)$$

It remains to find ν_{oe} from (7.1-4'). ν_{oi} is 1; and from (7.1-20), ν_{op} is

$$\nu_{op} = \iota G(\eta_c) \quad , \quad (7.1-21)$$

where we have made the convenient definition

$$G(x) = \beta^{1/2} e^{\beta x} (1 - \operatorname{erf} \sqrt{\beta x}) \quad . \quad (7.1-22)$$

Thus

$$\nu_{oe} = 1 - \iota G(\eta_c) \quad . \quad (7.1-23)$$

With the densities given by (7.1-6), (7.1-14), and (7.1-20), Poisson's equation (7.1-2') becomes

$$\eta'' = \left(1 + \frac{\eta}{\eta_i}\right)^{-1/2} - H [1 - \iota G(\eta_c)] e^{-\eta} (1 + \operatorname{erf} \sqrt{\eta_c - \eta}) - \iota G(\eta_c - \eta) \quad , \quad (7.1-24)$$

ν_i ν_e ν_p

where $H(\eta_c) = (1 + \operatorname{erf} \sqrt{\eta_c})^{-1}$

By means of the integrating factor η' , this can be integrated once:

$$\frac{1}{2} \eta'^2 = \int (\text{r. h. s.}) d\eta \quad . \quad (7.1-25)$$

The first term can be integrated easily:

$$\int \nu_i d\eta = 2\eta_i \left(1 + \frac{\eta}{\eta_i}\right)^{1/2} \quad . \quad (7.1-26)$$

The second term can be integrated with the help of (7.1-13), with $x = \eta_c - \eta$:

$$\int e^{-\eta} (1 + \operatorname{erf} \sqrt{\eta_c - \eta}) d\eta = -e^{-\eta} (1 + \operatorname{erf} \sqrt{\eta_c - \eta}) + \frac{2}{\sqrt{\pi}} e^{-\eta_c} \sqrt{\eta_c - \eta} . \quad (7.1-27)$$

The third term can similarly be integrated by (7.1-13):

$$\begin{aligned} \beta^{1/2} \int G(x) dx &= e^{\beta x} (1 - \operatorname{erf} \sqrt{\beta x}) + \frac{2}{\sqrt{\pi}} \sqrt{\beta x} \\ &= \beta^{-1/2} G(x) + \frac{2}{\sqrt{\pi}} \sqrt{\beta x} \end{aligned} \quad (7.1-28)$$

$$\therefore \int G(\eta_c - \eta) d\eta = -\beta^{-1} G(\eta_c - \eta) - \frac{2}{\sqrt{\pi}} \sqrt{\eta_c - \eta} . \quad (7.1-29)$$

Putting (7.1-26), (7.1-27), and (7.1-29) together, we obtain for (7.1-25)

$$\begin{aligned} \frac{1}{2} \eta'^2 &= 2\eta_i \left(1 + \frac{\eta}{\eta_i}\right)^{1/2} + H[1 - \iota G(\eta_c)] \left[e^{-\eta} (1 + \operatorname{erf} \sqrt{\eta_c - \eta}) - \frac{2}{\sqrt{\pi}} e^{-\eta_c} \sqrt{\eta_c - \eta} \right] \\ &\quad + \iota \left[\beta^{-1} G(\eta_c - \eta) + \frac{2}{\sqrt{\pi}} \sqrt{\eta_c - \eta} \right] + C , \end{aligned} \quad (7.1-30)$$

with $G(x)$ defined by (7.1-22).

In the case of temperature-limited emission, when ι is known, the boundary condition $\eta' = 0$ at $\eta = 0$ is put in at this point; and this equation can be integrated numerically to give the potential distribution for any given η_c . In the case of space-charge-limited emission, no additional quadrature is necessary to find the value of ι , since the two boundary conditions in this case, $\eta' = 0$

at $\eta = 0$ and $\eta = \eta_c$ are sufficient to give an algebraic equation for ι .

It remains to determine η_i from (7.1-1), in which $n_e + n_p$ is to be substituted for n_e . If we differentiate (7.1-6), (7.1-14), and (7.1-20) with respect to η and evaluate the derivatives at $\eta = 0$, then the condition $\nu'_{oi} = \nu'_{oe} + \nu'_{op}$ becomes

$$-\frac{1}{2\eta_i} = -H[1 - \iota G(\eta_c)] [1 + \operatorname{erf} \sqrt{\eta_c} + e^{-\eta_c} (\pi\eta_c)^{-1/2}] + \iota \beta [(\pi\eta_c)^{-1/2} - G(\eta_c)] . \quad (7.1-31)$$

Referring to the definition (7.1-22) for G and the expansion (7.1-11), we find that the last bracket in (7.1-31) differs from zero only by a higher order term in $(\beta\eta_c)^{-1/2}$. Similarly, from (7.1-12), the second bracket in (7.1-31) differs from 2 only by a higher order term in $\eta_c^{-1/2}$. Thus to first order in $\eta_c^{-1/2}$, we have

$$\eta_i = \frac{1}{2} \left[1 + \frac{1}{\sqrt{\pi\eta_c}} \left(\frac{1}{2} e^{-\eta_c} - \iota \right) \right]^{-1} \quad (7.1-32)$$

The dominant term is just $\eta_i = 1/2$, the value derived in Sec. 2.31, where n_p was 0, and the erf term in n_e was neglected. The magnitude of the correction term can be estimated by using the result of the next section, in which ι will be computed as a function of η_c for space charge limited emission when $\eta_i = 1/2$. It will turn out that ι varies approximately as $\eta_c^{1/2}$ for small η_c and approaches $(\frac{1}{2}\pi)^{1/2}$ at large η_c . For $\beta > 10$, the term $\iota(\pi\eta_c)^{-1/2}$ is about 15% for all $\eta_c < 20$ and is smaller for $\eta_c > 20$. Since ι is always less than the space charge limited value, the correction is always less than 15%.

If we go to terms in $\eta_c^{-3/2}$ in the expansion for $1 \pm \operatorname{erf} x$, the result is

$$\eta_i^{-1} = 2 + \frac{1}{\sqrt{\pi\eta_c}} \left(1 + \frac{e^{-\eta_c}}{2\sqrt{\pi\eta_c}}\right) (e^{-\eta_c} - 2\iota) - \frac{\iota}{\eta_c \sqrt{\pi\eta_c}} \left(1 + \frac{e^{-2\eta_c}}{2\pi} - \frac{1}{\beta}\right). \quad (7.1-33)$$

I II

We note that the terms containing ι have the effect of increasing η_i , while term I decreases it. This can be seen physically by making a schematic plot of the densities, as was done in Fig. 2.4.

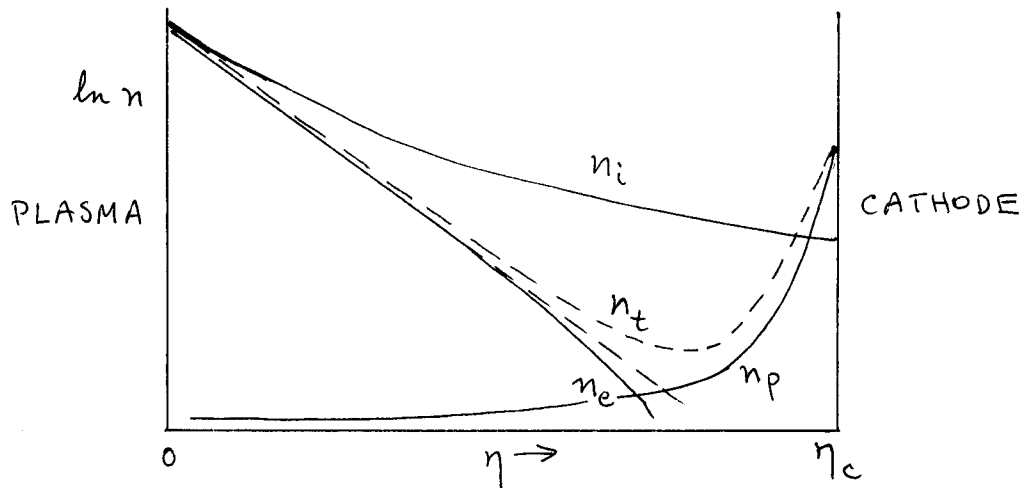


Fig. 7.2

In Fig. 7.2 the three densities n_i , n_e , and n_p are shown; the total electron density $n_t = n_e + n_p$ is shown by the dotted line. The effect of the positive slope of $\ln n_p$ at $\eta = 0$ is to decrease the (magnitude of the) slope of $\ln n_t$; this corresponds to the term II in (7.1-33) and results in a higher value of η_i since the slope of $\ln n_i$ decreases with η_i . The finite value of n_p at $\eta = 0$ also has the effect of shifting n_{oi} upwards at $\eta = 0$; this also increases η_i and corresponds to most of the terms in (7.1-33). Term I, which is independent of ι , reflects the deviation of $dn_e/d\eta$ from a straight line due to the truncation of the Maxwellian distribution. Unfortunately, this effect is not large enough, when ι is not zero, to ensure that $\eta_i < \eta_c$ for small η_c (less than 0.5). If $\eta_c < 1/2$, it is a little

hard to imagine how the ions can be accelerated to an energy $\eta_i = 1/2$,* and it must be assumed that our sheath criterion breaks down.

For large η_c , η_i can be set equal to $1/2$, and the error functions in (7.1-30) can be expanded by (7.1-11) and (7.1-12) to give a fairly simple equation. What limits the accuracy of our treatment for small η_c ? If the exact expression of η_i , Eq. (7.1-31), is substituted into (7.1-30), the resulting equation is exact providing that a) condition (7.1-1) is accurate (which is true if $\lambda \gg h$), b) the ions have no thermal speed, and c) the electron distribution is given exactly by (7.1-7). It is the last condition which probably limits the range of η_c to $\eta_c > 1$, since if electrons are lost quickly from the system, they do not have time to come to thermal equilibrium. To the extent that the electrons are in equilibrium, the calculation is good for any η_c , even below 1. However, for $1 < \beta < 10$ and $\eta_c < 2$, the exact expression (7.1-31) for η_i must be used. For larger η_c 's the approximate expression (7.1-33) for η_i may be used, or it may even be sufficiently accurate to let $\eta_i = 1/2$. Note that although the theory breaks down for very small η_c 's, it can give the right picture for the case $\beta = 1$, $\eta_c = 0$. In this case, the emitter can give back the electrons it collects and is effectively absent; hence $\eta = 0$ everywhere, and the value of η_i is irrelevant.

*One might think that this could happen even if $\eta_c = 0$, if a potential barrier of height $\eta > 1/2$ were built up in front of the cathode. However, since our treatment has implicitly assumed a monotonic potential, η_c is to be taken as the potential of this barrier if it exists, and not of the cathode itself. Fried and Heflinger [Space Technology Laboratories Rpt. TR59-0000-00870 (1959)] have treated the case of such a barrier, but the entire question of the plasma-sheath transition was side-stepped by assuming fixed ions, corresponding to $\eta_i = \infty$.

In the following section we shall for simplicity assume that $\eta_i = \frac{1}{2}$, but the numerical results given were computed exactly.

7.2 Space Charge Limited Emission

The condition for space charge limited emission is that the current emitted by the cathode, j_c , be so large that $d\eta/d\xi$ vanishes either at $\xi = 0$ or at some point ξ_m , as shown by the top curve in Fig. 7.1. When this happens, the current actually emitted into the plasma, j_p , is less than j_c , and the difference is the current reflected back to the cathode by the small potential hill.

If η_m is the magnitude of η at the top of this hill, we can calculate j_p by using (7.1-30) merely by replacing η_c by η_m . The difference between η_c and η_m is usually small and can be neglected. However if β is small, it may be necessary to calculate this difference; it is simply given by

$$j_p = j_c e^{-(\eta_m - \eta_c)/kT_p} \quad , \quad (7.2-1)$$

where j_c is, of course, given in terms of the cathode temperature by Richardson's equation.

We now have two boundary conditions for (7.1-30): $\eta' = 0$ at $\eta = 0$ and $\eta' = 0$ at $\eta = \eta_m$. It is a little more convenient to apply the second one first. At η_m we have

$$0 = 2\eta_i \left(1 + \frac{\eta_m}{\eta_i}\right)^{1/2} + H[1 - \iota G(\eta_m)] [e^{-\eta_m}] + \iota[\beta^{-1} G(0)] + C$$

$$-C = 2\eta_i \left(1 + \frac{\eta_m}{\eta_i}\right)^{1/2} + H e^{-\eta_m} [1 - \iota G(\eta_m)] + \iota \beta^{-1/2} \quad (7.2-2)$$

At $\eta = 0$, (7.1-30) becomes, with this value of C,

$$0 = 2\eta_i \left[1 - \left(1 + \frac{\eta_m}{\eta_i}\right)^{1/2}\right] + H [1 - \iota G(\eta_m)] \left[1 + \operatorname{erf} \sqrt{\frac{\eta_m}{\pi}} - \frac{2}{\sqrt{\pi}} e^{-\eta_m} \sqrt{\frac{\eta_m}{\pi}} - e^{-\eta_m}\right] \\ + \iota \left[\beta^{-1} G(\eta_m) + \frac{2}{\sqrt{\pi}} \sqrt{\frac{\eta_m}{\pi}} - \beta^{-1/2}\right] \quad (7.2-3)$$

With the abbreviation

$$F(\eta_m) = H \left[1 + \operatorname{erf} \sqrt{\frac{\eta_m}{\pi}} - e^{-\eta_m} \left(1 + 2\sqrt{\frac{\eta_m}{\pi}}\right)\right] \quad (7.2-4)$$

this becomes

$$2\eta_i \left[1 - \left(1 + \frac{\eta_m}{\eta_i}\right)^{1/2}\right] + F(1 - \iota G) + \iota (\beta^{-1} G + 2\sqrt{\frac{\eta_m}{\pi}} - \beta^{-1/2}) = 0 \quad (7.2-5)$$

This can be solved for ι :

$$\iota = \frac{2\eta_i \left(1 + \frac{\eta_m}{\eta_i}\right)^{1/2} - 2\eta_i - F}{2\sqrt{\frac{\eta_m}{\pi}} + \frac{G}{\beta} - \frac{1}{\sqrt{\beta}} - FG} \quad (7.2-6)$$

where G and F are to be evaluated at η_m and are defined by (7.1-22) and (7.2-4). This gives the space charge limited current as a function of β and η_m (essentially the voltage between the plasma and the emitter). It is therefore the plasma equivalent of the Child-Langmuir law (2.2-5). For small η_m (~ 1), Eq. (7.2-6) must be solved simultaneously with (7.1-31) for η_i (with the change

Improvements over Langmuir:

- 1) erf term in n_0 retained - hence get to lower V 's
- 2) erf term in η_p retained
- 3) u_0 not given explicitly by Langmuir

$\eta_c \rightarrow \eta_m$). The result is shown on Fig. 7.3. For large η_m , we can set $\eta_i = 1/2$, whereupon (7.2-6) becomes

$$\iota = \frac{(1 + 2\eta_m)^{1/2} - 1 - F}{2\sqrt{\eta_m/\pi} + \beta^{-1}G - \beta^{-1/2} - FG} \quad (7.2-7)$$

For large η_m , $G(\eta_m) \rightarrow (\pi\eta_m)^{-1/2}$ and $F(\eta_m) \rightarrow 1$. Thus for large voltages,

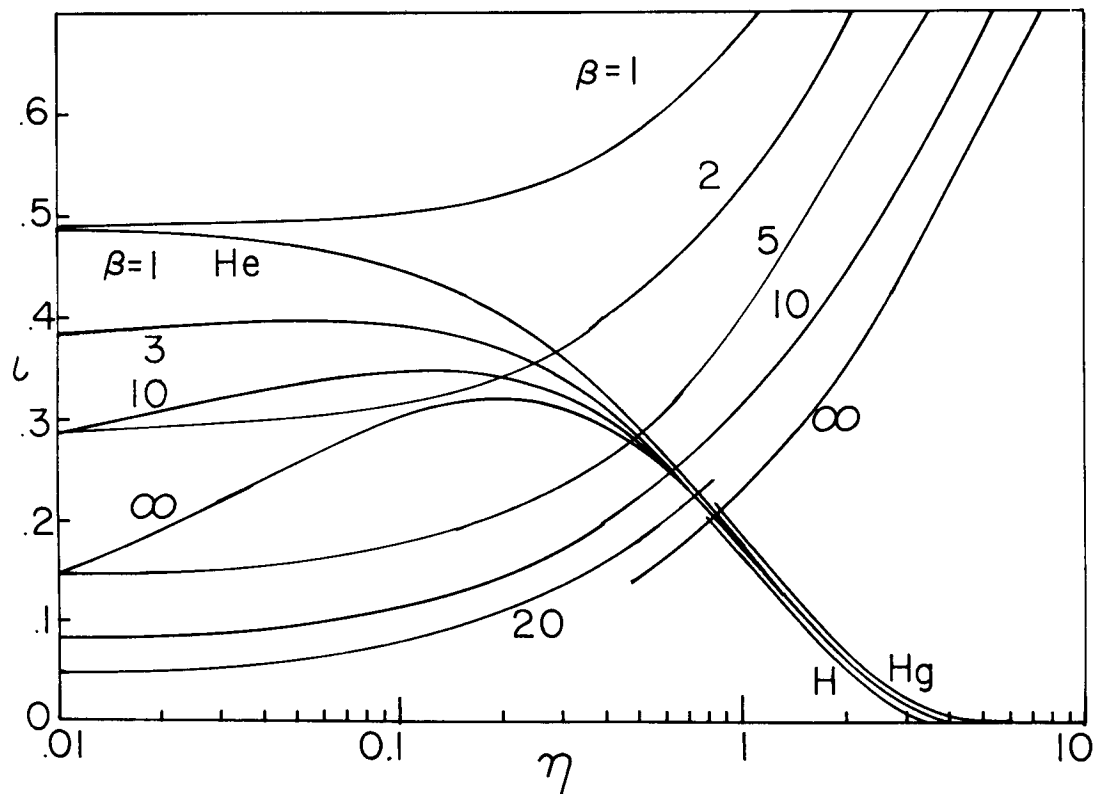
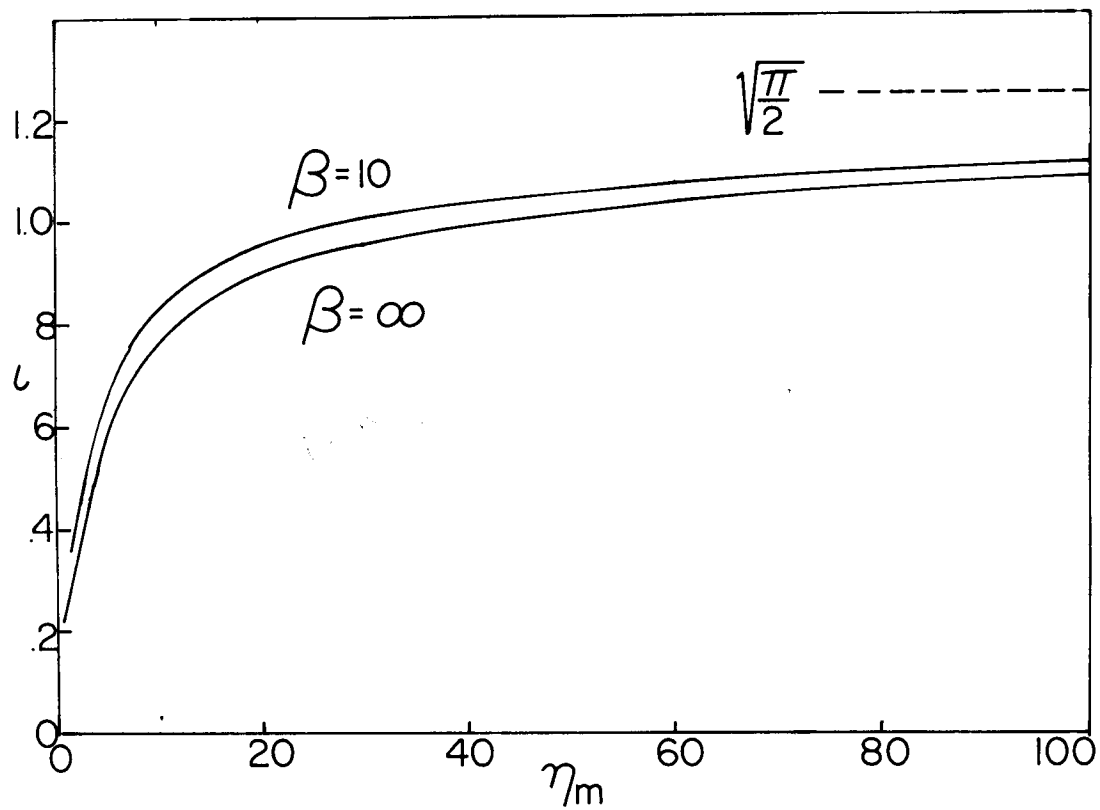
$$\iota \rightarrow (2\eta_m)^{1/2} / 2(\eta_m/\pi)^{1/2} = (\frac{1}{2}\pi)^{1/2} \quad (7.2-8)$$

In real units, the emitted current approaches (by (7.1-5)):

$$j_p \rightarrow (\frac{\pi}{2})^{1/2} n_{oi} (\frac{2kT_e}{m\pi})^{1/2} = n_{oi} (\frac{kT_e}{m})^{1/2} = j_i (\frac{M}{m})^{1/2} \quad (7.2-9)$$

This illustrates what is physically happening. In the presence of a plasma j_p is much larger than its value in a vacuum but has an upper bound proportional to the ion current. This is because it is the ions which cancel the space charge of the electrons, thus allowing more to be emitted. The factor $(M/m)^{1/2}$ merely reflects the fact that ions are more effective in producing space charge on account of their large mass and small velocity.

Since ι is a function only of η_m and β , the emitted current j_p , by (7.1-5), is proportional to plasma density n_{oi} . In a discharge in which the neutrals are ionized by the primaries, n_{oi} increases with j_p . Thus if η_m is fixed, n_{oi} and j_p can increase indefinitely. In practice the current is limited



either by j_c or by the external circuit. In the latter case η_m drops as j_p increases, until the ionization potential is approached and n_{oi} no longer increases with j_p . This explains why arcs tend to maintain a constant potential drop independent of current, the drop depending primarily on the ionization potential of the gas.

7.3 Emitting Probes

The results of the previous section can now be applied to probes which are heated to emission either purposely or accidentally. We first consider the case of a floating probe emitting a space charge limited current. We assume that kT_e is much larger than $kT_c (= kT_p)$, so that the difference between η_c and η_m can be neglected. The assumption of one-dimensionality will be valid whenever the probe is much larger than the Debye length or the electron gyroradius.

The condition that the probe be floating is that

$$j_i = j_e - j_p \quad , \quad (7.3-1)$$

where j_i and j_e are the ion and electron flux densities to the probe, and j_p is the flux density of emitted electrons. From (7.1-8), (7.1-23) and (3.34-1)

we obtain

$$j_p = \eta_{oi} \frac{v_e}{\sqrt{\pi}} H(1-\iota G) e^{-\eta_f - \frac{1}{2}} n_{oi} \left(\frac{kT_e}{M}\right)^{1/2} . \quad (7.3-2)$$

Using the definition of ι (7.1-5), we have

$$\iota = H(1-\iota G) e^{-\eta_f - \frac{1}{2}} \left(\frac{\pi}{2} \frac{m}{M}\right)^{1/2} = \frac{H e^{-\eta_f - \frac{1}{2}} \left(\frac{\pi}{2} \frac{m}{M}\right)^{1/2}}{1 + G H e^{-\eta_f}} . \quad (7.3-3)$$

The floating potential is then found by the intersection of this curve of ι vs. η and the curve of Fig. 7.3. The result for several values of M is shown in Fig. 7.4 on a logarithmic η scale.

The important point to note is that for the large β 's usually encountered ($\beta > 10$), the floating potential of an emitting probe is not much different from that of a cold probe. The reason is that the emitted electrons are of such low energy that a given current of them contributes more to the space charge than an equal current of incoming plasma electrons. Thus the emitted electrons become space charge limited at a small current and cannot effectively cancel the incoming current of electrons. The hope that a hot probe will float at space potential [Bohm et al, 1949], because if it were negative it would emit a large electron current and if it were positive it would collect a large electron current, is therefore in vain. A floating hot probe is only a little more positive than a cold probe, and the frequency response of the sheath cannot be improved this way. If β were smaller than 1, η_m would indeed be near 0, but then η_c would differ from η_m by an appreciable amount which depends on the exact probe temperature.

In using (6.1-1) for j_i we have implicitly assumed the result, since if the probe were indeed at space potential, the ion current would depend on kT_i and not kT_e . However, the effect of using kT_i instead of kT_e in j_i is to make η_f even larger, so that (6.1-1) is indeed the proper equation to use.

Although the space potential cannot be obtained directly from a floating hot probe, it can be measured from its probe characteristic. The procedure is to take two probe characteristics successively, one with the probe cold, and one

with it emitting. The current to the cold probe is given by

$$j(\eta) = j_i(\eta) - j_e(\eta) \quad . \quad (7.3-4)$$

The current to the hot probe is given by

$$j(\eta) = j_i(\eta) - j_e(\eta) + j_p(\eta) \quad , \quad (7.3-5)$$

where $j_p(\eta)$ is given by Fig. 7.3. When the probe is positive, $j_p = 0$, and the two characteristics coincide. As soon as the probe becomes negative, j_p begins to be emitted, and the characteristic of the hot probe will deviate from that of the cold probe. This is shown in Fig. 7.5.

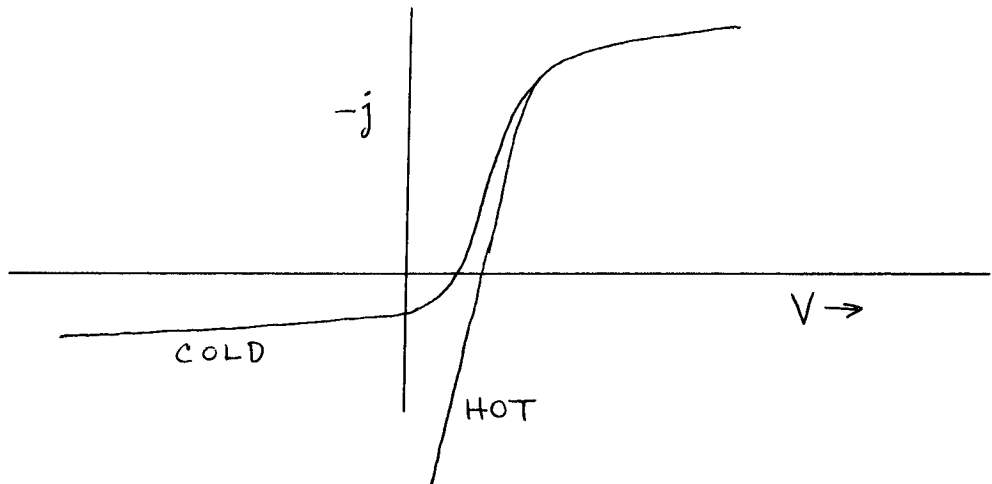


Fig. 7.5

The point of bifurcation of the superimposed characteristics then determines the space potential. The accuracy of this method is limited by the fact that the behavior of the ι - η curve is difficult to calculate near $\eta = 0$: either the deviation from planar geometry must be taken into account, or the plasma electron distribution must be calculated.

7.4 Secondary Emission

Secondary electrons can be emitted from bombardment by both electrons and ions. The primary effect of secondary emission on a probe characteristic will be to increase the apparent value of the saturation ion current at high negative probe voltages. This is because secondaries cannot leave the probe when it is positive, and because in the transition region neither ions nor electrons have sufficient energy to cause much secondary emission. We shall therefore be concerned only with part C of the characteristic.

Let δ be the secondary emission coefficient for ion bombardment, so that the emitted current j_p is

$$j_p = \delta j_i \quad . \quad (7.4-1)$$

If all emitted electrons are able to escape, the saturation ion current becomes

$$j_i + j_p = j_i(\eta)[1 + \delta(\eta)] \quad . \quad (7.4-2)$$

Since δ depends on the ion energy, it is a function of η . For most metals δ reaches a maximum at several hundred eV, and the maximum can be as large as 1 or greater; thus the correction is not always small. It is difficult to compute, however, because it depends sensitively on angle of incidence and cleanliness of the surface.

The potential distribution in the ion sheath can be computed from (7.1-30), with ι determined by (7.4-1). In terms of η_i this is

$$\iota = \delta (m\pi\eta_i/M)^{1/2} \quad . \quad (7.4-3)$$

In this case the slope of η at $\xi = 0$ is not known, but the value of ι is known, and (7.1-30) can be integrated numerically.

If the value of δ is large enough, it is conceivable for a double sheath to be formed and for the secondary current to be space charge limited. A necessary condition for this is that the density of emitted electrons be larger than that of ions near the probe surface. The density of ions there is:

$$n_i = \frac{j_i}{v_i} = j_i \left(\frac{M}{2kT_e} \right)^{1/2} (\eta + \eta_i)^{-1/2} \quad (7.4-4)$$

The density of emitted electrons is

$$n_p = \frac{j_p}{v_p} = j_p \left(\frac{m\pi}{2kT_p} \right)^{1/2} \quad (7.4-5)$$

Since $j_p = \delta j_i$, the necessary condition is

$$\eta + \eta_i > M/m\pi\beta\delta^2 \quad (7.4-6)$$

If we neglect η_i , this becomes

$$|eV| > MkT_p/m\pi\delta^2 \quad (7.4-7)$$

For δ 's of order 1 and kT_p of order 2 eV, the probe potential must be greater than about 1300 volts, even for hydrogen. This condition is rarely satisfied, and we conclude that (7.4-2) is valid since space charge limitation almost never occurs with secondary emission.

8. Practical Applications

When electrostatic probes are actually used experimentally, a number of considerations neglected in the foregoing theories must be taken into account. For example, a common experimental difficulty is a changing contact potential between the probe and the plasma, arising from a changing layer of impurities on the surface. This is important at low kT_e , when a change of tenths of a volt will affect the characteristic. Thus a probe must be kept clean. Another example is the macroscopic potential and density gradients in the discharge. These cause the conditions surrounding the probe to be asymmetric even if the probe itself is symmetric. The asymptotic values of \underline{V} and \underline{n} may be different in different directions. A third example is the effect of photoelectric emission. This becomes important when the plasma density and therefore the probe current is very small, as in the ionosphere.

For examples of difficulties arising in thermonuclear plasmas the reader is referred to review papers by F. F. Chen [1961] and Jones and Saunders [1961]. These papers also give representative diagrams of circuits used in probe work.

For an exposition of the use of floating probes in measuring correlation functions of potential fluctuations in a plasma, the reader is referred to the work of Kees Bol [1962] of this Laboratory.

SELECTED BIBLIOGRAPHY

I. Sheath Formation

1. I. Langmuir, Collected Works, ed. by C. G. Suits (Pergamon Press, New York, 1961), Vol. 5, pp. 140-224; Vol. 4, pp. 326-393; Vol. 3, pp.
2. D. Bohm, Characteristics of Electrical Discharges in Magnetic Fields, ed. by A. Guthrie and R. K. Wakerling (McGraw-Hill Book Co., New York, 1949), Chap. 3.
3. E. R. Harrison and W. B. Thompson, Proc. Phys. Soc. 74, Pt. 2, 145 (1959).

II. Probes, No Magnetic Field or Collisions

1. I. Langmuir, Collected Works, ed. by C. G. Suits (Pergamon Press, New York, 1961), Vol. 4, pp. 23-132.
2. J. E. Allen, R. L. F. Boyd, and P. Reynolds, Proc. Phys. Soc. 70B, 297 (1956).
3. D. Bohm, loc. cit., Chap. 2.
4. I. B. Bernstein and I. Rabinowitz, Phys. Fluids 2, 112 (1959).

III. Probes, with Collisions

1. B. Davydov and L. Zmanovskaja, Tech. Phys. USSR 3, No. 8, 715 (1936).
2. D. Bohm, loc. cit., Chap. 2.
3. R. L. F. Boyd, Proc. Phys. Soc. 64B, 795 (1951).
4. G. J. Schulz and S. C. Brown, Phys. Rev. 98, 1642 (1955).
5. C. H. Su and S. H. Lam, Princeton Aeronautical Sciences Dept. Rpt., to be published (1962).
6. I. Cohen, Thesis, Princeton Univ. (1962).

IV. Probes, with Magnetic Field

1. D. Bohm, loc. cit., Chap. 2.
2. G. V. Spivak and E. M. Reichrudel, Phys. Z. d. Sowjet, 9, 655 (1936); J.E.T.P. 8, 319 (1938); Izvestia Acad. Nauk, 1938, p. 479.
3. R. J. Bickerton and A. von Engel, Proc. Phys. Soc. 69, 468 (1955); also Bickerton, Thesis, Oxford Univ. (1954).
4. B. Bertotti, Phys. Fluids 4, 1047 (1961) ^{and 5, 1010 (1962)} ~~second article to be published, 1962. Receipt of preprint is hereby gratefully acknowledged.~~

V. Miscellaneous

1. E. O. Johnson and L. Malter, Phys. Rev. 80, 58 (1950). [Double probes]
2. D. Kamke and H.-J. Rose, Z. f. Physik 145, 83 (1956).
3. F. F. Chen, I.R.E. Trans. on Nuclear Sci. NS-8, No. 4, 150 (1961); also available as Princeton Plasma Physics Lab. Tech. Memo. 138 (1962).
4. H. W. Jones and P. A. H. Saunders, United Kingdom Atomic Energy Authority Report AERE-R3611 (1961), Her Majesty's Stationery Office, York House, Kingsway, London W. C. 2.
5. K. Bol, to be published (1962).